2015 年臺灣國際科學展覽會
優勝作品專輯

作品編號　**120006**

參展科別　環境科學

作品名稱　**Flexible Thermoelectric Module Application in Therapy Usage for Human Body**

得獎獎項　大會獎：四等獎

就讀學校　臺北市立建國高級中學

指導教師　朱旭山、李文禮

作者姓名　游皓任

關鍵字　**Waste Heat Recycle、Thermoelectric、Flexible**

作者簡介

我叫游皓任，目前就讀於台北市建國中學普通班三年級，在高一下時創立了專題研究社，因此為創社社長。

國小時是就讀體育班，國中則是念音樂班。游泳方面：目前是建國中學游泳校隊也曾任基隆市全國運動會代表隊。音樂方面：曾獲得建國中學校內合唱比賽最佳伴奏獎、台北市 102 學年度音樂比賽高中小提琴組甲等。至於接觸科展，要感謝我國中老師陳老師。熱電領域的接觸也是在那時開始的，在國中時，拿到基隆市環保科展第一名。關於高中的科展主題，其實早在國中科展做完時就有了將熱電晶片改良的想法。上了高中後，李文禮老師發現我對熱電領域的執著，提供了我機會完成國中沒有完成的夢想，才有機會走到現在。也謝謝一路上幫助我的人，沒有你們沒辦法成就今天的我。在未來，我將會成為熱電領域世界頂尖的人物。

摘要

福島核災的發生，更凸顯能源的重要性；又因近年來廢熱總量不斷提升與全球能源需求量增加，本研究利用熱電晶片冷端與熱端的溫度差產生電的特性，將環境廢熱回收成為可用的電能。

本研究設計之可撓性熱電晶片成功改良傳統熱電晶片的兩點缺點；其一 ：傳統的硬式平板狀晶片無法配合不同環境空間而改變其外型，其二 ： 硬式晶片的表面為陶瓷片，較易摔破導致晶片毀損，本研究之可撓性熱電晶片改良以往熱電晶片的陶瓷基板材料，改用具有可撓性的 FCCL 材料作為基板，因此可完整吸收表面彎曲物體的能源並將熱能轉換成電能。本研究之可撓式熱電晶片成功大幅降低熱電晶片之成本，有利於未來大量生產，成功應用人體體溫發電，同時也可利用 Peltier 效應，作為醫療用冷敷或熱敷之器材。

Abstract

Owing to the disaster of Fukushima nuclear power station, it reminded us the importance of energy again. Due to the amount of waste heat and energy demand increased in recent years. In this study, basing on the temperature difference between the hot and cold side of the thermoelectric module, electricity power was generated by conversion of environmental waste heat through the module.

The design of flexible thermoelectric module successfully improved the two disadvantages of traditional thermoelectric module. First, the hard flat module could not be bent to cover different shapes; second, the hard module was very fragile for its ceramic surface layer. The flexible thermoelectric module was improved the substrate of traditional thermoelectric module that it used the flexible material FCCL to be the substrate so it could completely absorb heat on curved surfaces and convert thermal energy into electrical energy. This study was successful reduced the cost substantially that it was favorability mass production. It was successfully applied to human body thermal energy conversion, and this power can be used to charge the cellphone, and so on... Basing on Peltier effect, it can convert electricity into thermal energy while the current flows into the module; and the temperature difference caused from thermal energy can also apply to therapy usage.

Chapter 1 Introduction

1.1 Global Energy Topic:

The disaster of Japan Fukushima nuclear power station (March 11, 2011) [1][2] revealed that, the nuclear power brought people a large amount of power, but it might bring people unimaginable tragedy if any mistakes happened. The energy consumption was increasing every year. (Figure 1-1) The prices of oil, gas and other energy rocketing which revealed the urgent shortage of available energy on earth.[3]

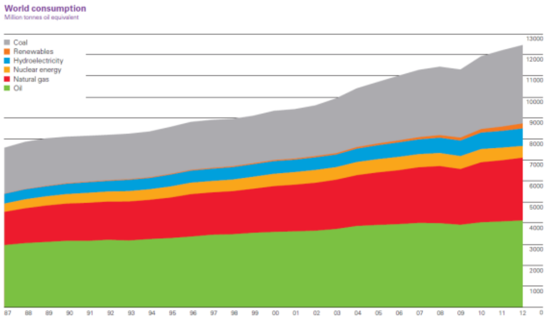

Figure 1-1: world energy consumption in 1987~2012 (Unit: 10^3 KLOE) [3]

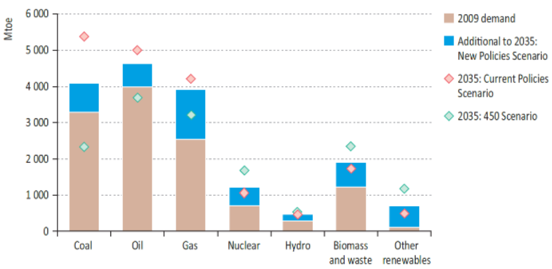

Figure 1-2: world primary energy demand by fuel and scenario in 2009~2035 [4]

The energy need would be much more than now.[4] (Figure 1-2) It was a very important topic about how to reduce inefficient energy and how to increase renewable energy.

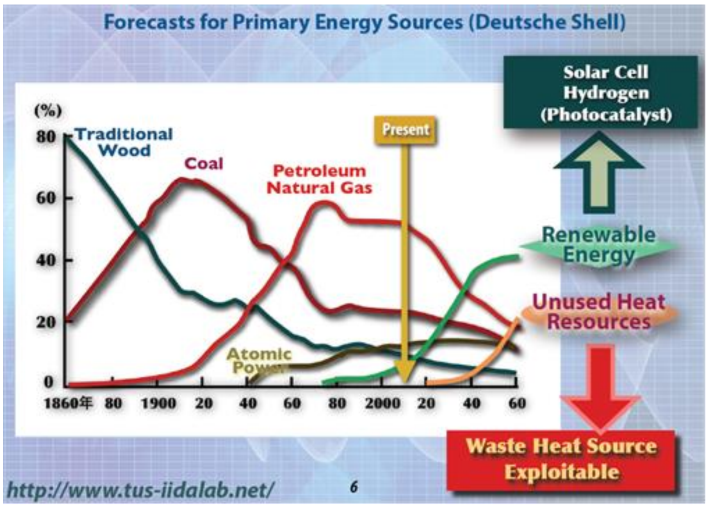

Figure 1-3: forecasts for primary energy sources [5]

The Deutsche Shell's forecasts for primary energy sources (Figure 1-3)[5] showed that renewable energy and waste heat would significantly increase. Waste heat was regarded as one of the causes of the greenhouse effect, so it was an important topic about how to reduce waste heat to alleviate the greenhouse effect.

1.2 Taiwan Thermal Energy Topic:

The thermal energy quantity continued to increase every year. (Table 1.1)(Figure 1-4) Therefore, it was a very important thing that how could we reduce thermal power or use thermal power effectively? And then, thermoelectric module (TEM) was convenient to use thermal power effectively because it could make thermal power transform to electric or electric transform thermal power.

Table 1.1: thermal of energy supply in 1997~2012 [6]

Year	Quantity	%(at that year)	Growth Rate (%)
1997	66.0	0.08	9.37
1998	70.1	0.08	6.20
1999	73.2	0.08	4.39
2000	77.3	0.08	5.61
2001	81.1	0.08	4.94
2002	84.3	0.08	3.98
2003	87.9	0.07	4.28
2004	92.7	0.07	5.42
2005	97.5	0.07	5.18
2006	102.4	0.08	5.02
2007	105.5	0.07	3.01
2008	109.5	0.08	3.84
2009	113.2	0.08	3.34
2010	114.3	0.08	0.99
2011	113.2	0.08	-0.96
2012	114.0	0.08	0.73

Unit: 10^3 KLOE

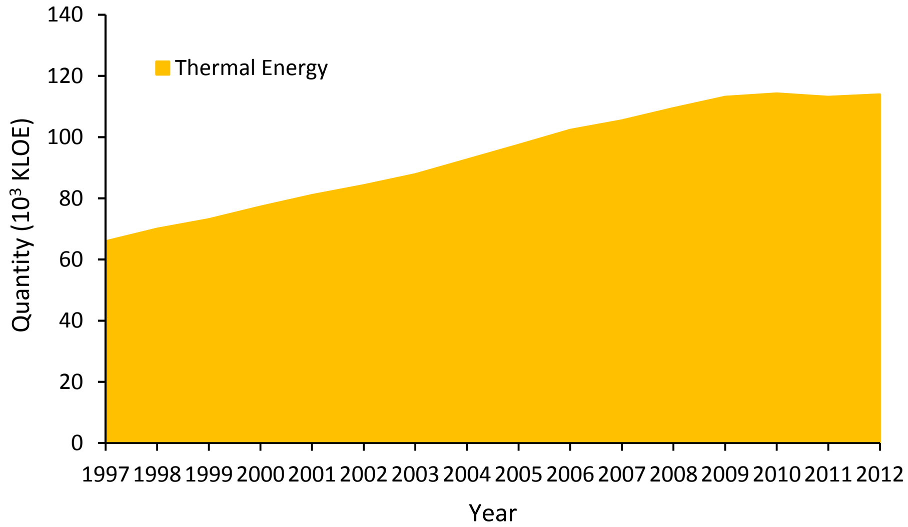

Figure 1-4: thermal energy quantity in 1997~2012

1.3 Thermoelectric Module (TEM):

Thermoelectric module (TEM) [7] was a kind of modules to use thermoelectric effect (the conversion between heat and electricity). Thermoelectric effect could be broadly divided into 3 parts: Seebeck effect, Peltier effect and Thomson effect; the following was the introduction of effects:

1.3.1 Seebeck effect [8][9]:

Thomas Johann Seebeck, in 1821, discovered that a compass needle would be deflected by a closed loop formed by two different metals joined in two places, with a temperature difference between the junctions. This was because the metals responded to the temperature difference in different ways, creating a current loop and a magnetic field. Seebeck did not recognize there was an electric current involved, so he called the phenomenon the thermomagnetic effect.

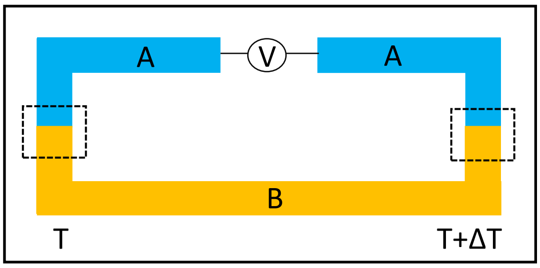

Figure 1-5: Seebeck effect schematic diagram

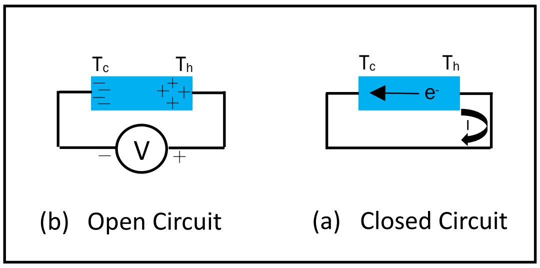

Figure 1-6: formation of electromotive force [9]

The effects could be explained in figure 1-6: when the right side of material was with higher temperature, the energy was larger and the electron mobility was in high speed; when the left side of material was with lower temperatures, the energy was less and the electron mobility was in low speed, which produced a net flow of electrons from right to left of the material. When electrons flow from right to left after a certain time, the left of material accumulated a considerable amount of electrons that have a large negative charges, so the material for forming a potential difference at both ends, and this would suppress the potential difference between electron flow continuously from right to left flows, and finally the state of equilibrium was reached.

The Seebeck coefficient could be expressed as Eq. (1.1).

$$S = \frac{V}{\Delta T} \qquad \text{Eq. (1.1)}$$

S (thermopower or Seebeck coefficient, V/ΔT)

V (voltage, W/A)

ΔT (temperature difference, K)

The voltage generated by the Seebeck effect could be expressed as Eq. (1.2).

$$V = \int_{T}^{T+\Delta T} [S_A\,(T) - S_B(T)]\; dT \qquad \text{Eq. (1.2)}$$

T and $T + \Delta T$ (temperature of the junction of both metals, K)

S_A (Seebeck coefficient of metal A, V/ΔT)

S_B (Seebeck coefficient of metal B, V/ΔT)

dT (temperature difference, K)

Assumed S_A and S_B were independent to temperature variable, the Eq. (1.2) could be expressed as Eq. (1.3).

$$V = (S_A - S_B) \cdot [(T + \Delta T) - T] \qquad \text{Eq. (1.3)}$$

1.3.2 Peltier effect [9]:

The Peltier effect was the presence of heating or cooling at an electrified junction of two different metals and was named for French physicist Jean Charles Athanase Peltier, who discovered it in 1834. When a current was made to flow through a junction between metal A and metal B, heat might be generated (or removed) at the junction.

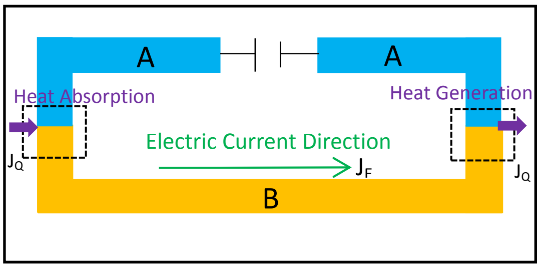

Figure 1-7: Peltier effect schematic diagram

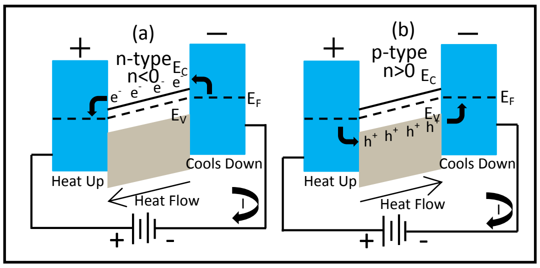

Figure 1-8: n-type p-type pairs schematic diagram

Figure 1-8(a): metal connected the n-type semiconductor, when electrons flowed from the n-type semiconductor to the right of metal, only electrons with higher energy overcame the energy barrier (E_C-E_F). These high-energy electrons flowed from the left of the metal to the n-type semiconductor; without any obstacles. It was endothermic phenomenon for right side of the conductor-energy electrons; left of the metal conductor with high-energy electrons accumulating more was exothermic.

Figure 1-8(b): metal connected the p-type semiconductor, electron hole was thermal carrier. The same, when the electron holes flowed from the left of metal into p-type semiconductor, only the higher energy electron hole to overcome the energy barrier (E_F-E_V). These high energy electron holes flowed from the right side of the metal to the N-type semiconductor had no barriers that it only had low energy electron hole at left side to cause endothermic. The right side of metal cumulated high energy electron holes to cause exothermic.

Peltier heat absorbed in a unit time could be expressed as Eq. (1.4).

$$Q = \Pi_{AB} I = (\Pi_B - \Pi_A) I \qquad \text{Eq. (1.4)}$$

Q (Peltier heat, W)

Π_{AB}(Peltier coefficient of metal A and metal B, V)

Π_A(Peltier coefficient of metal A, V)

Π_B(Peltier coefficient of metal B, V)

I (current, A)

1.3.3 Thomson effect[10]:

In many materials, the Seebeck coefficient was not constant in temperature, and so a spatial gradient in temperature could result in a gradient in the Seebeck coefficient. If a current was driven through this gradient then a continuous version of the Peltier effect would occur. This Thomson effect was predicted and subsequently observed by William Thomson (Lord Kelvin) in 1851. It described the heating or cooling of a current-carrying conductor with a temperature gradient.

Assumed a current density J was passed through a homogeneous conductor, the Thomson effect predicted a heat production rate q per unit volume that it could be expressed as Eq. (1.5).

$$q = -\kappa_t J \cdot dT \qquad \text{Eq. (1.5)}$$

q (heat production per unit volume, Jm^{-3})

J (current Density, Am^{-2})

κ_t(Thomson coefficient, VK)

1.4 Thermoelectric Bulk Materials (n-type and p-type):

Thermoelectric Junction was the n-type and p-type semiconductors upper and lower ends, using solder to the copper connect n-type p-type pairs. Finally, the ceramic plate welded to the upper and lower ends of thermoelectric Junction.

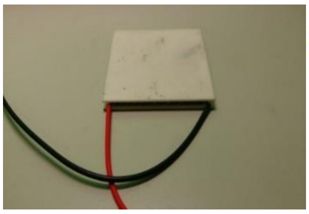

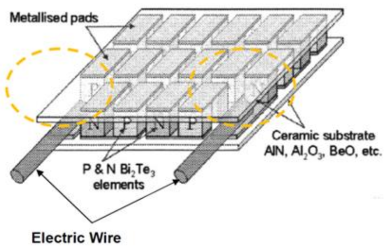

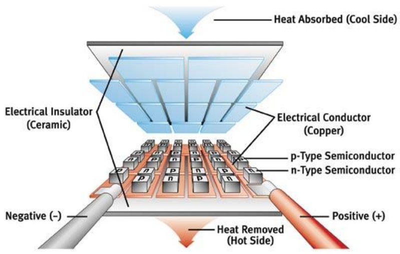

Figure 1-9: Traditional TEM Figure 1-10: TE schematic diagram[11] Figure 1-11: exploded view of TEM[12]

1.4.1 Selective Material:

The insulator had higher Seebeck coefficient, lower thermal conductivity, lower electrical conductivity and lower power factor. Although the metal had higher electrical conductivity and power factor ($\alpha^2\sigma$). The semiconductor had excellent power factor, its thermal conductivity was lower than metal, and its thermoelectric figure of merit ZT was much larger than the metal, so most of thermoelectric materials was semiconductor nowadays. (Figure 1-12)

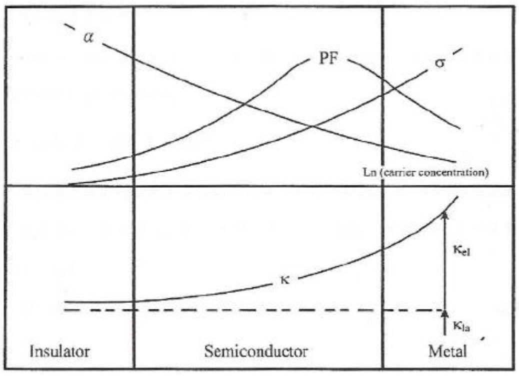

Figure 1-12: thermoelectric performance comparison chart of insulator, semiconductor and metal [13]

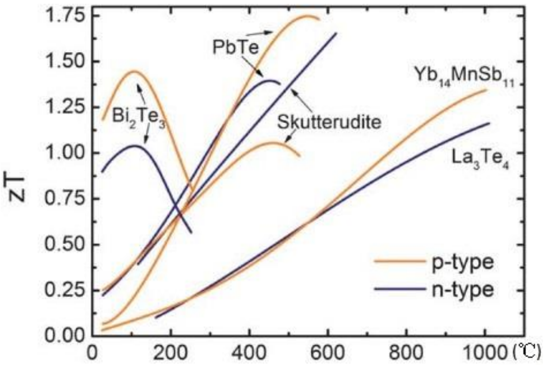

Figure 1-13: ZT and different temperature of n-type and p-type relationship diagram [14]

Table 1.2: Seebeck coefficient of the semiconductor and the metal [13]

Material	Seebeck coefficient	Material	Seebeck coefficient
Bi_2Te_3(P)	162	Bi_2Te_3(N)	-240
$Bi_{0.5}Sb_{1.5}Te_3$(P)	230	$Bi_{0.87}Sb_{0.13}$(N)	-100
$Al_{0.15}Ga_{0.85}As$	-350	$Al_{0.15}Ga_{0.85}As$	-670
Poly-Si(P)	190	Poly-Si(N)	-120
Poly-SiGe(P)	144	Poly-SiGe(N)	-136
ZnSb	220	InSb	-130
Cu	3.98	Ge	-210
W	5	TiO_2	-200
Ag	3.68	Al	-3.2

The figure 1-13 shows 3 points:

1. The maximum ZT value of Bi_2Te_3 material was about at 100℃.
2. The maximum ZT value of PbTe material was about during 420℃ to 520℃.
3. The maximum ZT value of $Yb_{14}MnSb_{11}$ and La_3Te_4 material were about at 1000℃.

1.4.2 Bulk Crystals of Bi_2Te_3 Thermoelectric Material:

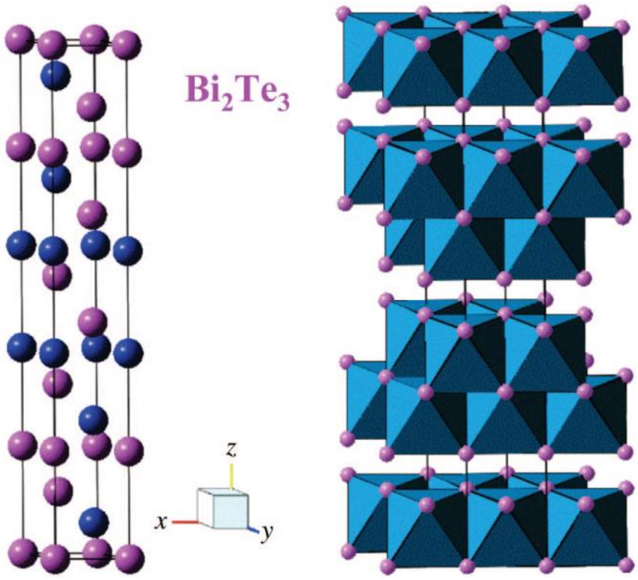

Figure 1-14: crystal structure of the state-of-the-art thermoelectric material, Bi_2Te_3.

(The blue atoms are Bi and the pink atoms are Te.) [15]

The n-type and p-type material Bi_2Te_3 was the most application in low temperature. The crystal of Bi_2Te_3 in a layer structure (Figure 1-14) with rhombohedral–hexagonal symmetry and space group $R\bar{3}m$ (D^5_{3d}). The hexagonal unit cell dimensions at room temperature were α = 3.8 Å and c = 30.5 Å. The layers stacked along the c-axis were ··· Te–Bi–Te–Bi–Te ··· Te–Bi–Te–Bi–Te ···. The Bi and Te layers were held together by strong covalent bonds, whereas the bonding between adjacent Te layers was of the van der Waals type. The optimum compositions for thermoelectric module were normally $Bi_2Te_{2.7}Se_{0.3}$ (n-type) and $Bi_{0.5}Sb_{1.5}Te_3$ (p-type) with ZT = 1 near room temperature. [15]

In the study, the experiment was conducted at room temperature, so it used compositions of $Bi_2Te_{2.7}Se_{0.3}$ and $Bi_{0.5}Sb_{1.5}Te_3$ as n-type and p-type.

1.4.3 Thermoelectric Properties of Bulk Materials:

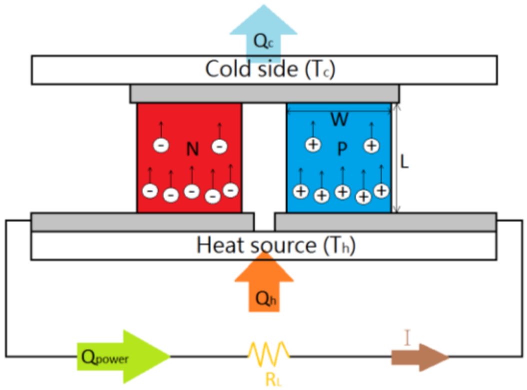

Figure 1-15: thermoelectric power generation schematic diagram

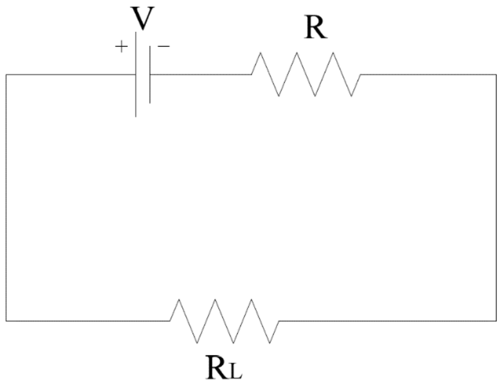

Figure 1-16: simplified circuit diagram of thermoelectric power generation

Generated voltage of a pair of bulk materials could be expressed as Eq. (1.6) for figure 1-15 and figure 1-16.

$$V = (S_p - S_n)(T_h - T_c) \qquad \text{Eq. (1.6)}$$

S_p(Seebeck coefficient of p-type material, V/ΔT)

S_n(Seebeck coefficient of n-type material, V/ΔT)

T_h(hot side temperature, K)

T_c(cold side temperature, K)

Resistance of a pair of bulk materials could be expressed as Eq. (1.7).

$$R = \frac{(\rho_p + \rho_n)L}{A} \qquad \text{Eq. (1.7)}$$

R (electric resistance, Ω)

ρ_p(electric resistivity of p-type material, Ωmm)

ρ_n(electric resistivity of n-type material, Ωmm)

L (length of bulk material, mm)

A (area of bulk material, mm^2)

Generated current of a pair of bulk materials could be expressed as Eq. (1.8).

$$I = \frac{V}{R + R_L} = \frac{(S_p - S_n)(T_h - T_c)}{R + R_L} \qquad \text{Eq. (1.8)}$$

R_L(resistance of load resistor, Ω)

Electric power of a pair of bulk materials could be expressed as Eq. (1.9).

$$p = I^2 R_L = \frac{[(S_p - S_n)(T_h - T_c)]^2 R_L}{(R + R_L)^2} \qquad \text{Eq. (1.9)}$$

p (electric power, W)

A pair of bulk materials could get the maximum power output when it had impedance matching ($R_L = R = R_p + R_n$, $R_p = \rho_p \frac{L}{W^2}$ and $R_n = \rho_n \frac{L}{W^2}$). Maximum power output could be expressed as Eq. (1.10).

$$\mathrm{P}_{max} = \frac{[(S_p - S_n)(T_h - T_c)]^2}{4R} = \frac{[(S_p - S_n)(T_h - T_c)W]^2}{4(\rho_p + \rho_n)L} \qquad \text{Eq. (1.10)}$$

P_{max}(maximum power output, W)

The thermal power flowing into hot side of a pair of bulk materials could be expressed as Eq. (1.11).

$$Q_h = (K_p + K_n)(T_h - T_c) + (S_p - S_n)IT_h - \frac{I^2R}{2} \qquad \text{Eq. (1.11)}$$

Q_h(thermal power, W)

K_p(thermal conductivity of p-type material, $K_p = \frac{\kappa_p W^2}{L}$, Wm^{-1}K^{-1})

K_n(thermal conductivity of n-type material, $K_n = \frac{\kappa_n W^2}{L}$, Wm^{-1}K^{-1})

$(S_p - S_n)IT_h$ represented the value of thermoelectric effect, $\frac{I^2R}{2}$ represented Joule heat, and $(K_p + K_n)(T_h - T_c)$ represented Fourier effect (thermal energy flowed from high temperature to low temperature).

The thermal power flowing out from cold side could be expressed as Eq. (1.12).

$$Q_c = (K_p + K_n)(T_h - T_c) + (S_p - S_n)IT_c + \frac{I^2R}{2} \qquad \text{Eq. (1.12)}$$

Q_c(thermal power, W)

According energy conservation effect, thermoelectric generator produced power of the value of Eq. (1.11) minuses Eq. (1.12). The power could be expressed as Eq. (1.13).

$$P = Q_h - Q_c = \frac{[(S_p - S_n)(T_h - T_c)]^2 R_L}{(R + R_L)^2} \qquad \text{Eq. (1.13)}$$

P (thermoelectric generator produces Power, W)

Conversion efficiency could be expressed as Eq. (1.14).

$$\eta = \frac{P}{Q_h} = \frac{T_h - T_c}{T_h} \frac{\sqrt{1 + Z(T_M)} - 1}{\sqrt{1 + Z(T_M)} + \frac{T_c}{T_h}} \qquad \text{Eq. (1.14)}$$

η (conversion efficiency, %)

T_M(the temperature between T_c and T_h, K)

Z (figure of merit, K^{-1})

V.E. Altenkirch [16] proposed the concept of figure of merit Z in 1957. Figure of Z stood for the performance of thermoelectric materials, Figure of Z could be expressed as Eq. (1.15).

$$Z = \frac{S^2\sigma}{\kappa} = \frac{S^2}{\kappa\rho} \qquad \text{Eq. (1.15)}$$

κ (thermal conductivity, W/K)

σ (electrical conductivity, Ω^{-1})

ρ (electrical resistivity, Ω)

A.F. Ioffe [17] added the temperature factor T into Eq. (1.15) that it could be expressed as Eq. (1.16). This was the most fundamental thermoelectric theory nowadays.

$$ZT = \frac{S^2\sigma}{\kappa}T = \frac{S^2}{\kappa\rho}T \qquad \text{Eq. (1.16)}$$

Conversion efficiency of cooler could be expressed as function (1.17):

$$\phi = \frac{Q_c}{W} = \frac{T_c}{T_h - T_c}\frac{\sqrt{1+Z(T_M)} - \frac{T_h}{T_c}}{\sqrt{1+Z(T_M)}+1} \qquad \text{Eq. (1.17)}$$

ϕ (conversion efficiency of cooler, %)

1.5 Thermoelectric Generator (TEG) [18]:

Thermoelectric generators (TEG) were based on the Seebeck effect of semiconductor materials to convert thermal energy to electricity directly [19] [20]. In recent years, thermoelectric technology was attracting more and more attention, mainly because of the following two aspects: one of them, there were not working fluids or other moving parts, so TE (thermoelectric device) had many good features, such as reliable operation, layout flexibility, adaptability and other characteristics [21] [22]. On the other hand, TEs did not produce secondary pollution gases such as carbon dioxide or other unfriendly polluting gases in the progress of using the daily lives' or industrial waste heat for electricity generation [23] [24].

The applications of Thermoelectric Generator currently:

The figure 1-17 and 1-18 from heat2power [25] showed TEG used in automotive exhaust pipe. The automotive exhaust pipe had a lot of thermal power (temperature different was about 500℃), that it made TEG produce electric power used for air-conditioning system or LED.

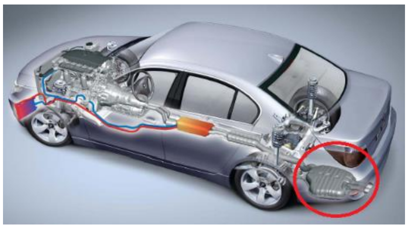

Figure 1-17: TEG used in automotive exhaust pipe schematic diagram [25]

Figure 1-18: TEG used in automotive exhaust pipe actual situation [25]

Figure 1-19: TEG used in China Steel Corporation (CSC) reheating furnace wall [26]

TEG could be applied to low grade waste heat recovery (below 500℃) and the installation capacity was flexible from a level of a few watts to several megawatts.

In response to the government carbon reduction policy to reduce industrial emissions and reuse waste heat, China Steel Corporation (CSC) had established a 200W pilot TEG on the wall of a reheating furnace. The wall surface temperature was about 130℃ and the TEG could generate electric energy from the waste heat of the reheating furnace wall basing on the thermoelectric effect. The TEG system was the first application using thermoelectric technology to recycle industrial waste heat in the country. The system was shown in the photo below. It had been running nearly two years and the power generation was stable. There were 216 thermoelectric modules installed in this 200W TEG system, with a total area of 5m^2, an average power density of 40W/m^2, and the average temperature difference was 82℃ with the average temperature of the hot and cold side of the TEG system being 115℃ and 33℃ respectively.[26]

1.6 Thermoelectric Cooler (TEC) [27]:

Thermoelectric coolers (TEC) were solid-state refrigerating devices that utilize the Peltier effect to pump heat. Thermoelectric coolers also offered the advantages of compact size, quiet operation, high reliability and exact temperature control, and thus they were widely used as refrigerating devices in many applications including military, aerospace, industrial and commercial areas. In recent years, there had been increased interest in the application of thermoelectric cooler to electronics cooling.

The applications of Thermoelectric Cooler currently:

Figure 1-20: AbsolutZero rapid beverage cooler [28]

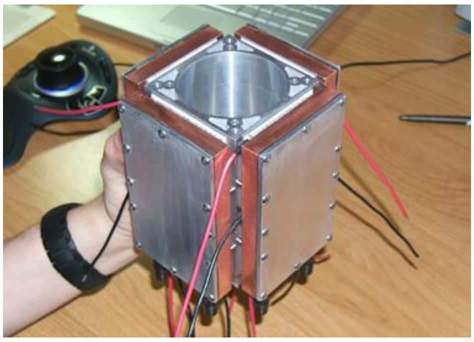

Figure 1-21: TEC cup holder [28]

AbsolutZero Rapid Beverage Cooler (Figure 1-20) was developed by Massachusetts Institute of Technology (MIT). It was a kind of application of thermoelectric cooler (TEC). AbsolutZero was using electricity to cool drinks, it even could cool drinks to 0℃. Figure 1-21 was the cup holder; it was composed with 4 pieces of TEC to assemble. This invention could be widely used in life.

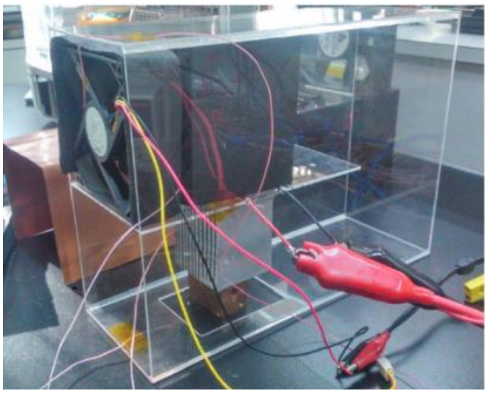

Figure 1-22: Thermoelectric Dehumidifier [29]

Thermoelectric Dehumidifier was an application of thermoelectric module from Industrial Technology Research Institute (ITRI). When the cold side temperature of the module was lower than the dew point temperature, the moisture in air would be condensed on the surface of fin, and successfully decreased the relative humidity of air.

1.7 Research purposes and question:

Because of the thermal energy increasing, it also caused the global warming. Along with the energy demand increasing, how to reuse waste thermal energy and increase the electric power was one of the important energy topics for people. The thermoelectric module (TEM) could reuse the waste thermal energy and turn to electric.

Most traditional TEM used hard ceramic for substrate, the volume was relatively restricted, and space restricts the usage. There were so many literatures about making small TEM and improving the restrictions of space that it must use sputtering and vacuum evaporation to make TEM. But the producing cost was very expensive and it was also difficult to mass production. By the way, the kind of TEM had two defects. First, the hard substrate could not be changed to meet the different needs under various circumstances. Second, the hard substrate was very fragile for its ceramic surface layer. The applications were almost used in high-temperature, it was seldom used in low-temperature. In fact, a lot of heat power had not been used effective in low-temperature. In this study, it was using human body heat power to increase the applications at low-temperature.

The study included 3 parts. First, design and producing the Basic Thermoelectric Module (BTEM) which was used for understanding how to make high efficiency module. The design was focused on the change of the structure (like the area and the thickness of copper foil…). Second, to improve the design and producing the Traditional Thermoelectric Module (TTEM) and 1st Flexible Thermoelectric Module (1st FTEM) by way of the result of the Basic Thermoelectric Module (BTEM) which was used for understanding how to make high efficiency module. The substrate of TTEM was ceramic, and the substrate of 1st is polyimide (PI). According to Eq. (1.15) $Z=S^2\sigma/\kappa$ for the different substrates of modules, power factor ($S^2\sigma$) was supposed constant. Then the relation of Z value and κ (thermal conductivity) was be inverse proportion. The ceramic had higher thermal conductivity, and the polyimide (PI) had less thermal conductivity; so it could be assumed that 1st FTEM had higher performance than TTEM. The study was verifying the assumption and comparing the generating efficiency and cooling efficiency of TTEM and 1st FTEM. That's the application of 1st FTEM to wristlet. Third, for improving the efficiency of 1st FTEM application in 1st wristlet, the study improved the 1st FTEM by design and producing 2nd FTEM, and compared the generating efficiency and cooling efficiency of 1st FTEM and 2nd FTEM. That was the application of 2nd FTEM to 2nd wristlet. The 2nd wristlet was not only using 2nd FTEM but also improving the cooler function. So the 2nd wristlet could be used for therapy usage. To take the 2nd FTEM application in clothes for warming and cooling human body could be the further development.

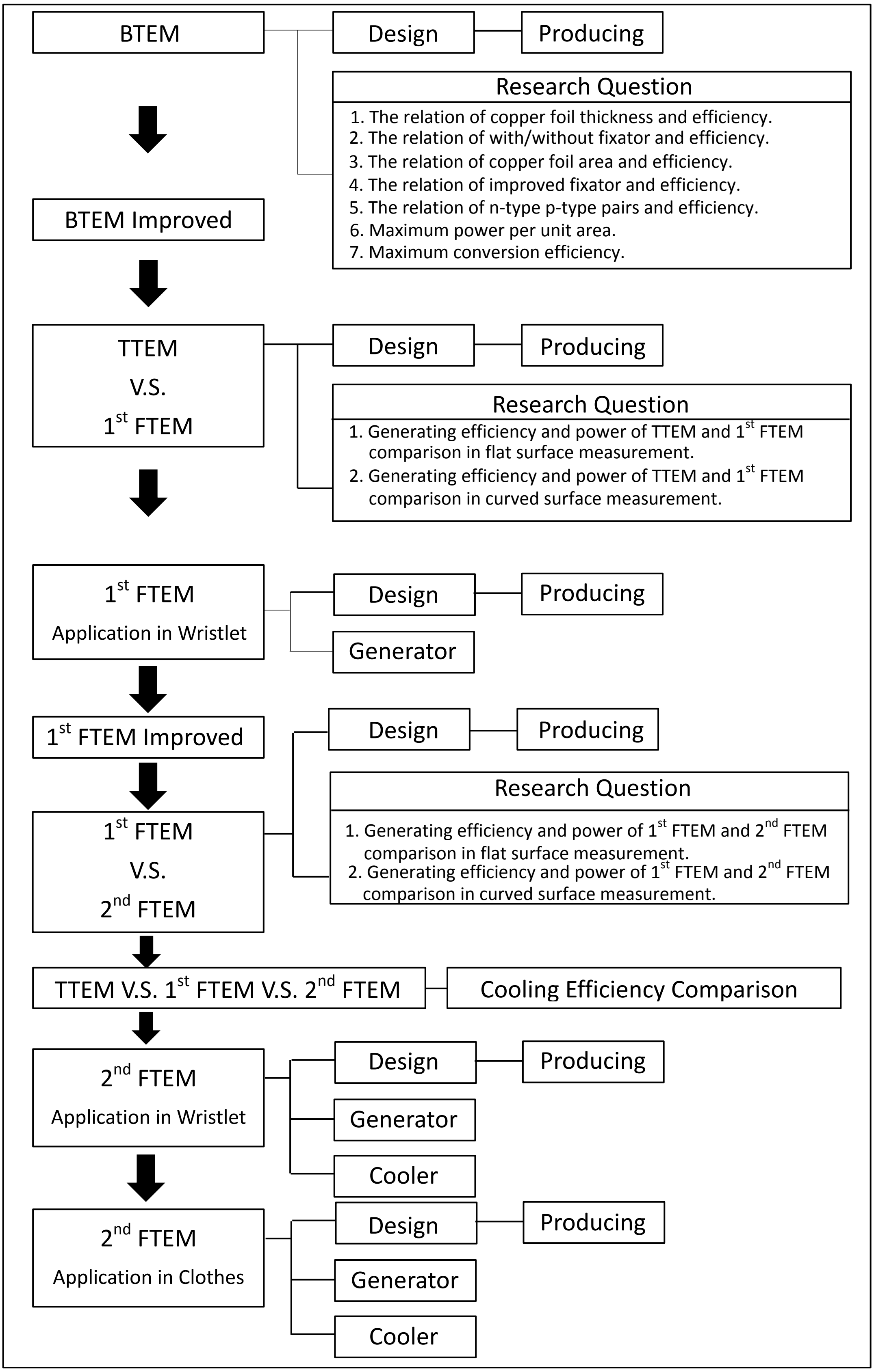

Figure 1-23: modules research history, processes and questions

1.8 Devices, Materials and Softwares:

Devices:

Table 1.3: devices

		
Precision electronics balance	Grinding	Programmable Controller Furnace
		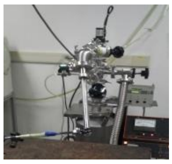
Hydraulic Machine	Water-Hydrogen Flame Machine	Vacuum Machine
		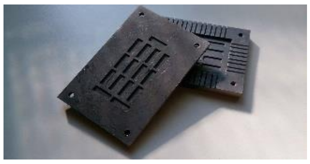
GL-800 Temperature Record	Thermostatic Water Bath	Fixator
		
Point Welding Machine	Hot Plate	Multimeter
		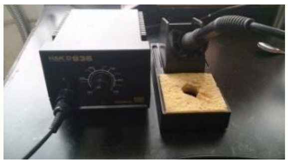
Laboratory DC Power Supply	Bulk material Cutting Machine	Welding Torch
		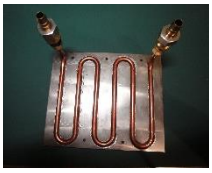
Reflow Soldering System FDS Maxi Power	Arch Cool Plate	Cool Plate
	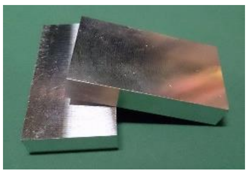	
Steel Plate	Aluminum	Thermoelectric Material testing Machine

Materials:

Table 1.4: materials

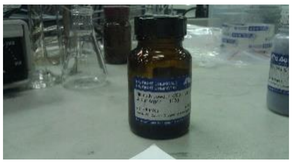		
Bismuth (Bi) (99.999%)	Stibium (Sb) (99.999%)	Selenium (Se) (99.999%)
		
Tellurium (Te) (99.999%)	N-type	P-type
	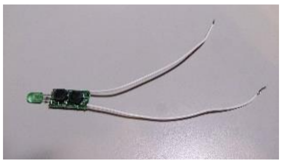	
Cotton Thread	Boost Converter Circuit	Sn/Ag/Cu Solder Paste
		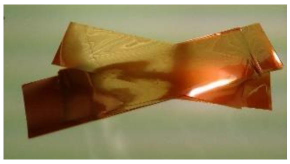
Bi/Sn Solder Paste	Thermocouple	Polyimide (PI)
		
Copper Foil	GRAPHIT 33	Ceramic Fiber

Softwares:

AutoCAD 2015:

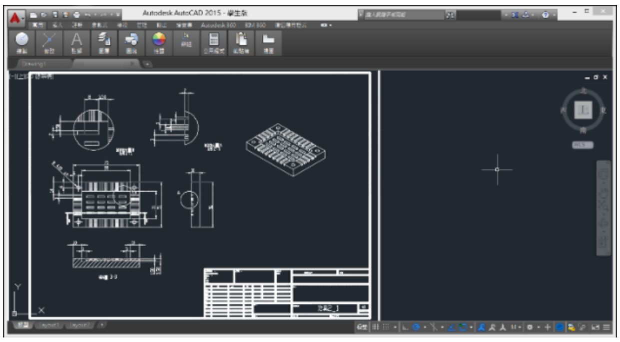

Figure 1-24: AutoCAD 2015

Chapter 2 Experimental Procedure

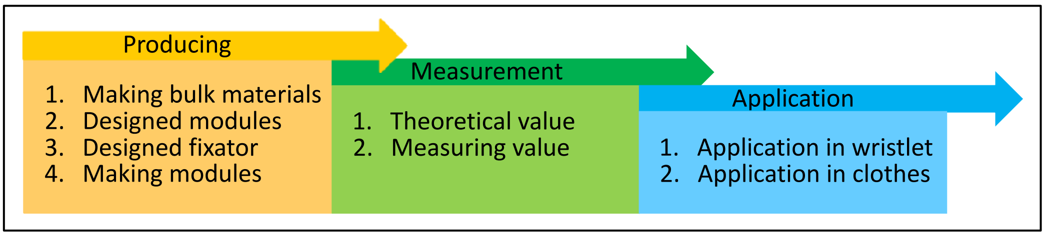

Figure 2-1: experimental procedure

2.1 Bulk Materials Making Process:

The making process was improved from "Review of Methods of Thermoelectric Materials Mass Production" [30].

Step A. Using four kinds of elements powder Bismuth (Bi), Selenium (Se), Tellurium (Te) and Antimony (Sb) to constitute N-type ($Bi_2Te_{2.7}Se_{0.3}$) and P-type ($Bi_{0.5}Sb_{1.5}Te_3$). N-type and P-type play in two difference quartz tubes.

Step B. Quartz tube was evacuated vacuum machine. (Figure 2-2)

Step C. Quartz plugged in the quartz tube and hydrogen flame melt let Quartz tube keep vacuum. (Figure 2-3)

Step D. The quartz tube put in Programmable Controller Furnace, and heated for 48 hours at 850℃. (Figure 2-4)

Step E. Cooling to 550℃ for 4 days.

Step F. Cooling to room temperature for 1 day.

Step G. The bulk material was ground into powder. (Figure 2-5)

Step H. Step A to Step G was repeated for three times. (Purified material)

Step I. Taking some powder to confirm crystal structure with X-Ray Diffraction (XRD).

Step J. Pressing the bulk material to 2.4mm thickness with hydraulic machine, and the lower end and the upper end of material gold-plated. (Figure 2-6)

Step K. Cutting bulk material became (3 X 3) mm^2 areas with bulk material cutting machine. (Bulk material size: 3mm x 3mm x 2.4mm)

Actual production status:

Figure 2-2: Step B

Figure 2-3: Step C

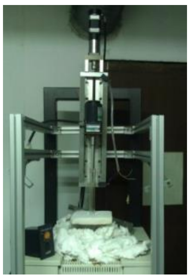

Figure 2-4: Step D

Figure 2-5: Step G

Figure 2-6: Step J

Actual production status process of Step J and step K:

Figure 2-7: cleaning

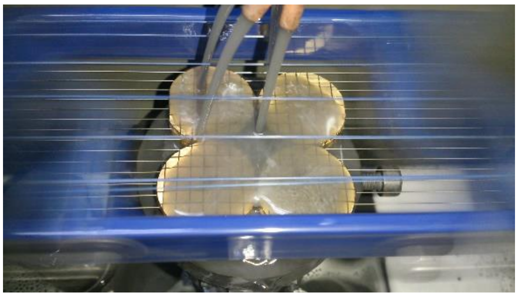

Figure 2-8: cutting

Figure 2-9: dried material

Figure 2-10: picked out the complete bulk material

2.2 Bulk Material (n-type and p-type) Performance:

Figure of Merit ZT:

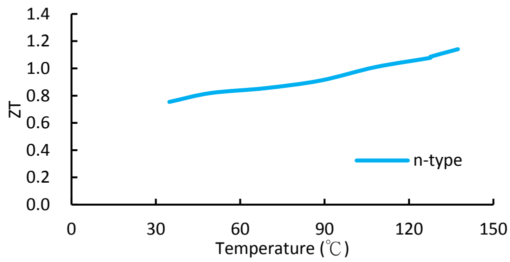

Figure 2-11: ZT of n-type

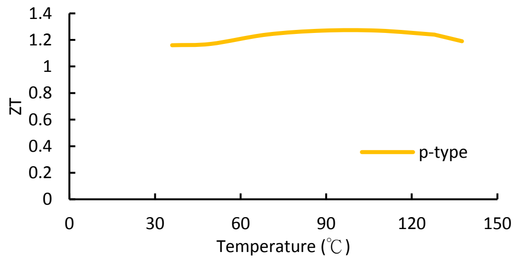

Figure 2-12: ZT of p-type

The ZT of n-type (Figure 2-11) was proportion to the temperature. The ZT of p-type (Figure 2-12) had maximum value at about 100℃.

X-Ray Diffraction (XRD):

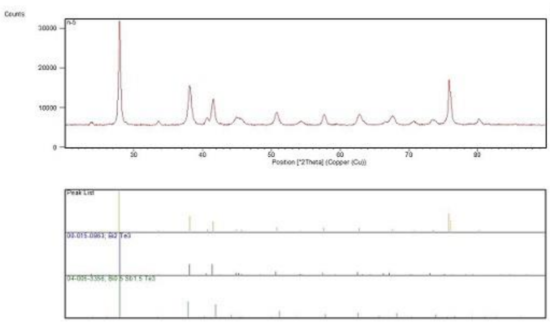

Figure 2-13: n-type powder XRD pattern

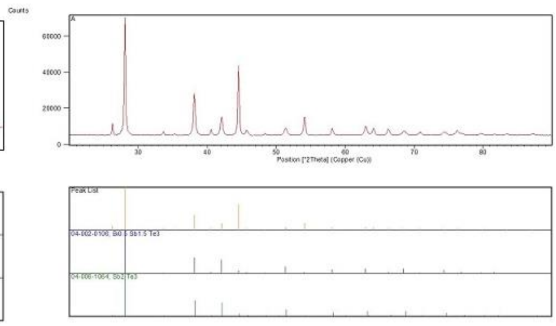

Figure 2-14: p-type powder XRD pattern

Scanning Electron Microscope (SEM):

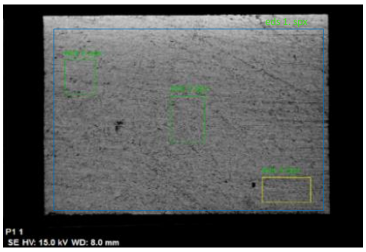

Figure 2-15: p-type-1

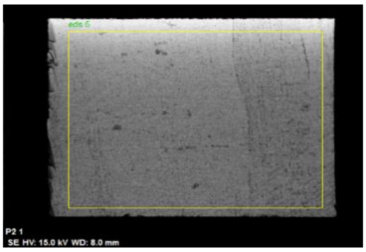

Figure 2-16: p-type-2

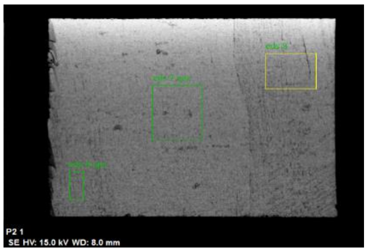

Figure 2-17: p-type-3

Table 2.1: the results of p-type and n-type in SEM

p-type								n-type			
eds	Bi (%)	Sb (%)	Te (%)	eds	Bi (%)	Sb (%)	Te (%)	eds	Bi (%)	Te (%)	Se (%)
1	20.00	34.85	45.15	5	20.01	34.83	45.16	9	53.15	43.81	3.04
2	19.93	34.85	45.22	6	19.95	34.87	45.18	10	53.15	43.82	3.03
3	19.96	34.83	45.21	7	19.96	34.85	45.19	11	53.16	43.81	3.03
4	20.04	34.85	45.11	8	20.02	34.83	45.15				

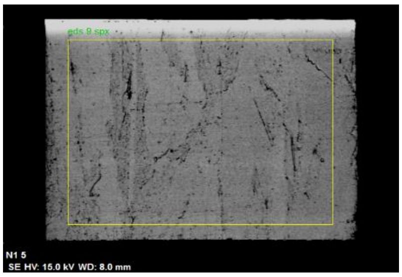

Figure 2-18: n-type-1

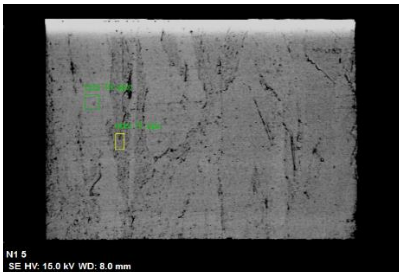

Figure 2-19: n-type-2

The materials of n-type and p-type were Bi_2Te_3 combination. There was almost no significant variation for the components of n-type and p-type materials.

2.3 Modules Making process:

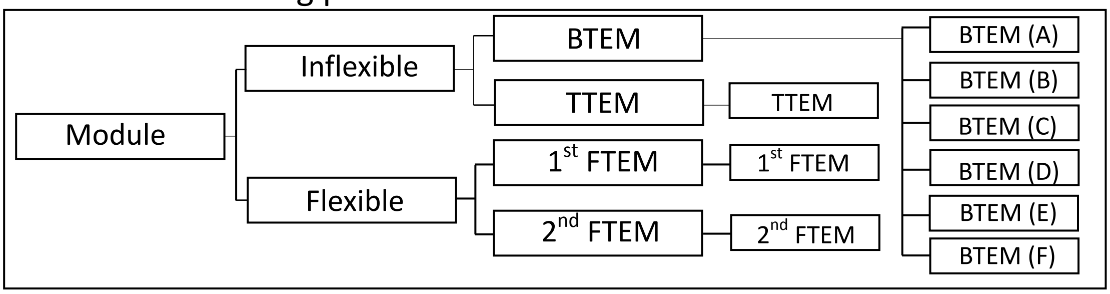

Figure 2-20: Module types

There were three ways to make modules in this project. The BTEM was improved the flexibility on TTEM. Because of the efficiency of the BTEM was not good enough, the 1st FTEM was improved with all the shortcomings. Besides, it also could be apply to the human clothing, for body cooling or warming.

2.3.1 Basic Thermoelectric Module (BTEM):

Table 2.2: BTEM menu

Module	Size	Further Explanation
BTEM (A)	80mm x 42mm x 4.5mm	1. 15 Pairs N-type P-type 2. Copper Foil Size: (1mm x 5mm x 16mm)
BTEM (B)	80mm x 42mm x 6.5mm	1. 15 Pairs N-type P-type 2. Copper Foil Size: (2mm x 5mm x 16mm)
BTEM (C)	80mm x 42mm x 4.5mm	1. Without Fixator 2. 15 Pairs N-type P-type 3. Copper Foil Size: (1mm x 5mm x 16mm)
BTEM (D)	55mm x 31mm x 4.5mm	1. 15 Pairs N-type P-type 2. Copper Foil Size: (1mm x 3mm x 9mm)
BTEM (E)	55mm x 31mm x 4.5mm	1. 15 Pairs N-type P-type 2. Copper Foil Size: (1mm x 3mm x 9mm) 3. Improved Fixator
BTEM (F)	99mm x 47mm x 4.5mm	1. 63 Pairs N-type P-type 2. Copper Foil Size: (1mm x 3mm x 9mm)

Although all of BTEM made roughly the same, BTEM (C) making without fixator and BTEM (E) making used the improve fixator.

Table 2.3: before improved and after improved fixator

<table>
<tr><th></th><th></th><th>Finished product</th><th>Design</th><th>Schematic</th></tr>
<tr><td rowspan="2">Before Improve</td><td>Lower end</td><td></td><td>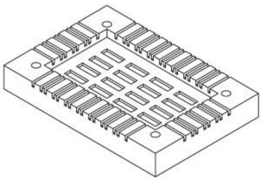</td><td rowspan="2">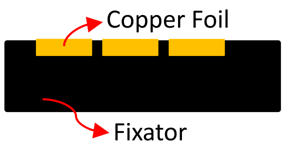
</td></tr>
<tr><td>Upper end</td><td></td><td>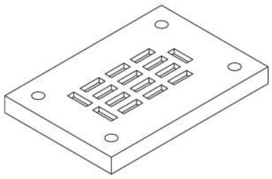</td></tr>
<tr><td rowspan="2">After Improve</td><td>Lower end</td><td></td><td>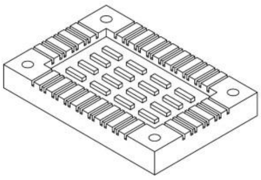</td><td rowspan="2">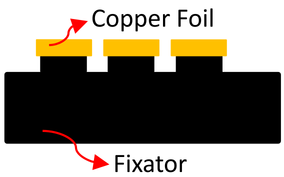
</td></tr>
<tr><td>Upper end</td><td></td><td>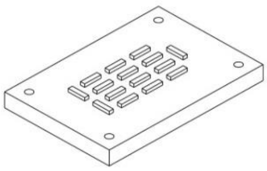</td></tr>
</table>

Fixator:

Table 2.4: fixator menu

BTEM (A)		
	Lower end	Upper end
Finished product		
Design	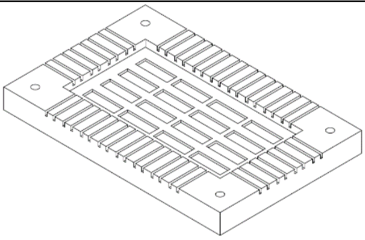	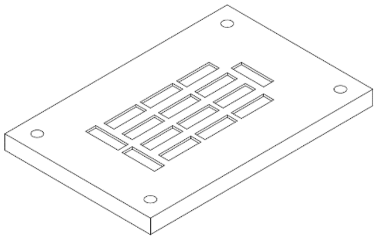
	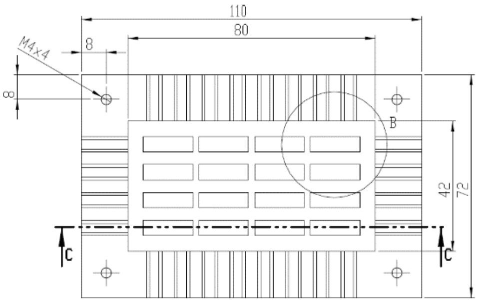	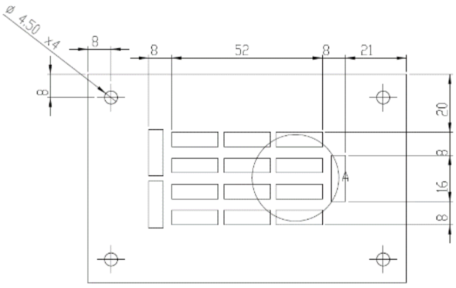
BTEM (B)		
	Lower end	Upper end
Finished product		
Design	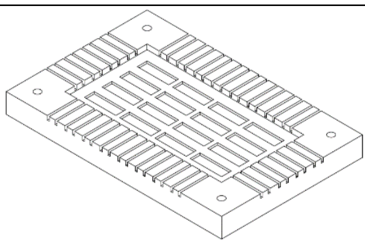	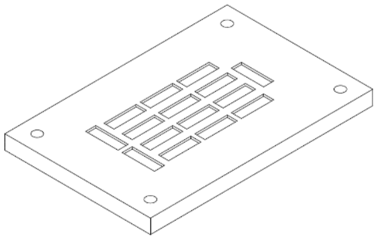
	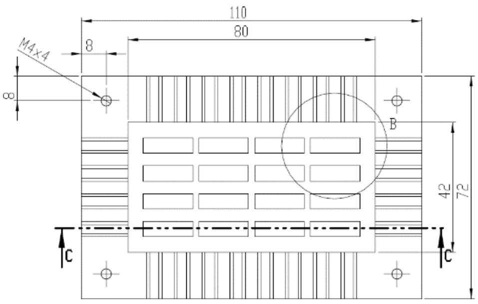	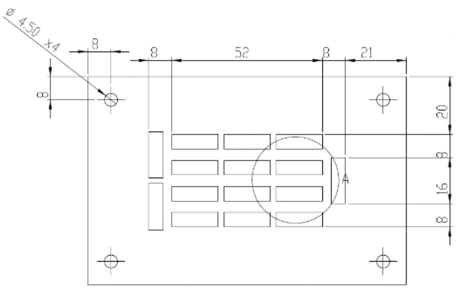

<table>
<tr><th colspan="3">BTEM (D)</th></tr>
<tr><th></th><th>Lower end</th><th>Upper end</th></tr>
<tr><td>Finished product</td><td></td><td></td></tr>
<tr><td rowspan="2">Design</td><td>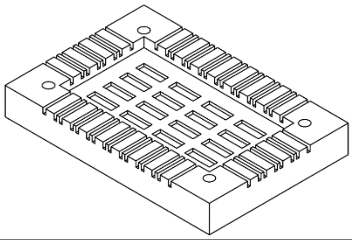</td><td>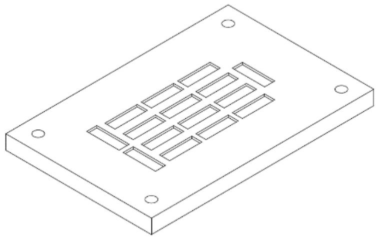</td></tr>
<tr><td>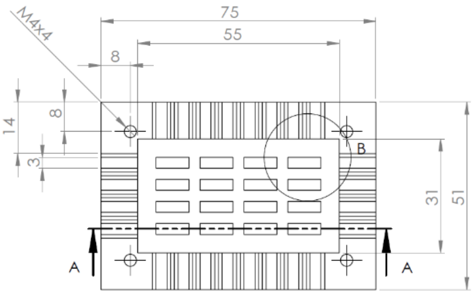
</td><td>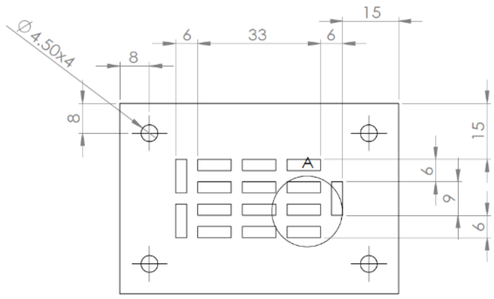
</td></tr>
</table>

<table>
<tr><th colspan="3">BTEM (E)</th></tr>
<tr><th></th><th>Lower end</th><th>Upper end</th></tr>
<tr><td>Finished product</td><td>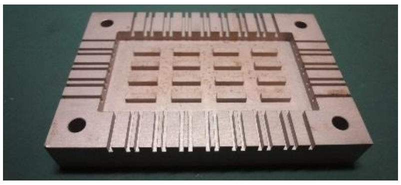</td><td>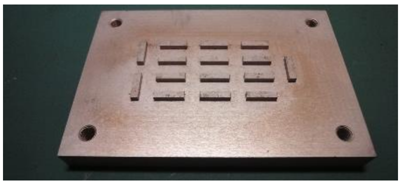</td></tr>
<tr><td rowspan="2">Design</td><td>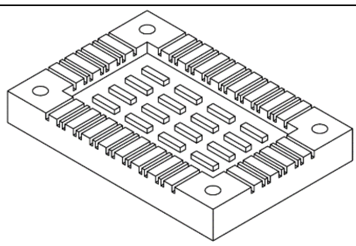</td><td>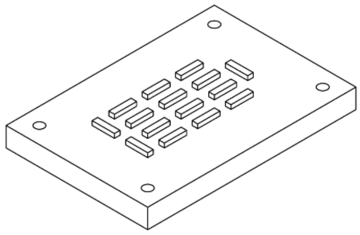</td></tr>
<tr><td>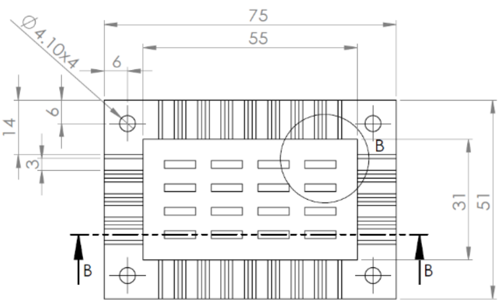
</td><td>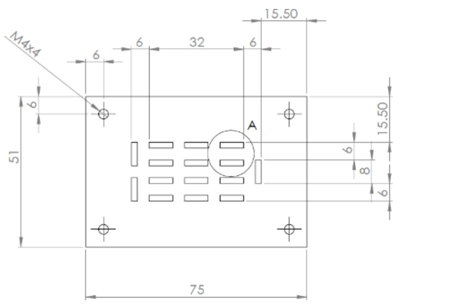
</td></tr>
</table>

BTEM (F)		
	Lower end	Upper end
Finished product		
Design	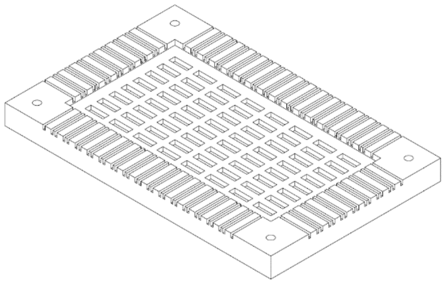	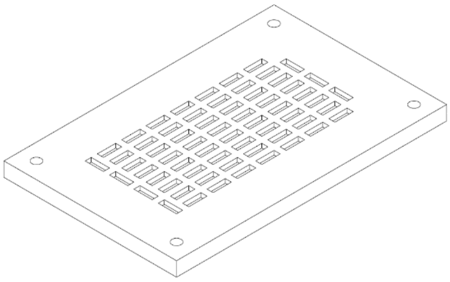
	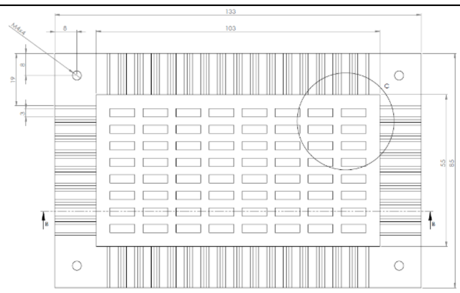	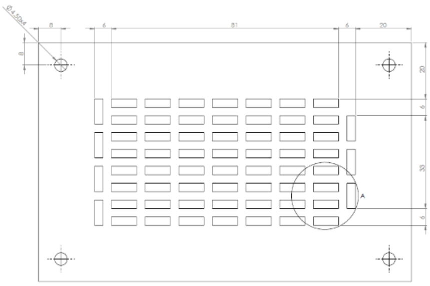

BTEM (A), (B) and (C) design surface:

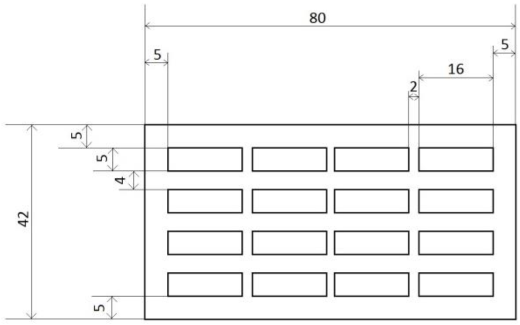

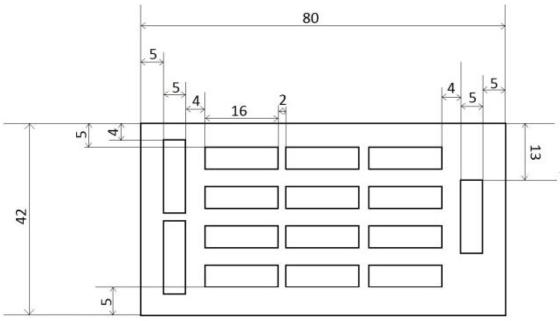

Figure 2-21: lower end design surface (Unit: mm) Figure 2-22: upper end design surface (Unit: mm)

BTEM (D) and (E) design surface:

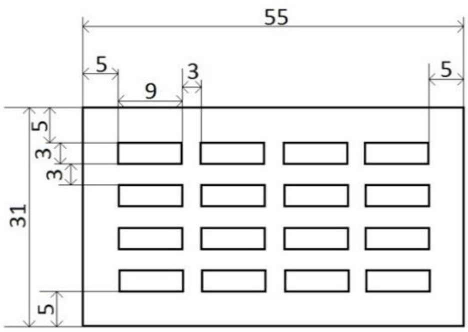

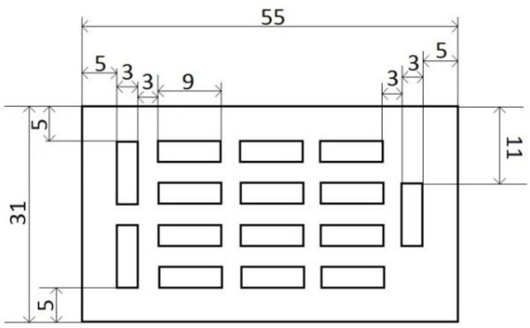

Figure 2-23: lower end design surface (Unit: mm) Figure 2-24: upper end design surface (Unit: mm)

BTEM (F) Design Surface:

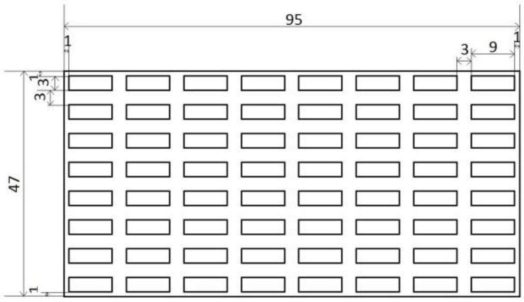

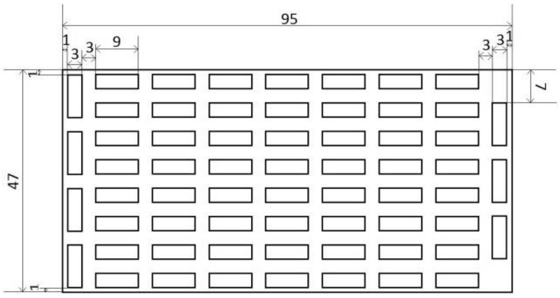

Figure 2-25: lower end design surface (Unit: mm) Figure 2-26: upper end design surface (Unit: mm)

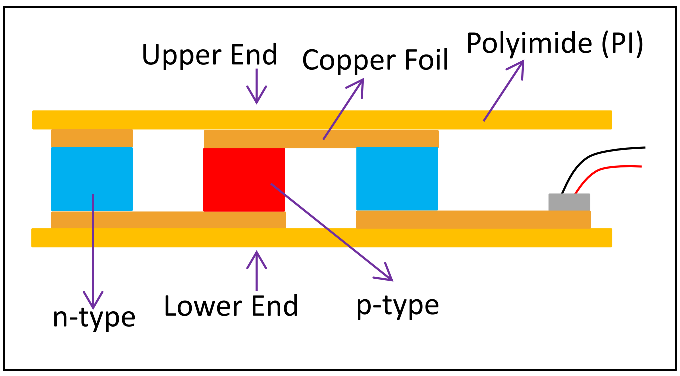

Figure 2-27: side face schematic

2.3.1.1 BTEM (A), (B), (D), (E) and (F) making process:

Step 1. To spray GRAFIT 33 on all fixators.

Step 2. To place the copper foils in the lower fixator. (Figure 2-28)

Step 3. To web the cotton threads around the fixator. (Figure 2-29)

Step 4. To make the Sn/Ag/Cu solder paste and to stick it on n-type and p-type. (figure 2-30)

Step 5. To place the n-type and p-type in the fixator. (Figure 2-31)

Step 6. To lock up the upper and lower of fixator with screws, and to heat it on the hot plate at 250℃ for 10 minutes. And then, to cool it down to room temperature and opened it.

Step 7. To place the copper foils in the upper fixator.

Step 8. To make the Bi/Sn solder pasting and to stick it on another side of n-type and p-type. (Figure 2-32)

Step 9. To lock up the upper and lower of fixator with screws, and heated it on the hot plate at 230℃ for 20 minutes. And then, cooled it down to room temperature and open it. (Figure 2-33)

Step 10. To use multimeter to test whether conductive or not.

Step 11. To weld wires on the circuit.

Step 12. To make the superglue pasting the polyimide (PI) on the circuit.

Step 13. To heat the module on hot plate at 100℃ for 10 minutes.

Step 14. After 10 minutes, to cool it down to room temperature.

Actual production status:

Figure 2-28: Step 2

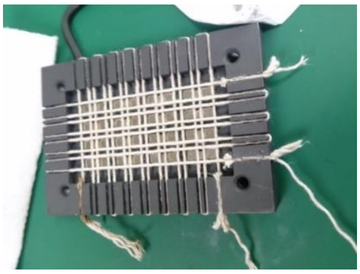

Figure 2-29: Step 3

Figure 2-30: Step 4

Figure 2-31: Step 5

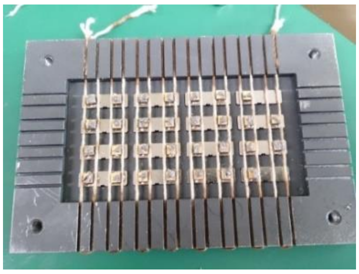

Figure 2-32: Step 8

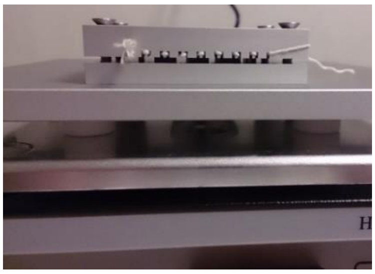

Figure 2-33: Step 9

2.3.1.2 BTEM (C) Making Process:

Step (1). To paste Sn/Ag/Cu solder pasting on the copper foils. (Figure 2-34)

Step (2). To place the copper foils on the hot plate.

Step (3). To place the n-type and p-type on the copper foils. (Figure 2-35)

Step (4). To heat them on hot plate at 245℃ for 10 minutes. After 10 minutes, to cool to room temperature. (Figure 2-36)

Step (5). To paste Bi/Sn solder on the upper n-type and p-type.

Step (6). To place the copper foils on the upper n-type and p-type.

Step (7). To heat them on the hot plate at 225℃ for 20 minutes. After 20 minutes, to cool to room temperature.

Step (8). To use multimeter to test whether conductive.

Step (9). To make the superglue paste the polyimide (PI) on the circuit.

Step (10). To heat the module on hot plate at 100℃ for 10 minutes.

Step (11). After 10 minutes, to cool to room temperature. (Figure 2-37)

Actual production status:

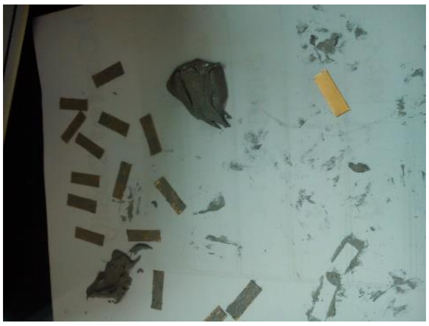

Figure 2-34: Step (1)

Figure 2-35: Step (3)

Figure 2-36: Step (4)

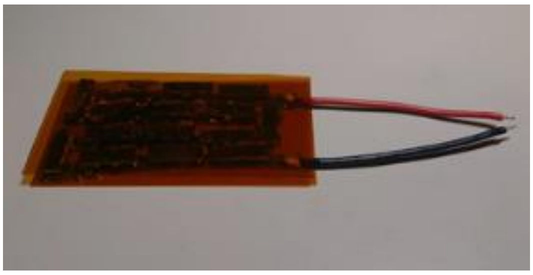

Figure 2-37: Step (11)

2.3.2 Traditional Module (TTEM) and 1st Flexible Module (1st FTEM):

The size of traditional module (TTEM) was the same as the 1st flexible module (1st FTEM), and the making process was also the same. The substrate of TTEM was using ceramic. The substrate of 1st FTEM module was using 2L FCCL. The 1st FTEM was improving the TTEM (TTEM was inflexible but FTEM was flexible). And the power of FTEM was increased.

Table 2.5: TTEM and 1st FTEM menu

Module	Size	Further descriptions
TTEM, 1st FTEM	40mm x 40mm x 2.6mm	1. 17 Pairs N-type P-type 2. Copper Foil Area: (3mm x 9mm)

Table 2.6: fixator

	Finished product	Design	Schematic
Lower end	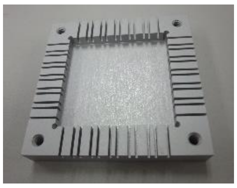	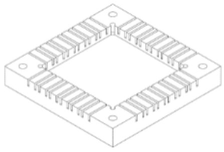	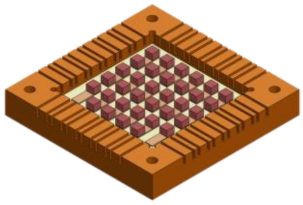
Upper end		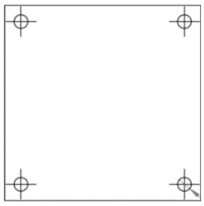	

TTEM and 1st FTEM design surface:

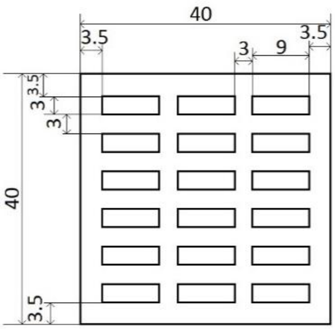

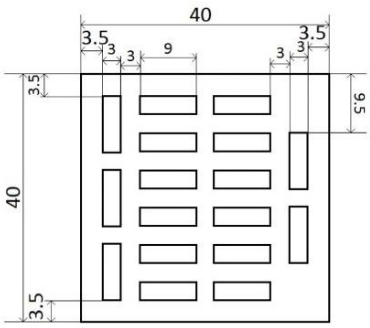

Figure 2-38: lower end design surface (Unit: mm) Figure 2-39: upper end design surface (Unit: mm)

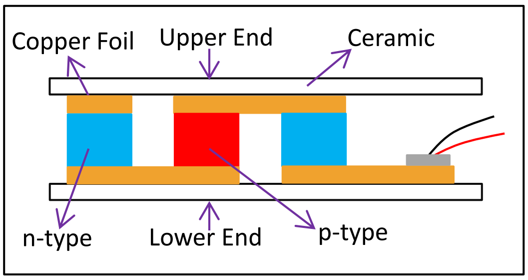

Figure 2-40: side face schematic of TTEM

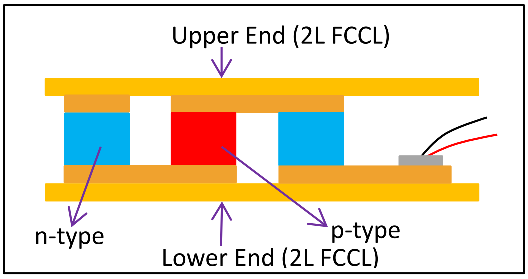

Figure 2-41: side face schematic of 1st FTEM

2.3.2.1 TTEM and 1st FTEM Making Process:

Step (A). To place some Sn/Ag/Cu solder to past on steel plate and to use solder paste to fill the holes of steel plate.(Figure 2-42, Figure 2-43)

Step (B). To place the substrate (2L FCCL or ceramic) in the fixator.

Step (C). To web the cotton threads around the fixator.

Step (D). To place the bulk materials (n-type and p-type) on the substrate, and to place the substrate on bulk materials. (Figure 2-44, Figure 2-45)

Step (E). To heat them with Reflow Soldering System FDS Maxi Power.

Step (F). To cool the module down to room temperature.

Actual production status:

Figure 2-42: Step (A)-1

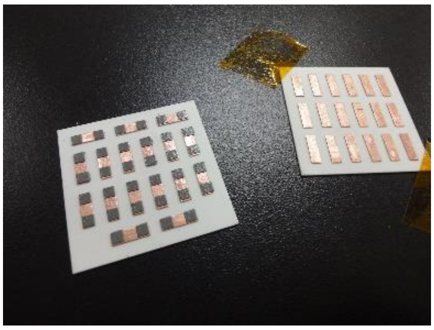

Figure 2-43: Step (A)-2

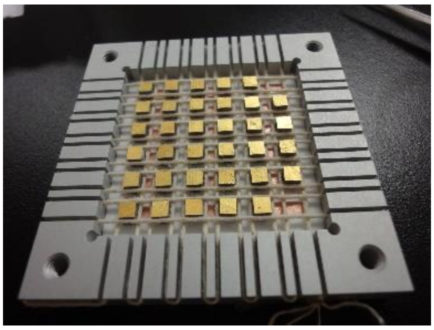

Figure 2-44: Step (D)-1

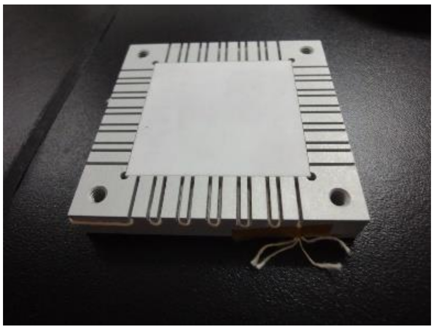

Figure 2-45: Step (D)-2

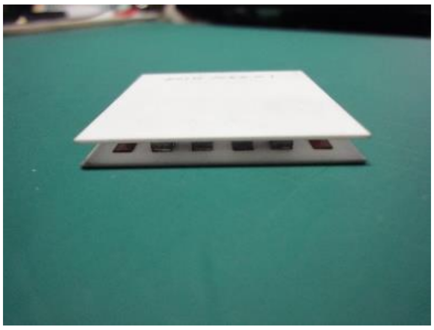

Figure 2-46: TTEM

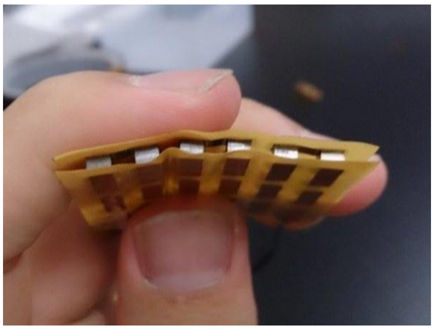

Figure 2-47: 1st FTEM

2.3.3 2nd Flexible Module (2nd FTEM):

2nd FTEM improved the substrate 2L FCCL of 1st FTEM to the substrate 3L FCCL of 2nd FTEM. The 2L FCCL had a layer of copper foil and a layer of polyimide, and the 3L FCCL had two layers of copper foil and layer of polyimide. The polyimide as between the two layers of copper foil. 2nd FTEM also improved the pairs of n-type p-type and improved the distance between n-type and p-type. And the middle of copper foil area was improved from 3mm x 3mm to 2mm x 1mm that it could make the flexible ability better. The making process of 2nd FTEM was the same as 1st FTEM.

Table 2.7: 2nd FTEM menu

Module	Size	Further descriptions
2nd FTEM	40mm x 40mm x 2.6mm	1. 31 Pairs N-type P-type 2. Copper Foil Area: (2 x 9mm^2 + 2mm^2)

Table 2.8: fixator

	Finished product	Design
Lower end	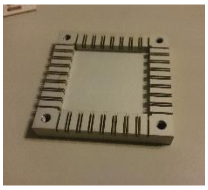	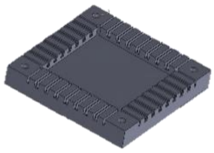
Upper end		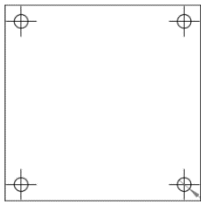

2nd FTEM design surface:

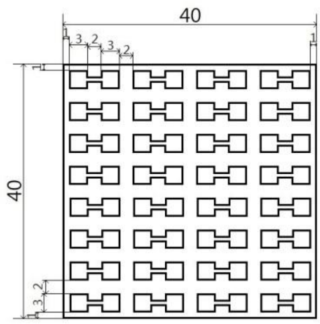

Figure 2-48: lower end design surface (Unit: mm)

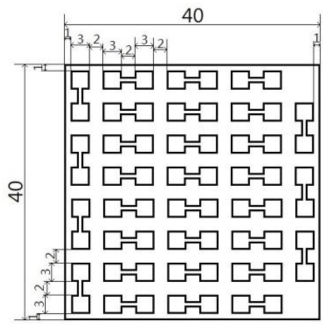

Figure 2-49: upper end design surface (Unit: mm)

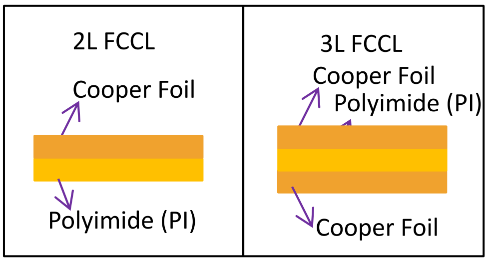

Figure 2-50: substrate 2L and 3L FCCL materials

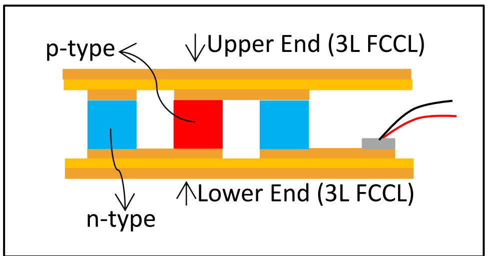

Figure 2-51: side face schematic (2nd FTEM)

2.3.2.1 2^{nd} FTEM Making Process:

Step (A). To place some Sn/Ag/Cu solder to paste steel plate and to use older paste to fill the holes of steel plate.(Figure 2-52)

Step (B). To place the substrate (3L FCCL) in the fixator. (Figure 2-53)

Step (C). To web the cotton threads around the fixator. (Figure 2-54)

Step (D). To place the bulk materials (n-type and p-type) on the substrate, and to place the substrate on bulk materials. (Figure2-55)

Step (E). To heat them with Reflow Soldering System FDS Maxi Power.

Step (F). To cool the module down to room temperature.

Actual production status:

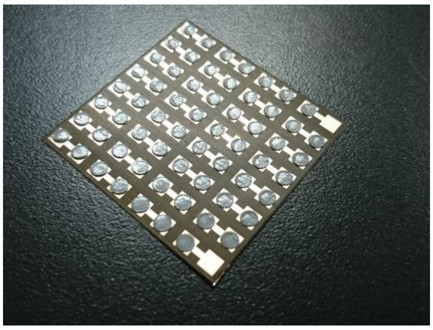

Figure 2-52: Step (A)

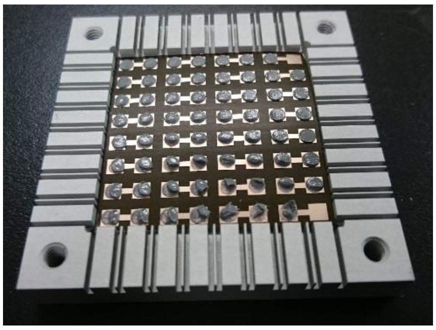

Figure 2-53: Step (B)

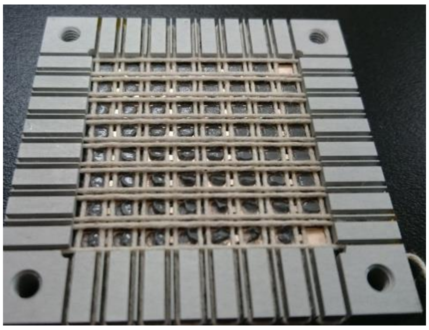

Figure 2-54: Step (C)

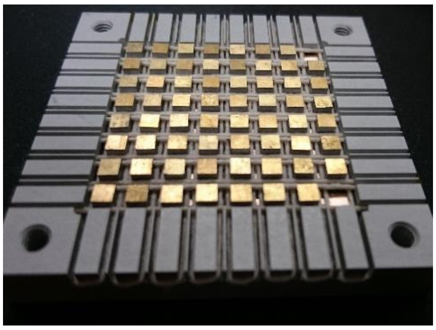

Figure 2-55: Step (D)-

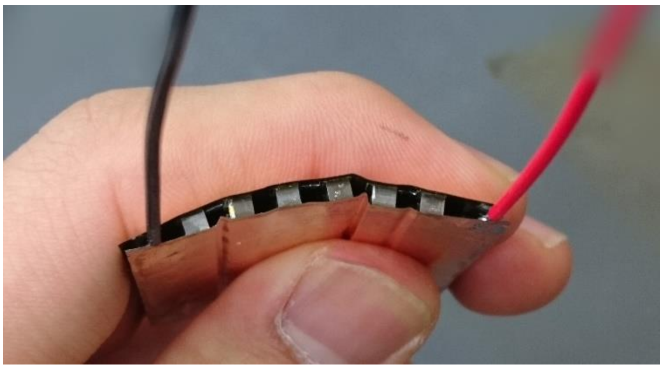

Figure 2-56: 2^{nd} FTEM

2.4 1st Wristlet:

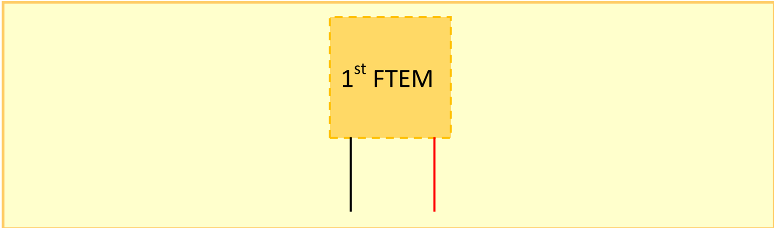

Figure 2-57: upper side of wristlet schematic

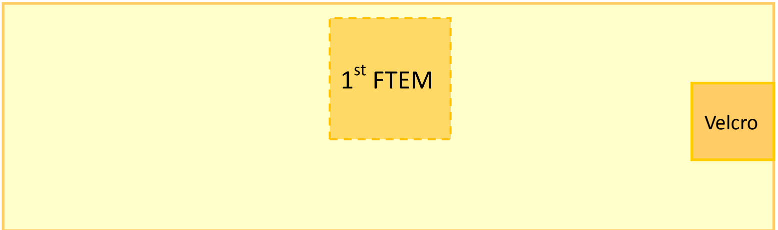

Figure 2-58: lower side of wristlet schematic

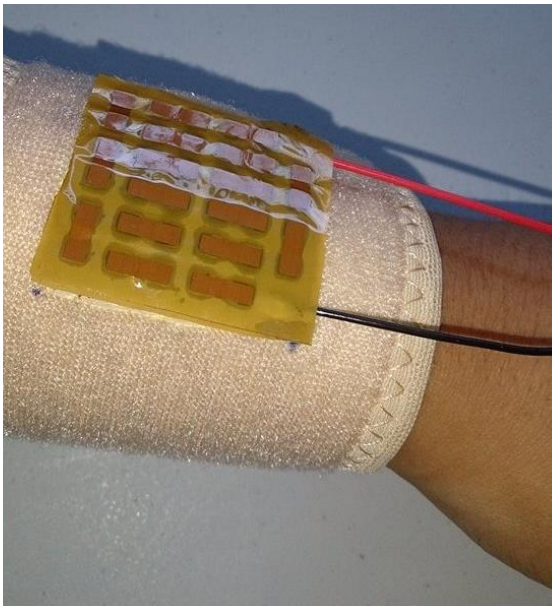

Figure 2-59: flexible module application in wristlet finished product

That was the application of 1st FTEM to wristlet. The wristlet was based on Seebeck effect to convert thermal energy to electricity directly.

2.5 2nd Wristlet:

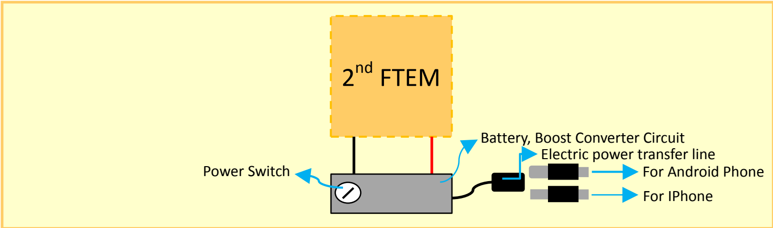

Figure 2-60: upper side of wristlet schematic

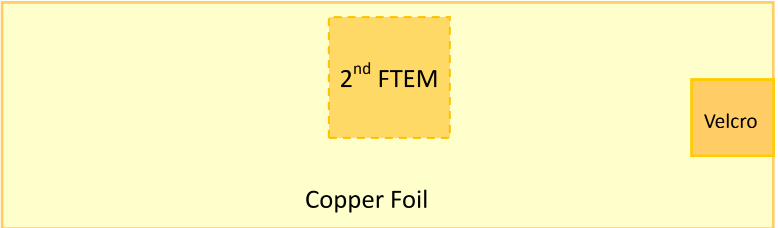

Figure 2-61: lower side of wristlet schematic

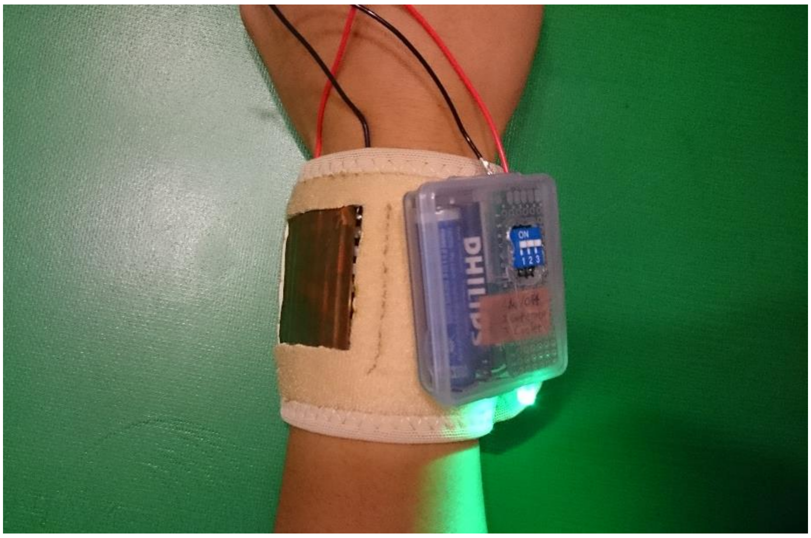

Figure 2-62: 2nd FTEM application in wristlet finished product

For raising the efficiency of 1st wristlet, the study improved 1st wristlet by increasing the copper foil area of 2nd wristlet inside and using 2nd FTEM. Increasing the copper foil area of 2nd wristlet inside could catch more thermal energy from human body that it could produce more electric energy for the cellphone or similar devices. And 2nd wristlet even improved the heater and cooler functions that could adjust temperature by power switch.

2.6 Application on Clothes for Body Warming up, Cooling down and for Battery Charging:

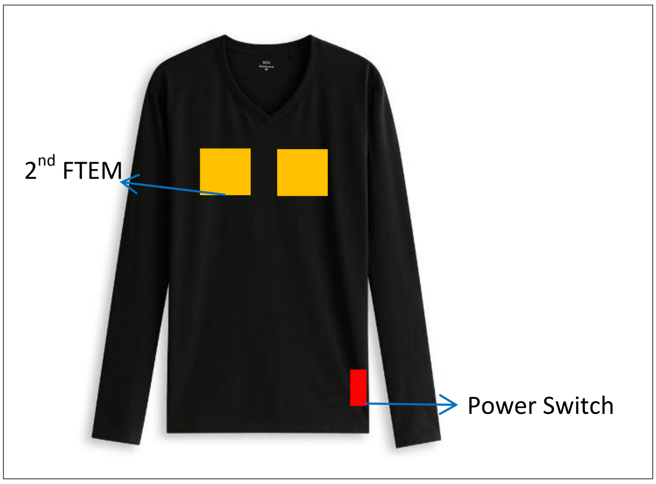

Figure 2-63: application on clothes schematic

Figure 2-64: finished product of application on clothes

It was the application of 2nd FTEM on clothes. It could keep body cool in summer, and keep body warm in winter. It could generate electric power to charge cellphones for example.

2.7 Measurement and BTEM Research Question:

2.7.1 Measurement:

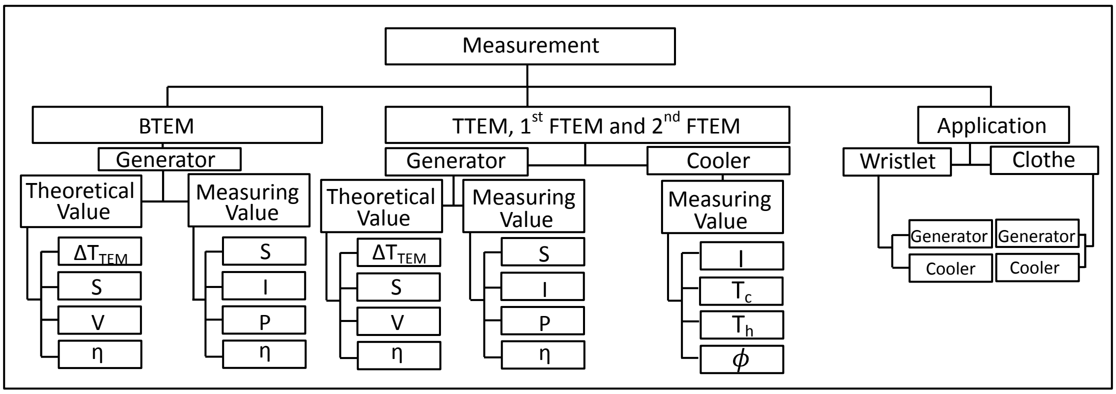

Figure2-65: Measuring Ways

Measuring Method:

1. Control variables:

   Cold side temperature (T_c): 22℃ (room temperature)

2. Independent variables:

   Hot side temperature (T_h):

   37℃ (human body temperature), 45℃ (the temperature of the bath water)

The setting of the study was using for imitating the realities of the situation effectively.

2.9.1 BTEM Research Question:

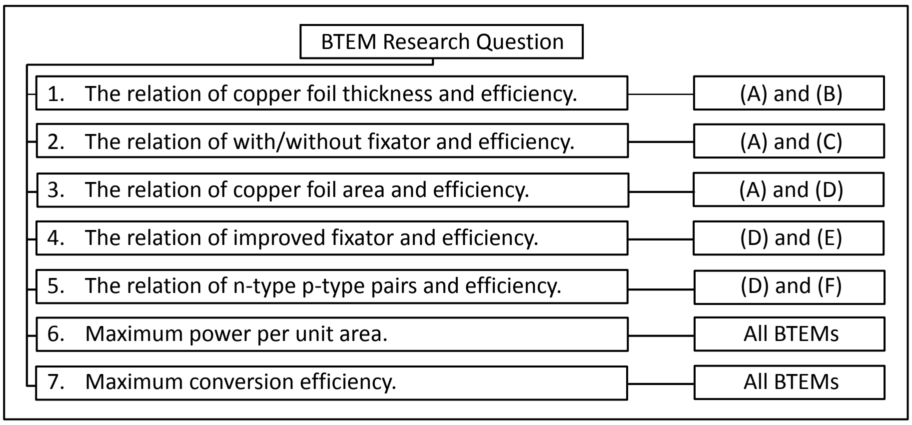

Figure 2-66: BTEM research question

In BTEM measurement that compared the theoretical value and measuring value in flat surface measurement of the questions (figure 2-65). It could understand how to make a high generating efficiency thermoelectric module by the study of BTEM.

2.8 Generating Measurement:

2.8.1 Theoretical Value:

In fact, a pair n-type p-type was crucial to a TEM generating electric energy. For assumed the practical temperature difference, the study used the equation of thermal resistivity to get the practical temperature difference.

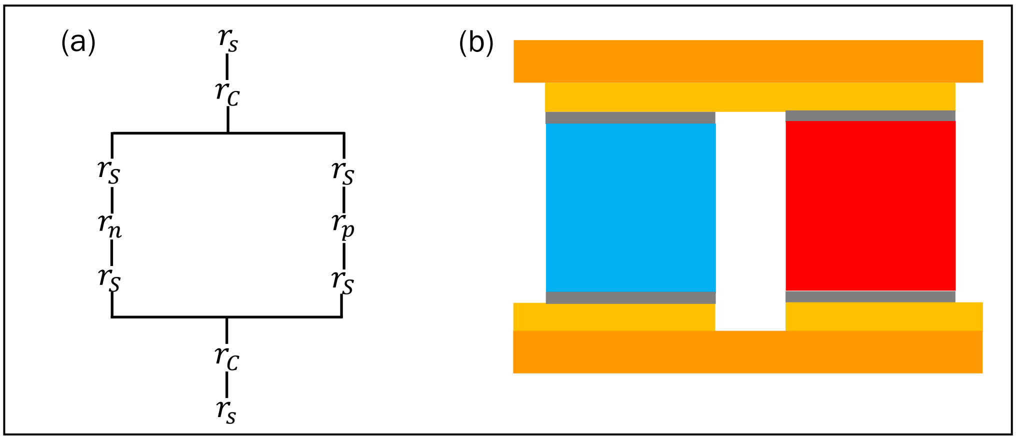

Figure 2-67: (a) a pair n-type p-type of TEM thermal resistivity schematic

(b) a pair n-type p-type of TEM schematic

The practical temperature difference could be expressed as Eq. (2.1).

$$\Delta T_{TEM} = (T_h - T_c) - [\frac{\frac{4r_S{}^2}{4r_S}\times(T_h - T_c)}{2(r_s + r_C) + \frac{4r_S{}^2}{4r_S}}] \qquad \text{Eq. (2.1)}$$

ΔT_{TEM} (practical temperature difference, K)

r_S (thermal resistivity of solder, KW^{-1})

r_s (thermal resistivity of substrate, KW^{-1})

r_C (thermal resistivity of copper foil, KW^{-1})

The definition of thermal resistivity could be expressed as Eq. (2.2).

$$r = \frac{L}{A\kappa} \qquad \text{Eq. (2.2)}$$

r (thermal resistivity, KW^{-1})

L (length, m)

A (touch area, m^2)

κ (thermal conductivity, $Wm^{-1}K^{-1}$)

The practical TEM generator electric energy could be expressed as Eq. (2.3).

$$V = (S_p - S_n) \times \Delta T_{TEM} \qquad \text{Eq. (2.3)}$$

S_p(Seebeck coefficient of p-type, V/ΔT)

S_n(Seebeck coefficient of n-type, V/ΔT)

2.8.2 Flat surface measurement:

The system was using for understanding the performance of modules (TTEM, 1st FTEM and 2nd FTEM) in flat surface measurement which simulated application in wall, ground, table… It could assume the system in conservation of energy that the system was covered the ceramic fiber up.

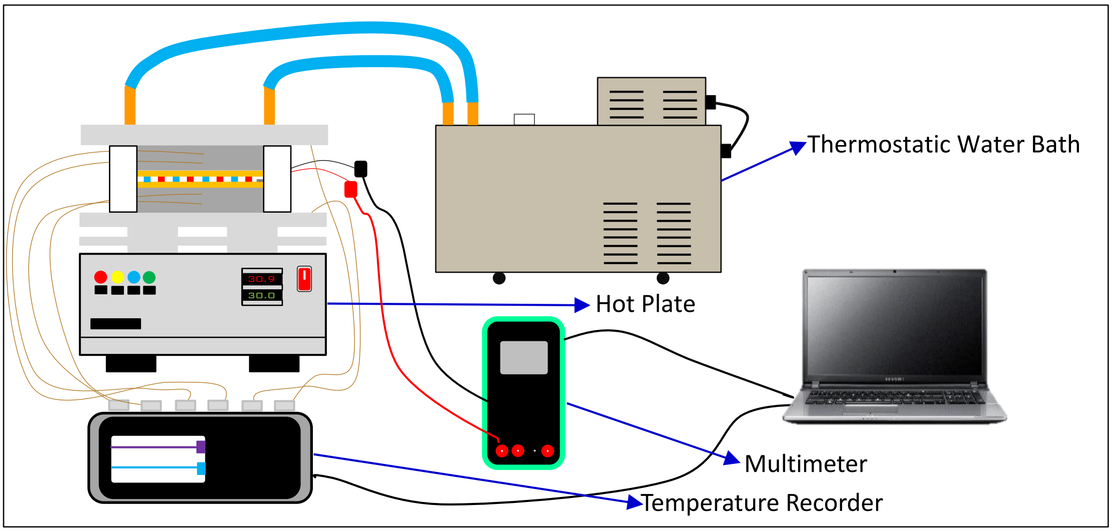

Figure 2-68: schematic of flat surface measurement system

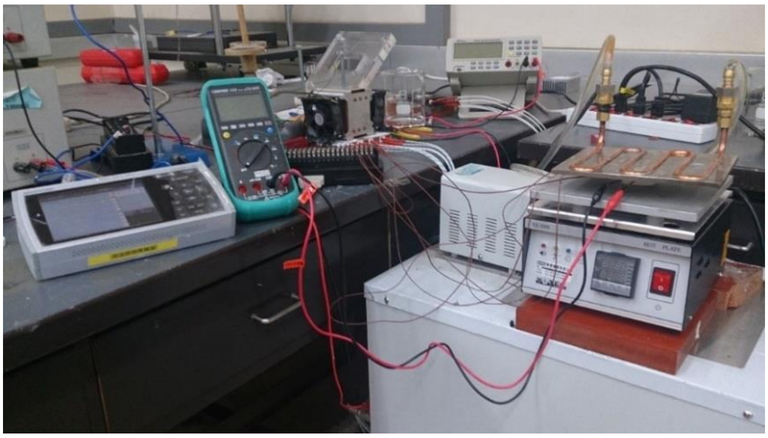

Figure 2-69: finished product of flat surface measurement system

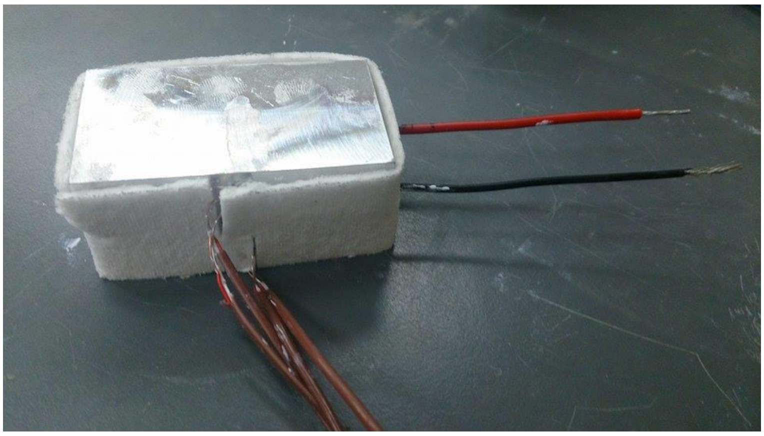

Figure 2-70: finished product of flat surface measurement system

2.8.3 Curved surface measurement:

The system was using for understanding the performance of modules (1st FTEM and 2nd FTEM) in curved surface measurement which simulated application in water pipe, air conditioner, human body... It could assume the system in conservation of energy that the system was covered the ceramic fiber up.

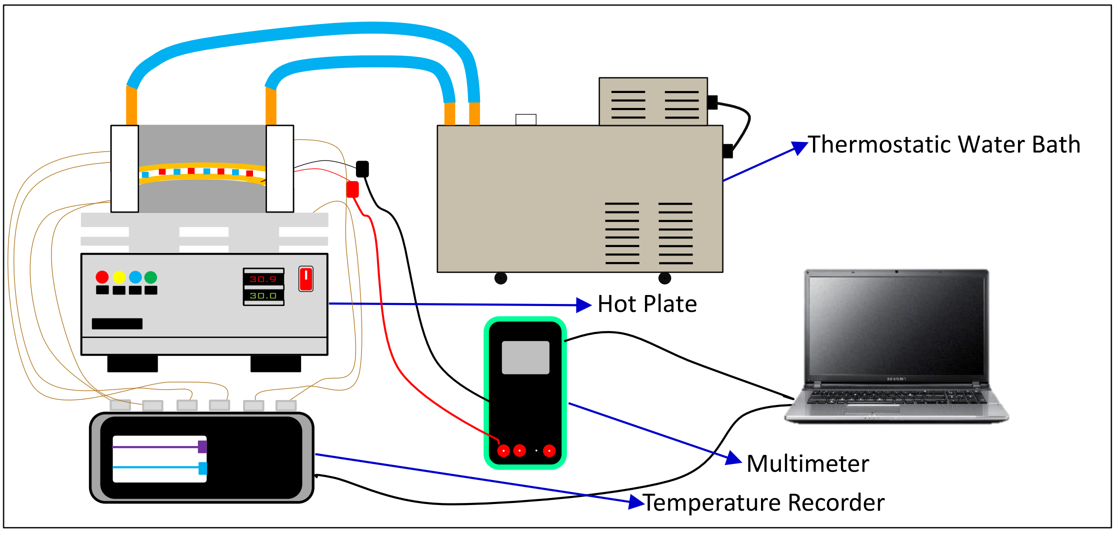

Figure 2-71: schematic of curved surface measurement system

Figure 2-72: finished product of curved surface measurement system

2.8.4 Generating Conversion Efficiency:

The thermal power of conversion efficiency of measuring value was using Fourier law. (Eq. (2.4)) The figure 2-74 and figure 2-75 were the design of thermal power measurement.

The thermal power flowing into module could be expressed as Eq. (2.4).

$$Q_h = K_a \times A_a \times \frac{T_1 - T_2}{X} \qquad \text{Eq. (2.4)}$$

Q_h(heat flux, W)

K_a(thermal conductivity of aluminum, $Wm^{-1}K^{-1}$)

A_a(area of aluminum, m^2)

T (temperature of hot side, ℃)

X (distance, m)

The efficiency of module could be expressed as Eq. (2.5)

$$\eta = \frac{VI}{Q_h} = \frac{P}{Q_h} \qquad \text{Eq. (2.5)}$$

η (generating conversion efficiency, %)

V (voltage, V)

I (current, A)

P (power, W)

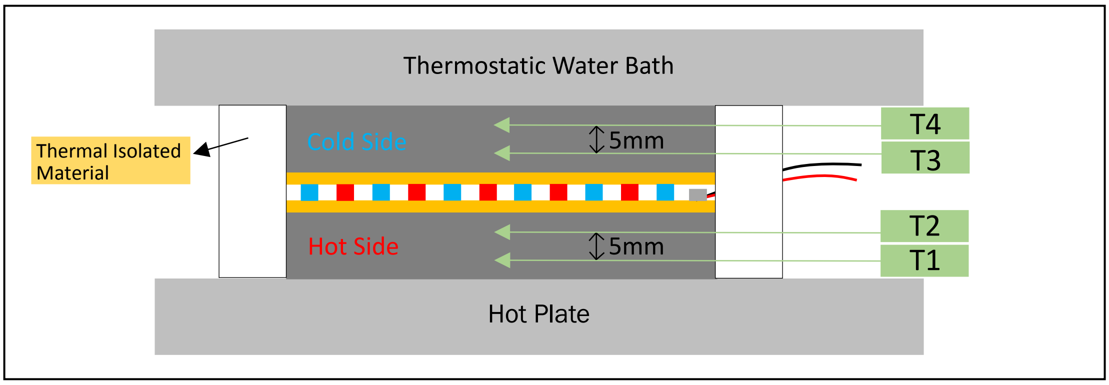

Figure 2-73: schematic of thermal power measurement

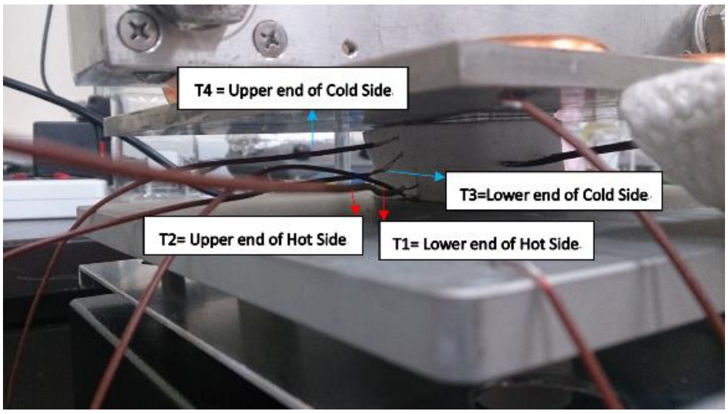

Figure 2-74: finished product of thermal power measurement

2.9 Cooling Measurement:

2.9.1 Measuring Value:

The system was using for understanding the 10 points of TTEM and FTEMs cold side and hot side temperature and the cooling stability of modules when the Laboratory DC power supply imported the electric power. The points T_{c1} and T_{h1} were placed at the middle of module. The T_{c2} to T_{c5} and T_{h2} to T_{h5} were the temperature of the four corners of the module.

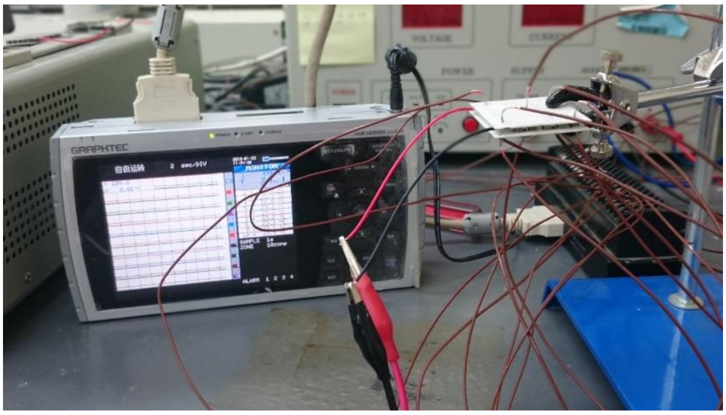

Figure 2-75: finished product of cooling measurement system

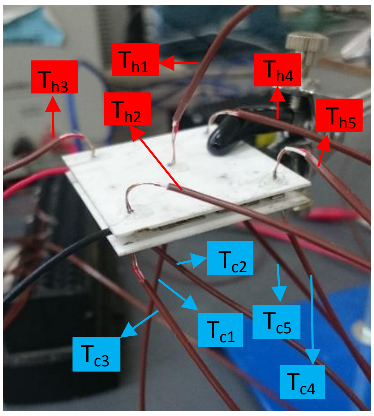

Figure 2-76: measuring points

2.9.2 Cooling Conversion Efficiency:

The cooling conversion efficiency of measuring value was using Eq. (1.4) and Eq. (1.17). So, the completely cooling conversion efficiency could be expressed as Eq. (2.6).

$$\phi = \frac{[S_p \times (T_{ha} - T_{ca}) - S_n \times (T_{ha} - T_{ca})] \times I_{in}}{V_{in} \times I_{in}} = \frac{Q}{P_{in}} \qquad \text{Eq. (2.6)}$$

ϕ (cooling conversion efficiency, %)

S_p (Seebeck coefficient of p-type, V/ΔT)

S_n (Seebeck coefficient of p-type, V/ΔT)

T_{ha}(average hot side temperature, ℃)

T_{ca}(average cold side temperature, ℃)

I_{in}(inputted current, A)

V_{in}(inputted voltage, V)

Q (Peltier heat, W)

P_{in}(inputted electric power, W)

Where $[S_p \times (T_{ha} - T_{ca}) - S_n \times (T_{ha} - T_{ca})]$ was Peltier coefficient of n-type and p-type (Π_{np}). Therefore, the Eq. (2.6) could be simplified as Eq. (2.7).

$$\phi = \frac{\Pi_{np}}{V_{in}} \qquad \text{Eq. (2.7)}$$

Π_{np}(Peltier coefficient of n-type and p-type, V)

Chapter 3 Results and Discussion

3.1 Generating Performance:

3.1.1 Theoretical Value Comparison of BTEM:

The data (table 3.1 to 3.9 and figure 3-1, 3-2) of BTEMs showed the theoretical of temperature difference, Seebeck coefficient and voltage every BTEM at (T_c=22℃, T_h=37℃) and (T_c=22℃, T_h=45℃).

Table 3.1: data of BTEM (A)

Material	n-type	p-type	Copper	Polyimide	Sn/Ag/Cu Solder	Bi/Sn Solder	Thermal grease
Touch Area(m^2)	9 x 10^{-6}	9 x 10^{-6}	9 x 10^{-6}	9 x 10^{-6}	9 x 10^{-6}	9 x 10^{-6}	9 x 10^{-6}
Length (m)	2.4 x 10^{-3}	2.4 x 10^{-3}	1 x 10^{-3}	2.5 x 10^{-4}	5 x 10^{-5}	5 x 10^{-5}	2 x 10^{-5}
Seebeck coefficient (VK^{-1})	-1.50 x 10^{-4}	1.96 x 10^{-4}	N/A	N/A	N/A	N/A	N/A
Resistivity (Ωm)	1.89 × 10^{-5}	1.53 × 10^{-5}	1.7 x 10^{-8}	N/A	1.2 x 10^{-8}	3 x 10^{-8}	N/A
Thermal conductivity ($Wm^{-1}K^{-1}$)	1.75	1.57	401	1.65 x 10^{-1}	50	2 x 10^{-1}	1
Thermal resistivity (KW^{-1})	1.524 x 10^{2}	1.698 x 10^{2}	2.8 x 10^{-1}	1.684 x 10^{2}	1.1 x 10^{-1}	3 x 10^{-1}	2.22222
Z (K^{-1})	2.45 x 10^{-3}	3.77 x 10^{-3}	N/A	N/A	N/A	N/A	N/A

Table 3.2: data of BTEM (B)

Material	n-type	p-type	Copper	Polyimide	Sn/Ag/Cu Solder	Bi/Sn Solder	Thermal grease
Touch Area(m^2)	9 x 10^{-6}	9 x 10^{-6}	9 x 10^{-6}	9 x 10^{-6}	9 x 10^{-6}	9 x 10^{-6}	9 x 10^{-6}
Length (m)	2.4 x 10^{-3}	2.4 x 10^{-3}	2 x 10^{-3}	2.5 x 10^{-4}	5 x 10^{-5}	5 x 10^{-5}	2 x 10^{-5}
Seebeck coefficient (VK^{-1})	-1.50 x 10^{-4}	1.96 x 10^{-4}	N/A	N/A	N/A	N/A	N/A
Resistivity (Ωm)	1.89 × 10^{-5}	1.53 × 10^{-5}	1.7 x 10^{-8}	N/A	1.2 x 10^{-8}	3 x 10^{-8}	N/A
Thermal conductivity ($Wm^{-1}K^{-1}$)	1.75	1.57	401	1.65 x 10^{-1}	50	2 x 10^{-1}	1
Thermal resistivity (KW^{-1})	1.524 x 10^{3}	1.698 x 10^{2}	5.5 x 10^{-1}	1.684 x 10^{2}	1.1 x 10^{-1}	3 x 10^{-1}	2.22222
Z (K^{-1})	2.45 x 10^{-3}	3.77 x 10^{-3}	N/A	N/A	N/A	N/A	N/A

Table 3.3: data of BTEM (C)

Material	n-type	p-type	Copper	Polyimide	Sn/Ag/Cu Solder	Bi/Sn Solder	Thermal grease
Touch Area(m^2)	9 x 10^{-6}	9 x 10^{-6}	9 x 10^{-6}	9 x 10^{-6}	9 x 10^{-6}	9 x 10^{-6}	9 x 10^{-6}
Length (m)	2.4 x 10^{-3}	2.4 x 10^{-3}	1 x 10^{-3}	2.5 x 10^{-4}	5 x 10^{-5}	5 x 10^{-5}	2 x 10^{-5}
Seebeck coefficient (VK^{-1})	-1.50 x 10^{-4}	1.96 x 10^{-4}	N/A	N/A	N/A	N/A	N/A
Resistivity (Ωm)	1.89 × 10^{-5}	1.53 × 10^{-5}	1.7 x 10^{-8}	N/A	1.2 x 10^{-8}	3 x 10^{-8}	N/A
Thermal conductivity ($Wm^{-1}K^{-1}$)	1.75	1.57	401	1.65 x 10^{-1}	50	2 x 10^{-1}	1
Thermal resistivity (KW^{-1})	1.524 x 10^{3}	1.698 x 10^{2}	2.8 x 10^{-1}	1.684 x 10^{2}	1.1 x 10^{-1}	3 x 10^{-1}	2.22222
Z (K^{-1})	2.45 x 10^{-3}	3.77 x 10^{-3}	N/A	N/A	N/A	N/A	N/A

Table 3.4: data of BTEM (D)

Material	n-type	p-type	Copper	Polyimide	Sn/Ag/Cu Solder	Bi/Sn Solder	Thermal grease
Touch Area(m^2)	9×10^{-6}	9×10^{-6}	9×10^{-6}	9×10^{-6}	9×10^{-6}	9×10^{-6}	9×10^{-6}
Length (m)	2.4×10^{-3}	2.4×10^{-3}	1×10^{-3}	2.5×10^{-4}	5×10^{-5}	5×10^{-5}	2×10^{-5}
Seebeck coefficient (VK^{-1})	-1.50×10^{-4}	1.96×10^{-4}	N/A	N/A	N/A	N/A	N/A
Resistivity (Ωm)	1.89×10^{-5}	1.53×10^{-5}	1.7×10^{-8}	N/A	1.2×10^{-8}	3×10^{-8}	N/A
Thermal conductivity ($Wm^{-1}K^{-1}$)	1.75	1.57	401	1.65×10^{-1}	50	2×10^{-1}	1
Thermal resistivity (KW^{-1})	1.524×10^{3}	1.698×10^{2}	2.8×10^{-1}	1.684×10^{2}	1.1×10^{-1}	3×10^{-1}	2.22222
Z (K^{-1})	2.45×10^{-3}	3.77×10^{-3}	N/A	N/A	N/A	N/A	N/A

Table 3.5: data of BTEM (E)

Material	n-type	p-type	Copper	Polyimide	Sn/Ag/Cu Solder	Bi/Sn Solder	Thermal grease
Touch Area(m^2)	9×10^{-6}	9×10^{-6}	9×10^{-6}	9×10^{-6}	9×10^{-6}	9×10^{-6}	9×10^{-6}
Length (m)	2.4×10^{-3}	2.4×10^{-3}	1×10^{-3}	2.5×10^{-4}	5×10^{-5}	5×10^{-5}	2×10^{-5}
Seebeck coefficient (VK^{-1})	-1.50×10^{-4}	1.96×10^{-4}	N/A	N/A	N/A	N/A	N/A
Resistivity (Ωm)	1.89×10^{-5}	1.53×10^{-5}	1.7×10^{-8}	N/A	1.2×10^{-8}	3×10^{-8}	N/A
Thermal conductivity ($Wm^{-1}K^{-1}$)	1.75	1.57	401	1.65×10^{-1}	50	2×10^{-1}	1
Thermal resistivity (KW^{-1})	1.524×10^{3}	1.698×10^{2}	2.8×10^{-1}	1.684×10^{2}	1.1×10^{-1}	3×10^{-1}	2.22222
Z (K^{-1})	2.45×10^{-3}	3.77×10^{-3}	N/A	N/A	N/A	N/A	N/A

Table 3.6: data of BTEM (F)

Material	n-type	p-type	Copper	Polyimide	Sn/Ag/Cu Solder	Bi/Sn Solder	Thermal grease
Touch Area(m^2)	9×10^{-6}	9×10^{-6}	9×10^{-6}	9×10^{-6}	9×10^{-6}	9×10^{-6}	9×10^{-6}
Length (m)	2.4×10^{-3}	2.4×10^{-3}	1×10^{-3}	2.5×10^{-4}	5×10^{-5}	5×10^{-5}	2×10^{-5}
Seebeck coefficient (VK^{-1})	-1.50×10^{-4}	1.96×10^{-4}	N/A	N/A	N/A	N/A	N/A
Resistivity (Ωm)	1.89×10^{-5}	1.53×10^{-5}	1.7×10^{-8}	N/A	1.2×10^{-8}	3×10^{-8}	N/A
Thermal conductivity ($Wm^{-1}K^{-1}$)	1.75	1.57	401	1.65×10^{-1}	50	2×10^{-1}	1
Thermal resistivity (KW^{-1})	1.524×10^{3}	1.698×10^{2}	2.8×10^{-1}	1.684×10^{2}	1.1×10^{-1}	3×10^{-1}	2.22222
Z (K^{-1})	2.45×10^{-3}	3.77×10^{-3}	N/A	N/A	N/A	N/A	N/A

Table 3.7: equations of BTEMs practical temperature difference (ΔT_{TEM})

Module	ΔT_{TEM} Equation
BTEM (A)	$\Delta T_{BTEM\ (A)} = 0.99939271 \times (T_h - T_c)$
BTEM (B)	$\Delta T_{BTEM\ (B)} = 0.99939368 \times (T_h - T_c)$
BTEM (C)	$\Delta T_{BTEM\ (C)} = 0.99939271 \times (T_h - T_c)$
BTEM (D)	$\Delta T_{BTEM\ (D)} = 0.99939271 \times (T_h - T_c)$
BTEM (E)	$\Delta T_{BTEM\ (E)} = 0.99939271 \times (T_h - T_c)$
BTEM (F)	$\Delta T_{BTEM\ (F)} = 0.99939271 \times (T_h - T_c)$

Table 3.8: BTEMs theoretical value at T_c=22℃, T_h=37℃

Module	BTEM (A)	BTEM (B)	BTEM (C)	BTEM (D)	BTEM (E)	BTEM (F)
ΔT_{TEM} (℃)	14.990891	14.990905	14.990891	14.990891	14.990891	14.990891
Seebeck coefficient (mV/ΔT)	5.1868482	5.1868532	5.1868482	5.1868482	5.1868482	21.784762
Voltage (mV)	77.802722	77.802798	77.802722	77.802722	77.802722	326.77143

Table 3.9: BTEMs theoretical value at T_c=22℃, T_h=45℃

Module	BTEM (A)	BTEM (B)	BTEM (C)	BTEM (D)	BTEM (E)	BTEM (F)
ΔT_{TEM} (℃)	22.986032	22.986055	22.986032	22.986032	22.986032	22.986032
Seebeck coefficient (mV/ΔT)	5.1868482	5.1868532	5.1868482	5.1868482	5.1868482	21.784762
Voltage (mV)	119.29751	119.29762	119.29751	119.29751	119.29751	501.05002

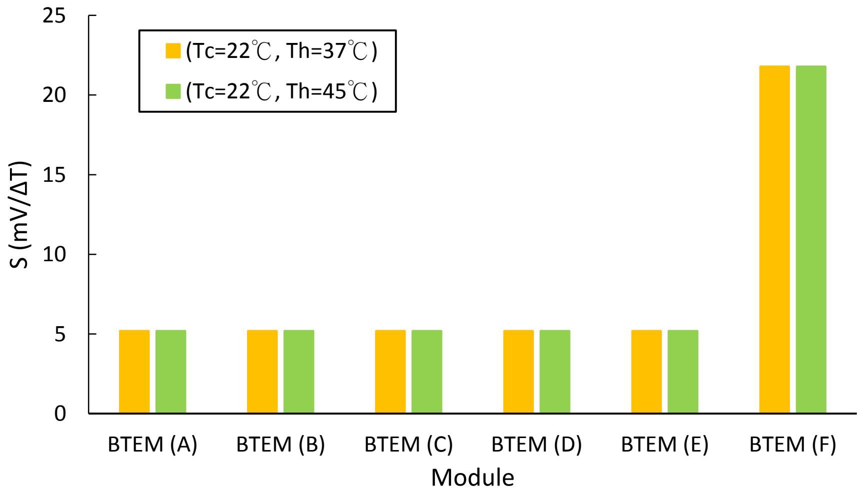

Figure 3-1: Seebeck coefficient of all BTEMs at (T_c=22℃, T_h=37℃) and (T_c=22℃, T_h=45℃)

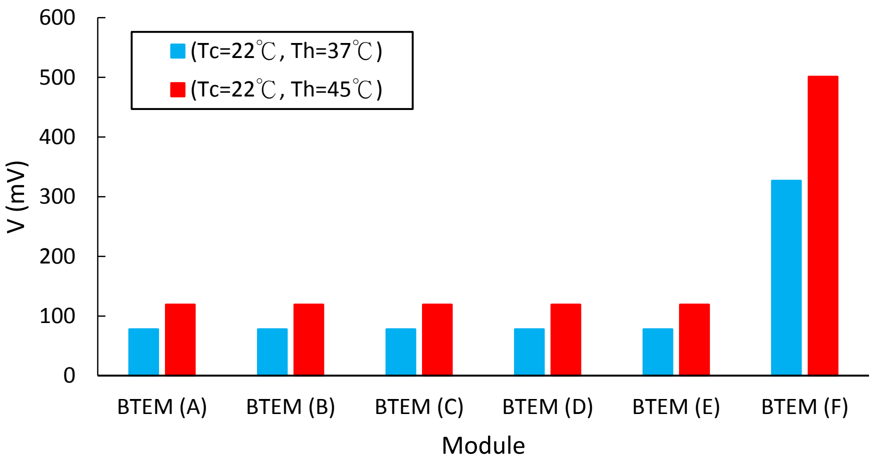

Figure 3-2: voltage of all BTEMs at (T_c=22℃, T_h=37℃) and (T_c=22℃, T_h=45℃)

The data (table 3.8, 3.9 and figure 3-1, 3-2) showed that every BTEM had the same Seebeck coefficient at (T_c=22℃, T_h=37℃) and (T_c=22℃, T_h=45℃) itself, and the more the n-type p-type pairs (BTEM (F)) were, the voltage were higher. It also showed which it couldn't be understand the soldering different in the data.

3.1.2 Measuring Value of BTEM (Flat Surface Measurement):

BTEM (A):

Table 3.10: Seebeck coefficient and current of BTEM (A) at (T_c=22℃, T_h=37℃) and (T_c=22℃, T_h=45℃)

Seebeck coefficient and Current (I) / Time (Min)	Tc=22℃, Th=37℃, ΔT=15℃		Tc=22℃, Th=45℃, ΔT=23℃	
	S (mV/ΔT)	I (mA)	S (mV/ΔT)	I (mA)
0.5	2.693333333	6.84	2.782608696	10.79
1	2.701986755	6.82	2.786956522	10.77
1.5	2.697368421	6.79	2.774891775	10.76
2	2.710526316	6.78	2.774891775	10.77
2.5	2.717105263	6.77	2.786956522	10.76
3	2.717105263	6.76	2.774891775	10.76
3.5	2.699346405	6.74	2.779220779	10.77
4	2.699346405	6.73	2.751072961	10.78
4.5	2.717105263	6.72	2.786956522	10.81
5	2.692810458	6.72	2.739316239	10.83
5.5	2.68627451	6.72	2.75862069	10.81
6	2.703947368	6.73	2.782608696	10.8
6.5	2.715231788	6.76	2.735042735	10.8
7	2.708609272	6.78	2.770562771	10.83
7.5	2.708609272	6.78	2.794759825	10.87
8	2.72	6.79	2.782608696	10.88
8.5	2.713333333	6.8	2.782608696	10.87
9	2.695364238	6.81	2.782608696	10.85
9.5	2.724832215	6.8	2.790393013	10.84
10	2.724832215	6.79	2.782608696	10.85

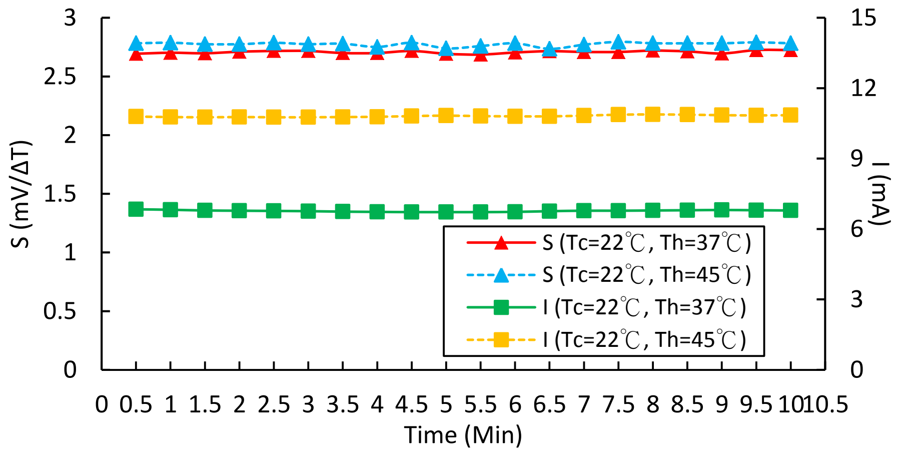

Figure 3-3: S-I-T of BTEM (A) at (T_c=22℃, T_h=37℃) and (T_c=22℃, T_h=45℃)

Table 3.10 and figure 3-3 showed that the Seebeck coefficient at (T_c=22℃, T_h=45℃) was higher than Seebeck coefficient at (T_c=22℃, T_h=37℃), and the current also.

Table 3.11: power and conversion efficiency of BTEM (A) at (T_c=22℃, T_h=37℃) and (T_c=22℃, T_h=45℃)

Time (Min) \ Power and conversion efficiency (η)	Tc=22℃, Th=37℃, ΔT=15℃		Tc=22℃, Th=45℃, ΔT=23℃	
	Power (µW)	η (x 10^{-6})	Power (µW)	η (x 10^{-6})
0.5	276.336	1.020636103	690.56	1.667671288
1	278.256	1.091960518	690.357	1.605433606
1.5	278.39	0.919988526	689.716	1.493326197
2	279.336	1.031716484	690.357	1.494714047
2.5	279.601	1.032695251	689.716	1.493326197
3	279.188	1.031169852	689.716	1.546659276
3.5	278.362	1.028119054	691.434	1.497045894
4	277.949	1.026593654	690.998	1.446231833
4.5	277.536	1.089135021	692.921	1.500265445
5	276.864	1.02258625	694.203	1.556721185
5.5	276.192	1.020104244	691.84	1.401284619
6	276.603	1.085473648	691.2	1.446654611
6.5	277.16	1.023679514	691.2	1.607394012
7	277.302	1.024203985	693.12	1.554292603
7.5	277.302	1.024203985	695.68	1.617812307
8	277.032	1.023206751	696.32	1.619300635
8.5	276.76	1.086089763	695.68	1.506239044
9	277.167	1.087686954	694.4	1.55716295
9.5	276.08	1.083421238	692.676	1.499734988
10	275.674	1.018191032	694.4	1.453352086

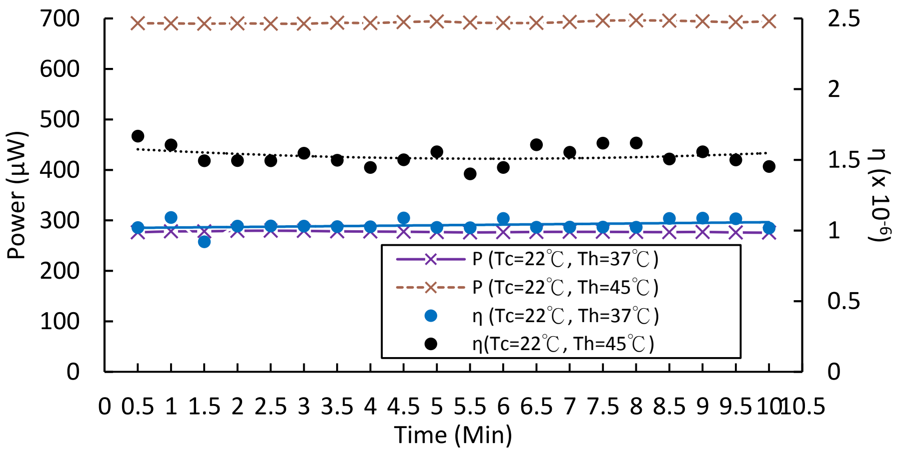

Figure 3-4: P-η-T of BTEM (A) at (T_c=22℃, T_h=37℃) and (T_c=22℃, T_h=45℃)

Table 3.12 and figure 3-4 showed that the conversion efficiency and power at (T_c=22 ℃, T_h=45℃) were higher than conversion efficiency and power at (T_c=22℃, T_h=37℃). The conversion efficiency had minimum value at 1.5 second at (T_c=22℃, T_h=37℃) and it had minimum value at 5.5 second at (T_c=22℃, T_h=45℃).

BTEM (B):

Table 3.12: Seebeck coefficient and current of BTEM (B) at (T_c=22℃, T_h=37℃) and (T_c=22℃, T_h=45℃)

Seebeck coefficient and Current (I) / Time (Min)	Tc=22℃, Th=37℃, ΔT=15℃		Tc=22℃, Th=45℃, ΔT=23℃	
	S (mV/ΔT)	I (mA)	S (mV/ΔT)	I (mA)
0.5	3.02	11.69	4.623430962	17.92
1	3.013333333	11.65	4.656903766	17.93
1.5	3.02	11.61	4.609053498	17.91
2	3.013333333	11.59	4.648760331	17.9
2.5	3.013333333	11.58	4.665289256	17.94
3	3.026845638	11.56	4.639344262	17.95
3.5	3.006666667	11.56	4.647540984	17.93
4	3.026845638	11.57	4.674897119	17.9
4.5	3.013333333	11.56	4.709543568	17.88
5	3.026845638	11.57	4.685950413	17.89
5.5	3.040540541	11.59	4.658436214	17.88
6	3.020134228	11.6	4.68879668	17.88
6.5	3.020134228	11.6	4.731092437	17.88
7	2.993377483	11.62	4.69874477	17.85
7.5	3.013333333	11.63	4.686192469	17.84
8	3	11.67	4.658333333	17.84
8.5	3.013333333	11.69	4.708860759	17.83
9	2.993377483	11.71	4.716101695	17.81
9.5	3.033557047	11.72	4.752136752	17.79
10	3.006666667	11.72	4.668067227	17.78

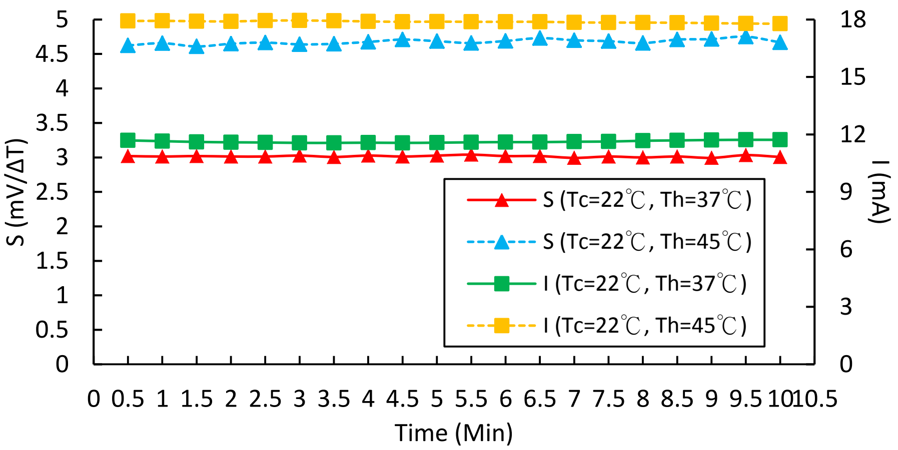

Figure 3-5: S-I-T of BTEM (B) at (T_c=22℃, T_h=37℃) and (T_c=22℃, T_h=45℃)

Table 3.12 and figure 3-5 showed that the Seebeck coefficient at (T_c=22℃, T_h=45℃) was higher than Seebeck coefficient at (T_c=22℃, T_h=37℃), and the current also.

Table 3.13: power and conversion efficiency of BTEM (B) at (T_c=22℃, T_h=37℃) and (T_c=22℃, T_h=45℃)

Time (Min) \ Power and conversion efficiency (η)	Tc=22℃, Th=37℃, ΔT=15℃		Tc=22℃, Th=45℃, ΔT=23℃	
	Power (μW)	η (x 10^{-6})	Power (μW)	η (x 10^{-6})
0.5	529.557	2.55771	1980.160	6.54379
1	526.58	2.54333	1995.609	6.96122
1.5	525.933	2.54021	2005.920	6.99719
2	523.868	2.34950	2013.750	6.65479
2.5	523.416	2.34748	2025.426	6.35871
3	521.356	2.51810	2031.940	6.71490
3.5	521.356	2.33824	2033.262	5.80301
4	521.807	2.18424	2033.440	5.80351
4.5	522.512	2.34342	2029.380	5.79193
5	521.807	2.34026	2028.726	6.36907
5.5	521.55	2.51904	2024.016	6.68872
6	522	2.52121	2020.440	5.51570
6.5	522	2.52121	2013.288	5.26717
7	525.224	2.19855	2004.555	5.24432
7.5	525.676	2.35761	1998.080	4.18190
8	528.651	2.37096	1994.512	4.03978
8.5	528.388	2.36978	1989.828	5.20579
9	529.292	2.55643	1982.253	5.18597
9.5	529.744	2.37586	1978.248	5.40052
10	528.572	2.07428	1975.358	5.63775

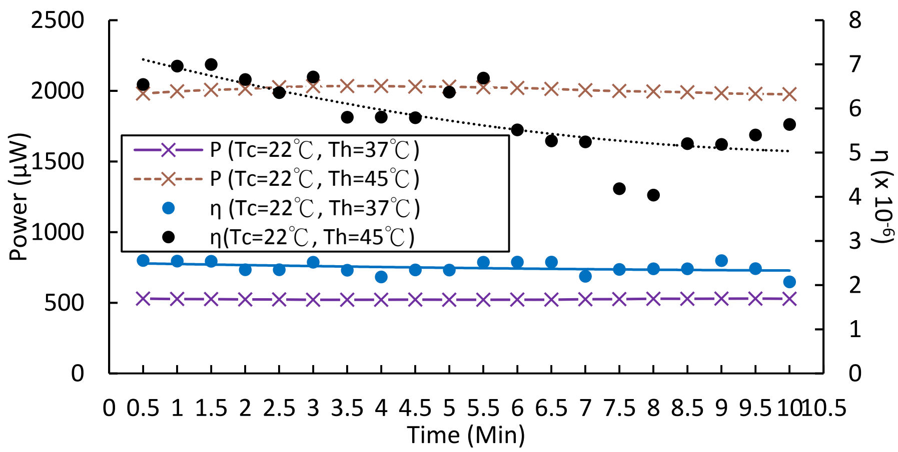

Figure 3-6: P-η-T of BTEM (A) at (T_c=22℃, T_h=37℃) and (T_c=22℃, T_h=45℃)

Table 3.13 and figure 3-6 showed that the conversion efficiency and power at (T_c=22℃, T_h=45℃) were higher than conversion efficiency and power at (T_c=22℃, T_h=37℃). But, the conversion efficiency was getting lower belong the time at (T_c=22℃, T_h=37℃), and (T_c=22℃, T_h=45℃).

BTEM (C):

Table 3.14: Seebeck coefficient and current of BTEM (C) at (T_c=22℃, T_h=37℃) and (T_c=22℃, T_h=45℃)

Seebeck coefficient and Current (I) / Time (Min)	Tc=22℃, Th=37℃, ΔT=15℃		Tc=22℃, Th=45℃, ΔT=23℃	
	S (mV/ΔT)	I (mA)	S (mV/ΔT)	I (mA)
0.5	2.510204082	5.43	2.337662338	8.21
1	2.510204082	5.45	2.337662338	8.23
1.5	2.510204082	5.44	2.368421053	8.23
2	2.517006803	5.43	2.317596567	8.23
2.5	2.523809524	5.41	2.378854626	8.24
3	2.513513514	5.39	2.303418803	8.24
3.5	2.52027027	5.39	2.313304721	8.25
4	2.527027027	5.39	2.293617021	8.27
4.5	2.516778523	5.39	2.278481013	8.28
5	2.5	5.39	2.343478261	8.28
5.5	2.5	5.38	2.303418803	8.28
6	2.473684211	5.37	2.299145299	8.27
6.5	2.513333333	5.36	2.318965517	8.3
7	2.536912752	5.37	2.339130435	8.3
7.5	2.52	5.38	2.412556054	8.3
8	2.52	5.37	2.376106195	8.31
8.5	2.52	5.36	2.334782609	8.31
9	2.530201342	5.35	2.324675325	8.31
9.5	2.506666667	5.35	2.289361702	8.31
10	2.5	5.36	2.299145299	8.3

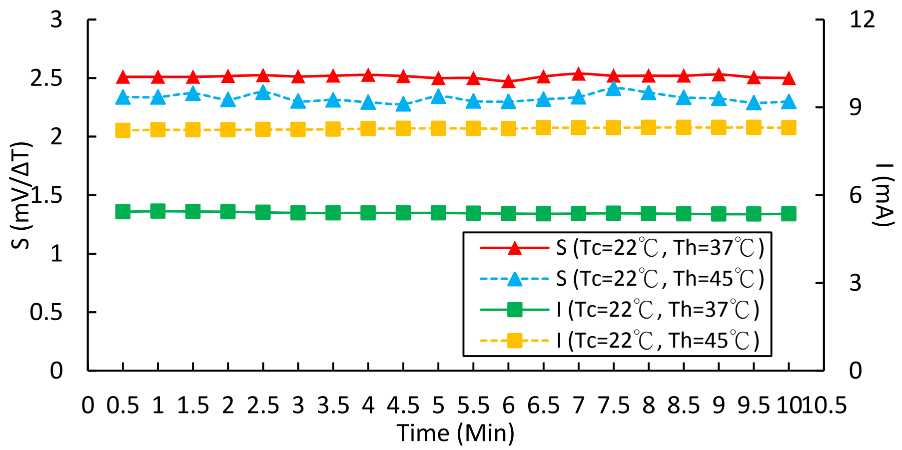

Figure 3-7: S-I-T of BTEM (C) at (T_c=22℃, T_h=37℃) and (T_c=22℃, T_h=45℃)

Table 3.14 and figure 3-7 showed that the Seebeck coefficient at (T_c=22℃, T_h=37℃) was higher than Seebeck coefficient at (T_c=22℃, T_h=45℃), but the current at (T_c=22℃, T_h=45℃) was higher the current at (T_c=22℃, T_h=37℃).

Table 3.15: power and conversion efficiency of BTEM (C) at (T_c=22℃, T_h=37℃) and (T_c=22℃, T_h=45℃)

Power and conversion efficiency (η) / Time (Min)	Tc=22℃, Th=37℃, ΔT=15℃		Tc=22℃, Th=45℃, ΔT=23℃	
	Power (μW)	η (x 10^{-6})	Power (μW)	η (x 10^{-6})
0.5	200.367	0.503232369	443.340	2.319733273
1	201.105	0.467672125	444.420	2.536782837
1.5	200.736	0.484768396	444.420	2.325384268
2	200.91	0.485188598	444.420	2.536782837
2.5	200.711	0.466755873	444.960	1.862567812
3	200.508	0.484217786	444.136	2.535161744
3.5	201.047	0.485519447	444.675	2.147740182
4	201.586	0.486821108	445.753	2.544391702
4.5	202.125	0.488122769	447.120	2.807414105
5	202.125	0.470044148	446.292	2.547468354
5.5	201.75	0.46917208	446.292	2.547468354
6	201.912	0.469548813	444.926	2.539671124
6.5	202.072	0.487994776	446.540	2.336476961
7	202.986	0.490202045	446.540	2.156747964
7.5	203.364	0.491114898	446.540	2.156747964
8	202.986	0.472046414	446.247	2.334943867
8.5	202.608	0.454339964	446.247	2.334943867
9	201.695	0.487084338	446.247	2.334943867
9.5	201.16	0.505224031	447.078	2.551954902
10	201	0.485405944	446.540	2.548883957

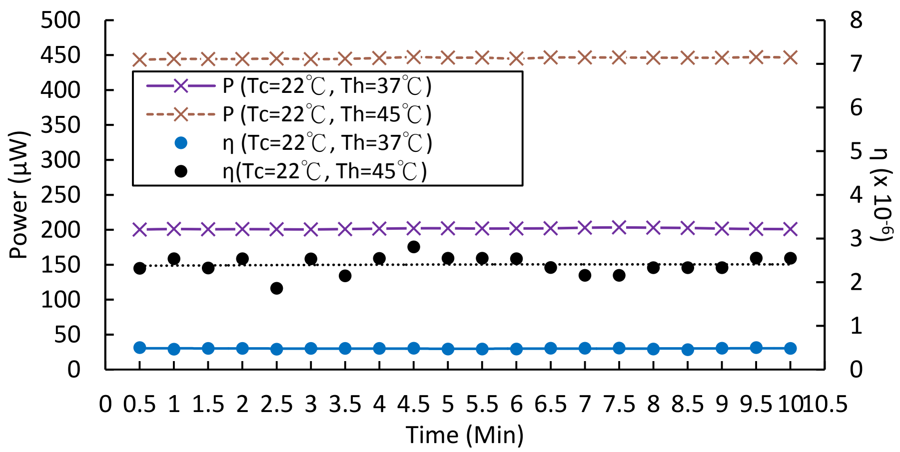

Figure 3-8: P-η-T of BTEM (C) at (T_c=22℃, T_h=37℃) and (T_c=22℃, T_h=45℃)

Table 3.15 and figure 3-8 showed that the conversion efficiency and power at (T_c=22℃, T_h=45℃) were higher than conversion efficiency and power at (T_c=22℃, T_h=37℃). The conversion efficiency was getting higher belong the time at (T_c=22℃, T_h=37℃), and it had the maximum at 4.5 second at (T_c=22℃, T_h=45℃).

BTEM (D):

Table 3.16: Seebeck coefficient and current of BTEM (D) at (T_c=22℃, T_h=37℃) and (T_c=22℃, T_h=45℃)

Seebeck coefficient and Current (I) / Time (Min)	Tc=22℃, Th=37℃, ΔT=15℃		Tc=22℃, Th=45℃, ΔT=23℃	
	S (mV/ΔT)	I (mA)	S (mV/ΔT)	I (mA)
0.5	3.094594595	8.44	2.780172414	13.62
1	3.108843537	8.4	2.733050847	13.53
1.5	3.060402685	8.36	2.771551724	13.46
2	3.081081081	8.33	2.752136752	13.42
2.5	3.080536913	8.29	2.740425532	13.43
3	3.108108108	8.27	2.768240343	13.42
3.5	3.087248322	8.25	2.797413793	13.42
4	3.087248322	8.25	2.82173913	13.43
4.5	3.06	8.26	2.80952381	13.43
5	3.108108108	8.27	2.830434783	13.43
5.5	3.06	8.29	2.855263158	13.43
6	3.039735099	8.29	2.793991416	13.47
6.5	3.150684932	8.3	2.872246696	13.5
7	3.052980132	8.29	2.872246696	13.54
7.5	3.100671141	8.32	2.839130435	13.56
8	3.100671141	8.34	2.847161572	13.59
8.5	3.039473684	8.34	2.847161572	13.58
9	3.128378378	8.34	2.876651982	13.58
9.5	3.11409396	8.34	2.915178571	13.61
10	3.11409396	8.35	2.876651982	13.63

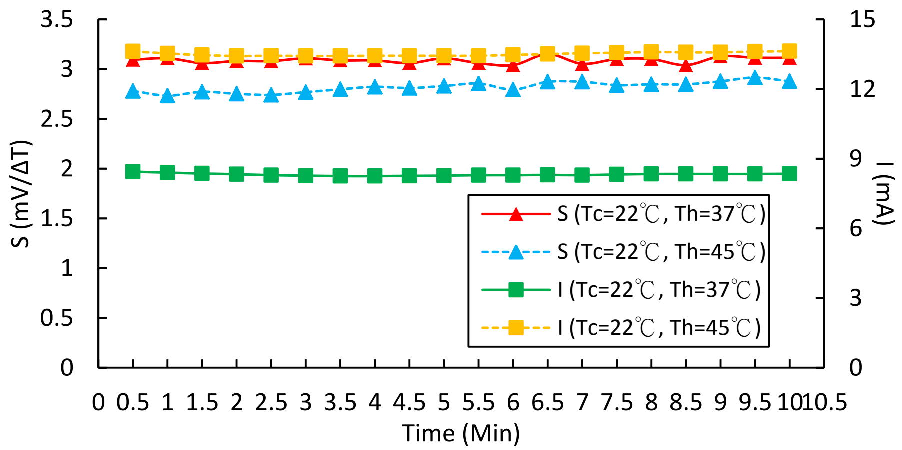

Figure 3-9: S-I-T of BTEM (C) at (T_c=22℃, T_h=37℃) and (T_c=22℃, T_h=45℃)

Table 3.16 and figure 3-9 showed that the Seebeck coefficient at (T_c=22℃, T_h=37℃) was higher than Seebeck coefficient at (T_c=22℃, T_h=45℃), but the current at (T_c=22℃, T_h=45℃) was higher the current at (T_c=22℃, T_h=37℃).

Table 3.17: power and conversion efficiency of BTEM (D) at (T_c=22℃, T_h=37℃) and (T_c=22℃, T_h=45℃)

Time (Min) \ Power and conversion efficiency (η)	Tc=22℃, Th=37℃, ΔT=15℃		Tc=22℃, Th=45℃, ΔT=23℃	
	Power (µW)	η (x 10^{-6})	Power (µW)	η (x 10^{-6})
0.5	386.552	6.832932958	878.490	6.394184683
1	383.88	7.9166512	872.685	8.998570845
1.5	381.216	11.7925684	865.478	6.693192645
2	379.848	5.875125283	864.248	7.638491901
2.5	380.511	7.847173243	864.892	8.23219791
3	380.42	5.230197717	865.590	7.650352914
3.5	379.5	5.869742752	870.958	8.289935191
4	379.5	6.708277431	871.607	5.676287493
4.5	379.134	6.701807788	871.607	6.344086022
5	380.42	5.230197717	874.293	6.01010101
5.5	380.511	7.847173243	874.293	6.363636364
6	380.511	11.77075986	876.897	9.042002301
6.5	381.8	3.936877967	880.200	6.807045547
7	382.169	9.457638863	882.808	6.068635174
7.5	384.384	5.284696702	885.468	8.428043985
8	385.308	5.959575337	886.068	9.136567801
8.5	385.308	11.91915067	885.416	9.129844793
9	386.142	4.77797988	886.774	7.315078098
9.5	386.976	5.320332768	888.733	5.236598618
10	387.44	5.326712064	890.039	7.342011375

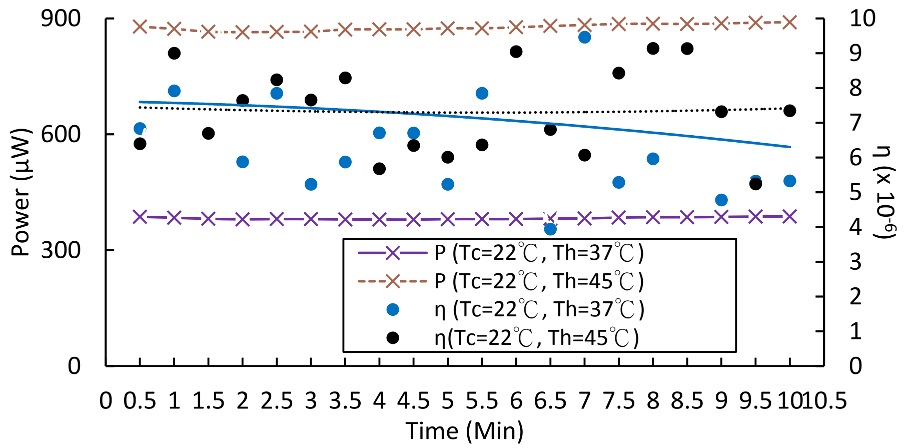

Figure 3-10: P-η-T of BTEM (D) at (T_c=22℃, T_h=37℃) and (T_c=22℃, T_h=45℃)

Table 3.17 and figure 3-10 showed that the conversion efficiency and power at (T_c=22℃, T_h=45℃) were higher than conversion efficiency and power at (T_c=22℃, T_h=37℃). The conversion efficiency was getting lower belong the time at (T_c=22℃, T_h=37℃), and it was getting higher belong the time at (T_c=22℃, T_h=45℃).

BTEM (E):

Table 3.18: Seebeck coefficient and current of BTEM (E) at (T_c=22℃, T_h=37℃) and (T_c=22℃, T_h=45℃)

Seebeck coefficient and Current (I) / Time (Min)	Tc=22℃, Th=37℃, ΔT=15℃		Tc=22℃, Th=45℃, ΔT=23℃	
	S (mV/ΔT)	I (mA)	S (mV/ΔT)	I (mA)
0.5	3.860927152	8.09	3.815789474	12.19
1	3.873333333	8.1	3.824561404	12.24
1.5	3.88590604	8.12	3.812227074	12.27
2	3.879194631	8.14	3.816593886	12.25
2.5	3.879194631	8.15	3.804347826	12.23
3	3.88590604	8.16	3.825327511	12.23
3.5	3.866666667	8.17	3.825327511	12.24
4	3.899328859	8.16	3.813043478	12.24
4.5	3.822368421	8.14	3.834061135	12.23
5	3.828947368	8.13	3.813043478	12.2
5.5	3.828947368	8.13	3.813043478	12.2
6	3.803921569	8.14	3.829694323	12.2
6.5	3.810457516	8.14	3.813043478	12.2
7	3.816993464	8.13	3.813043478	12.19
7.5	3.848684211	8.13	3.842105263	12.17
8	3.816993464	8.12	3.804347826	12.14
8.5	3.828947368	8.13	3.804347826	12.15
9	3.797385621	8.14	3.825327511	12.2
9.5	3.854304636	8.13	3.842105263	12.21
10	3.847682119	8.12	3.825327511	12.2

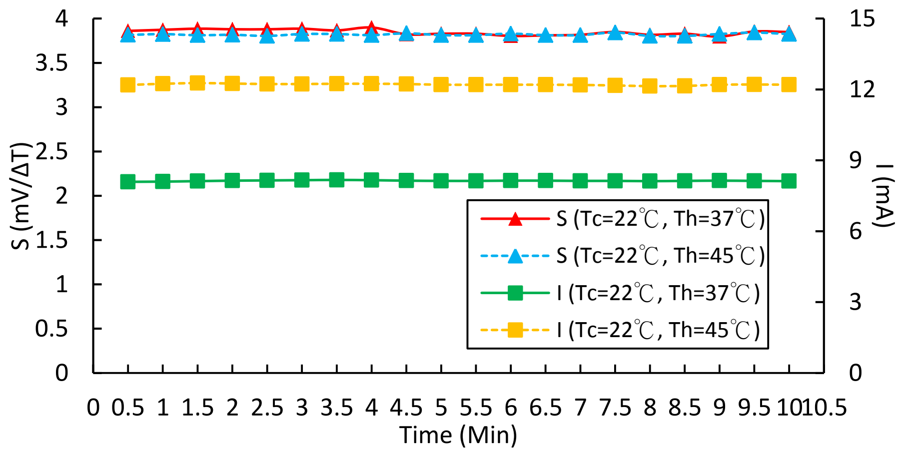

Figure 3-11: S-I-T of BTEM (E) at (T_c=22℃, T_h=37℃) and (T_c=22℃, T_h=45℃)

Table 3.18 and figure 3-11 showed that the Seebeck coefficient at (T_c=22℃, T_h=37℃) was higher than Seebeck coefficient at (T_c=22℃, T_h=45℃), but the current at (T_c=22℃, T_h=45℃) was higher the current at (T_c=22℃, T_h=37℃).

Table 3.19: power and conversion efficiency of BTEM (E) at (T_c=22℃, T_h=37℃) and (T_c=22℃, T_h=45℃)

Time (Min) \ Power and conversion efficiency (η)	Tc=22℃, Th=37℃, ΔT=15℃		Tc=22℃, Th=45℃, ΔT=23℃	
	Power (μW)	η (x 10^{-6})	Power (μW)	η (x 10^{-6})
0.5	471.647	19.45329159	1060.530	10.93550862
1	470.61	19.41052006	1067.328	12.00611483
1.5	470.148	14.5435985	1071.171	12.0493438
2	470.492	19.4056531	1070.650	12.0434832
2.5	471.07	19.42949297	1070.125	12.0375776
3	472.464	29.23048369	1071.348	11.04705693
3.5	473.86	14.65842583	1072.224	12.06118875
4	474.096	14.66572627	1073.448	12.07495723
4.5	472.934	29.25956173	1073.794	12.0788493
5	473.166	19.51594343	1069.940	12.03549658
5.5	473.166	19.51594343	1069.940	12.03549658
6	473.748	29.30992242	1069.940	12.03549658
6.5	474.562	29.36028311	1069.940	12.03549658
7	474.792	19.58300853	1069.063	12.02563142
7.5	475.605	14.71240581	1066.092	11.99221136
8	474.208	19.55892118	1062.250	11.94899363
8.5	473.166	29.27391514	1063.125	11.95883629
9	472.934	19.50637448	1068.720	12.0217731
9.5	473.166	14.63695757	1069.596	12.03162701
10	471.772	19.45844727	1068.720	12.0217731

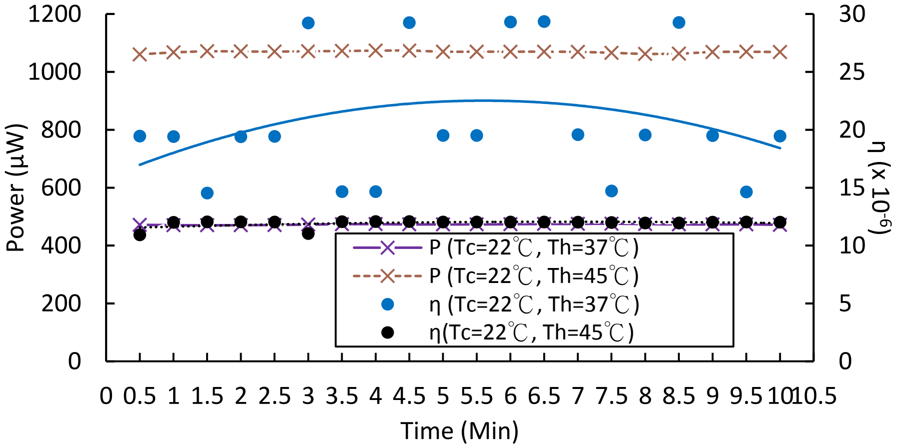

Figure 3-12: P-η-T of BTEM (E) at (T_c=22℃, T_h=37℃) and (T_c=22℃, T_h=45℃)

Table 3.19 and figure 3-12 showed that the conversion efficiency and power at (T_c=22℃, T_h=45℃) were higher than conversion efficiency and power at (T_c=22℃, T_h=37℃). The conversion efficiency was getting lower belong the time at (T_c=22℃, T_h=37℃), and it was getting higher belong the time at (T_c=22℃, T_h=45℃).

BTEM (F):

Table 3.20: Seebeck coefficient and current of BTEM (F) at (T_c=22℃, T_h=37℃) and (T_c=22℃, T_h=45℃)

Seebeck coefficient and Current (I) / Time (Min)	Tc=22℃, Th=37℃, ΔT=15℃		Tc=22℃, Th=45℃, ΔT=23℃	
	S (mV/ΔT)	I (mA)	S (mV/ΔT)	I (mA)
0.5	8.52173913	21.81	9.043859649	33.89
1	9.119205298	21.7	9.052631579	33.89
1.5	8.63125	21.63	9.070175439	33.92
2	8.65	21.65	9.074561404	33.92
2.5	8.65	21.67	9.03930131	33.93
3	8.561728395	21.61	9.056768559	33.97
3.5	8.627329193	21.56	9.061135371	34.04
4	8.574074074	21.56	9.056768559	34.08
4.5	8.567901235	21.58	9.114035088	34.09
5	8.543209877	21.59	9.082969432	34.1
5.5	8.577639752	21.59	9.091703057	34.12
6	8.577639752	21.61	9.056521739	34.16
6.5	8.63125	21.65	9.060869565	34.22
7	8.565217391	21.69	9.069565217	34.21
7.5	8.552795031	21.73	9.043290043	34.19
8	8.527950311	21.76	9.047619048	34.13
8.5	8.616352201	21.76	9.086956522	34.09
9	8.658227848	21.78	9.051948052	34.08
9.5	8.525	21.8	9.104347826	34.09
10	8.566037736	21.81	9.060606061	34.12

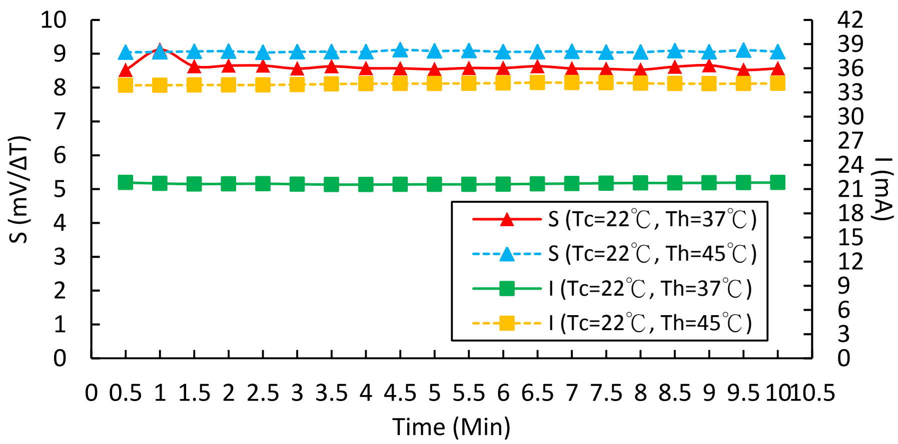

Figure 3-13: S-I-T of BTEM (F) at (T_c=22℃, T_h=37℃) and (T_c=22℃, T_h=45℃)

Table 3.20 and figure 3-13 showed that the Seebeck coefficient at (T_c=22℃, T_h=45℃) was higher than Seebeck coefficient at (T_c=22℃, T_h=37℃), and the current also.

Table 3.21: power and conversion efficiency of BTEM (F) at (T_c=22℃, T_h=37℃) and (T_c=22℃, T_h=45℃)

Power and conversion efficiency (η) / Time (Min)	Tc=22℃, Th=37℃, ΔT=15℃		Tc=22℃, Th=45℃, ΔT=23℃	
	Power (μW)	η (x 10^{-6})	Power (μW)	η (x 10^{-6})
0.5	2992.332	9.81528322	6988.118	14.47707864
1	2988.09	6.534245896	6994.896	13.7665644
1.5	2987.103	10.68887055	7014.656	13.14805124
2	2996.36	10.72199525	7018.048	13.1544091
2.5	2999.128	10.73190009	7023.510	13.82287925
3	2997.307	9.831601942	7045.378	13.86591738
3.5	2994.684	10.71599795	7063.300	13.90118943
4	2994.684	10.71599795	7068.192	13.91081732
4.5	2995.304	9.825031811	7083.902	13.27784377
5	2988.056	9.047314448	7092.800	13.29452191
5.5	2981.579	9.780011819	7103.784	13.31510997
6	2984.341	10.67898718	7115.528	14.00397868
6.5	2989.865	9.807191102	7131.448	14.03531063
7	2991.051	9.811081354	7136.206	13.37588075
7.5	2992.221	9.814919123	7142.291	14.79647431
8	2987.648	9.79991902	7133.170	14.03869968
8.5	2981.12	9.778506232	7124.810	13.35452045
9	2979.504	9.773205518	7126.128	16.49981224
9.5	2973.52	9.753577129	7138.446	16.5283333
10	2970.522	9.743743254	7141.316	14.05473171

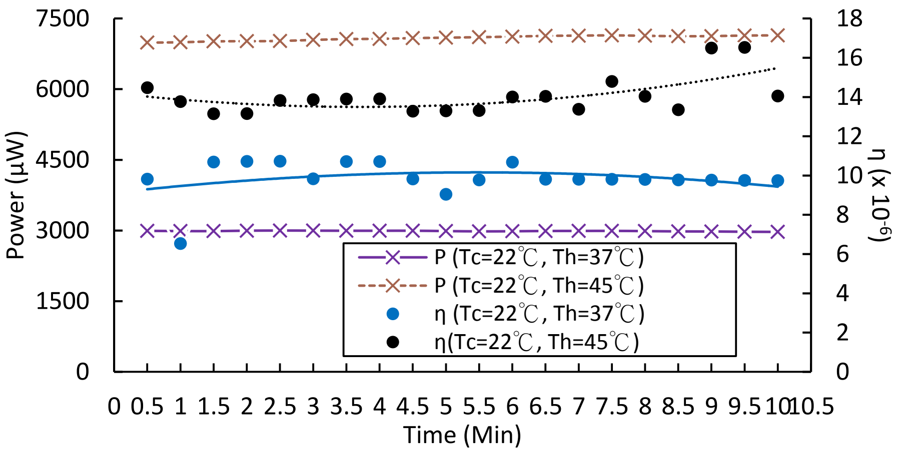

Figure 3-14: P-η-T of BTEM (F) at (T_c=22℃, T_h=37℃) and (T_c=22℃, T_h=45℃)

Table 3.21 and figure 3-14 showed that the conversion efficiency and power at (T_c=22℃, T_h=45℃) were higher than conversion efficiency and power at (T_c=22℃, T_h=37℃). The conversion efficiency was getting lower belong the time at (T_c=22℃, T_h=37℃), and it was getting higher belong the time at (T_c=22℃, T_h=45℃).

3.1.2.1 The Relation of Copper Foil Thickness and Efficiency:

Table 3.22: BTEM (A) and BTEM (B) menu

Module	BTEM (A)	BTEM (B)
Finished product	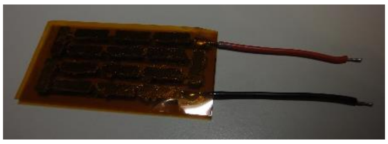	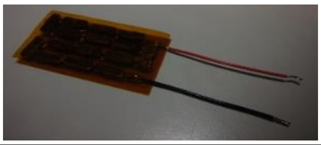
Size	80mm x 42mm x 4.5mm	80mm x 42mm x 6.5mm
Further Explanation	1. 15 Pairs N-type P-type 2. Copper Foil Size: (1mm x 5mm x 16mm)	1. 15 Pairs N-type P-type 2. Copper Foil Size: (2mm x 5mm x 16mm)

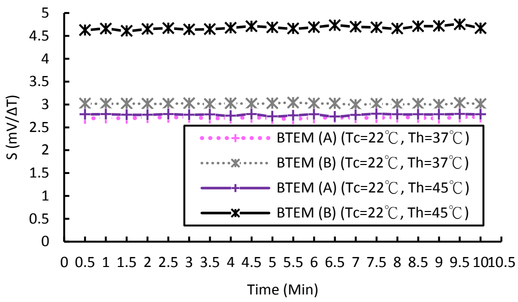

Figure 3-15: S-t in T_c=22℃, T_h=37℃ and 45℃

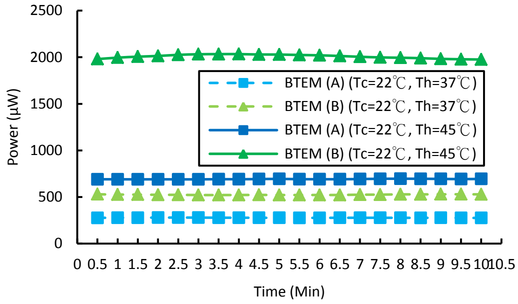

Figure 3-16: P-t in T_c=22℃, T_h=37℃ and 45℃

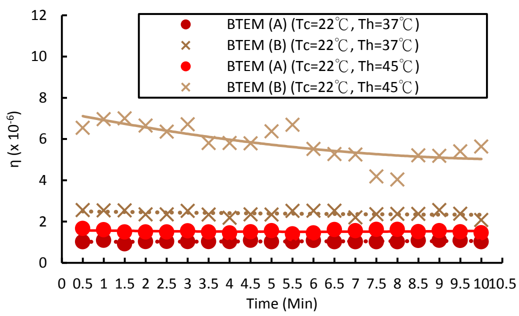

Figure 3-17: η-t in T_c=22℃, T_h=37℃ and 45℃

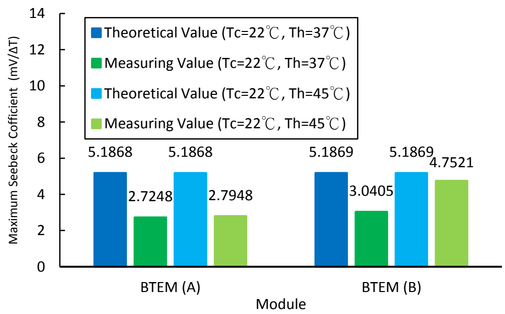

Figure 3-18: maximum Seebeck coefficient of theoretical value and measuring value

The data (Figure 3-15, 3-16, 3-17, 3-18) showed that the copper foil thickness was thicker (BTEM (B)), then the Seebeck coefficient, power output and the conversion efficiency were higher, because the copper foil thickness thicker and the resistivity were lower. The bulk n-type and p-type of BTEM (B) was had higher temperature difference by copper foil thickness thicker was conducted more thermal energy. Although the copper foil thickness thicker could conduct more thermal energy, the conversion efficiency of BTEM (B) was more changeful than BTEM (A). The BTEM (B) at (T_c=22℃, T_h=37℃) in figure 3-18, it had an important point which the measuring value was higher than the theoretical value, but the measuring value still included the deviation value. So, it still was rationalizing value.

3.1.2.2 The Relation of With/Without Fixator and Efficiency:

Table 3.23: BTEM (A) and BTEM (C) menu

Module	BTEM (A)	BTEM (C)
Finished product	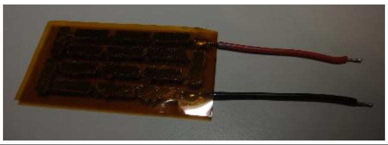	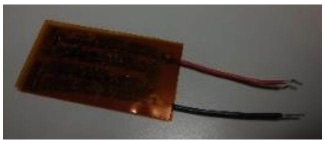
Size	80mm x 42mm x 4.5mm	80mm x 42mm x 4.5mm
Further Explanation	1. 15 Pairs N-type P-type 2. Copper Foil Size: (1mm x 5mm x 16mm)	1. Without Fixator 2. 15 Pairs N-type P-type 3. Copper Foil Size: (1mm x 5mm x 16mm)

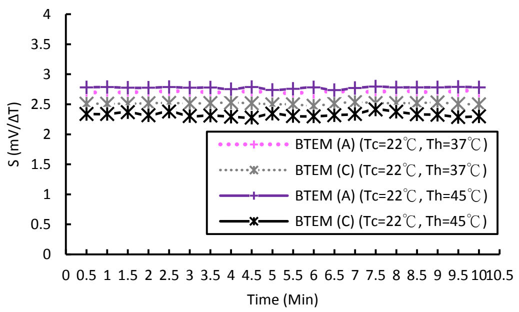

Figure 3-19: S-t in T_c=22℃, T_h=37℃ and 45℃

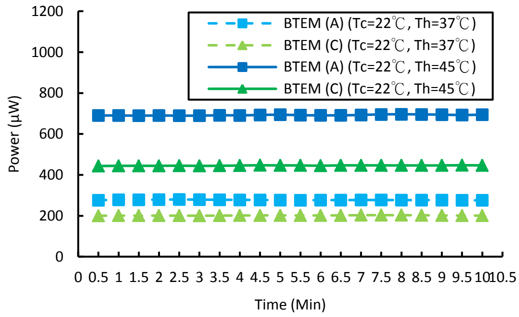

Figure 3-20: P-t in T_c=22℃, T_h=37℃ and 45℃

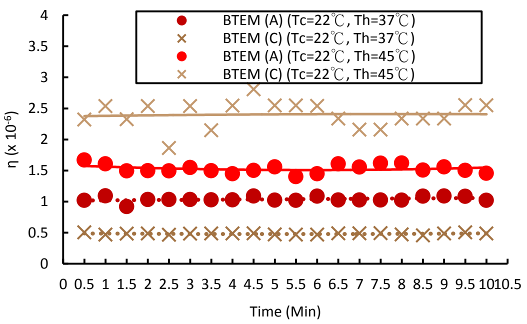

Figure 3-21: η-t in T_c=22℃, T_h=37℃ and 45℃

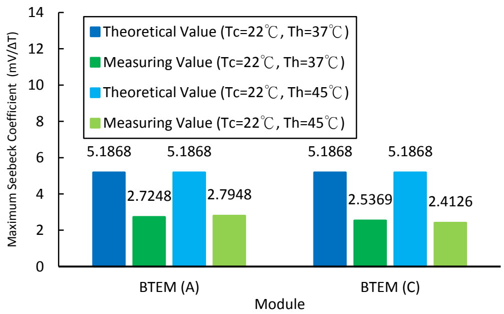

Figure 3-22: maximum Seebeck coefficient of theoretical value and measuring value

The data (Figure 3-19, 3-20, 3-21, 3-22) showed that the power output and Seebeck coefficient of making BTEM (A) with fixator was higher than making BTEM (C) without fixator. Because BTEM (A) was soldered well than BTEM (C), the resistivity of BTEM (A) was lower than BTEM (C). In making method, the pressure was the most crucial variable. It assumed the pressure less that made the solder couldn't melt uniformly in making process. Oppositely, it assumed the pressure more that made the solder could melt uniformly. It caused the conversion efficiency of BTEM (C) was more changeful than BTEM (A) because the solder couldn't melt uniformly, and the temperature couldn't conduct uniformly.

3.1.2.3 The Relation of Copper Foil Area and Efficiency:

Table 3.24: BTEM (A) and BTEM (D) menu

Module	BTEM (A)	BTEM (D)
Finished product	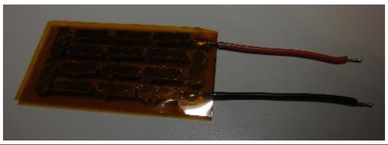	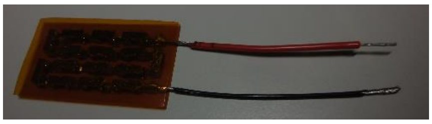
Size	80mm x 42mm x 4.5mm	55mm x 31mm x 4.5mm
Further Explanation	1. 15 Pairs N-type P-type 2. Copper Foil Size: (1mm x 5mm x 16mm)	1. 15 Pairs N-type P-type 2. Copper Foil Size: (1mm x 3mm x 9mm)

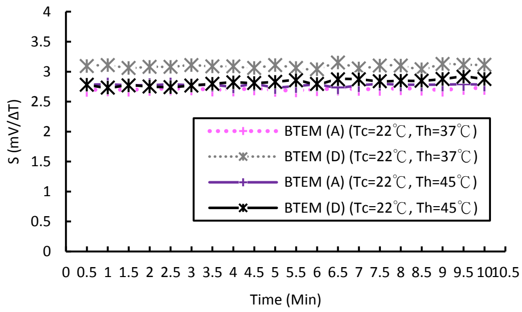

Figure 3-23: S-t in T_c=22℃, Th=37℃ and 45℃

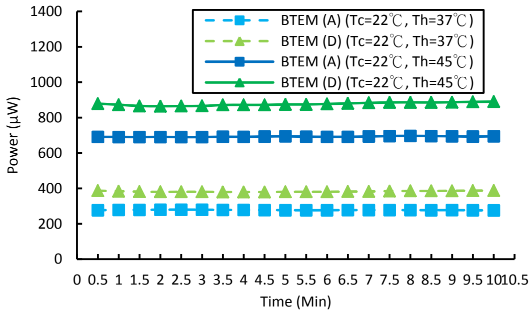

Figure 3-24: P-t in T_c=22℃, T_h=37℃ and 45℃

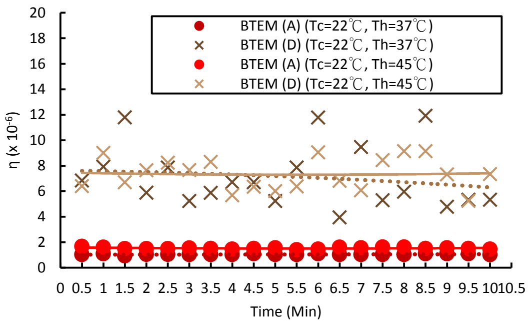

Figure 3-25: η-t in T_c=22℃, T_h=37℃ and 45℃

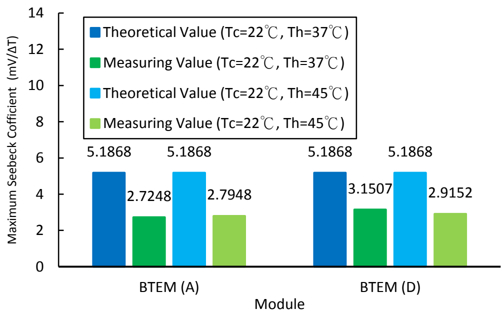

Figure 3-26: maximum Seebeck coefficient of theoretical value and measuring value

The data (Figure 3-23, 3-24, 3-25, 3-26) showed that the copper foil area was smaller (BTEM (D)), the Seebeck coefficient, power output and conversion efficiency were higher, because the circuit was less and the resistivity was lower. The figure 3-23 showed the Seebeck coefficient of BTEM (A) and BTEM (D) were getting higher belong the time. The figure 3-26 BTEM (A) showed that the measuring value at (T_c=22℃, T_h=45℃) was higher than it at (T_c=22℃, T_h=37℃), but the measuring value of BTEM (D) at (T_c=22℃, T_h=37℃) was higher than the measuring value of BTEM (D) at (T_c=22℃, T_h=45℃).

3.1.2.4 The Relation of Improved Fixator and Efficiency:

Table 3.25: BTEM (D) and BTEM (E) menu

Module	BTEM (D)	BTEM (E)
Finished product	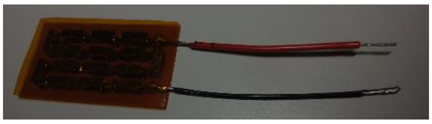	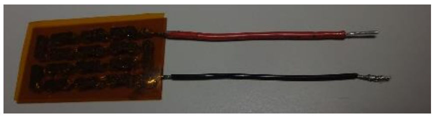
Size	55mm x 31mm x 4.5mm	55mm x 31mm x 4.5mm
Further Explanation	1. 15 Pairs N-type P-type 2. Copper Foil Size: (1mm x 3mm x 9mm)	1. 15 Pairs N-type P-type 2. Copper Foil Size: (1mm x 3mm x 9mm) 3. Use Improved Fixator

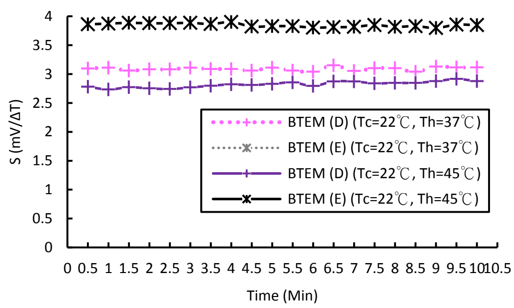

Figure 3-27: S-t in T_c=22℃, T_h=37℃ and 45℃

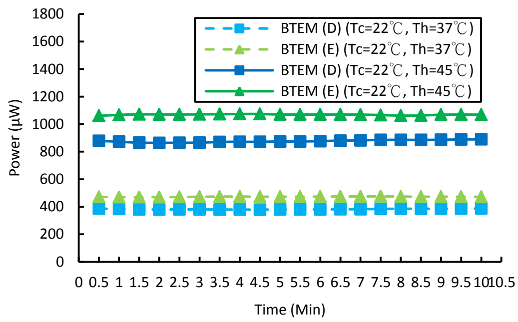

Figure 3-28: P-t in T_c=22℃, T_h=37℃ and 45℃

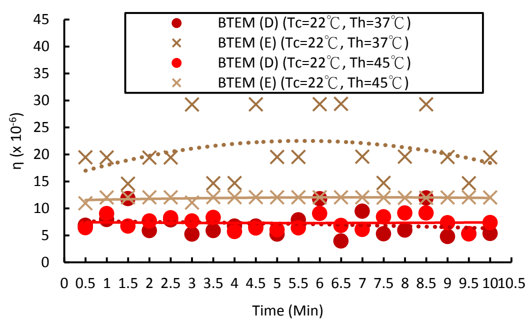

Figure 3-29: η-t in T_c=22℃, T_h=37℃ and 45℃

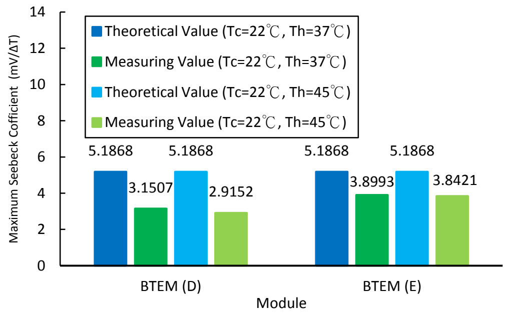

Figure 3-30: maximum Seebeck coefficient of theoretical value and measuring value

The data (Figure 3-27, 3-28, 3-29, 3-30) showed that the power output and conversion efficiency of making BTEM (E) with improved fixator was higher than making BTEM (D) with before improved fixator. Because the BTEM (E) was soldered well than BTEM (D), the resistivity of BTEM (E) was lower than BTEM (D).

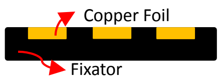

Figure 3-31: fixator of BTEM (D) in schematic

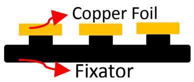

Figure 3-32: fixator of BTEM (E) in schematic

When making BTEM (E) with fixator, the flux could not flow on the fixator.(figure 3-32) But the flux could flow on the fixator when making BTEM (D) with fixator that it let the copper foil stick on fixator to hardly take the copper foil out.(figure 3-31)

3.1.2.5 The Relation of N-type P-type Pairs and Efficiency:

Table 3.26: BTEM (D) and BTEM (F) menu

Module	BTEM (D)	BTEM (F)
Finished product	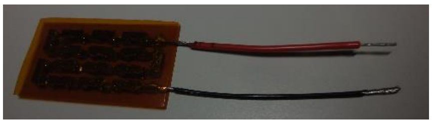	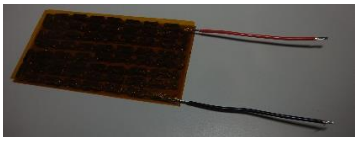
Size	55mm x 31mm x 4.5mm	99mm x 47mm x 4.5mm
Further Explanation	1. 16 Pairs N-type P-type 2. Copper Foil Size: (1mm x 3mm x 9mm)	1. 64 Pairs N-type P-type 2. Copper Foil Size: (1mm x 3mm x 9mm)

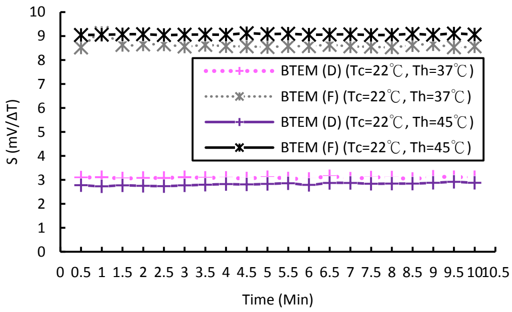

Figure 3-33: S-t in T_c=22℃, T_h=37℃ and 45℃

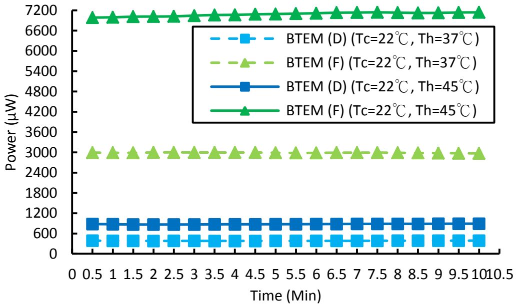

Figure 3-34: P-t in T_c=22℃, T_h=37℃ and 45℃

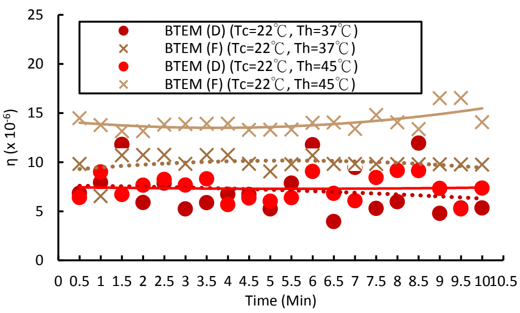

Figure 3-35: η-t in T_c=22℃, T_h=37℃ and 45℃

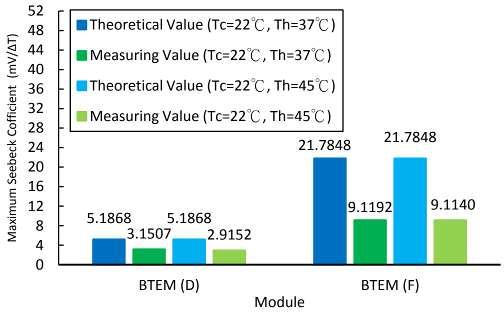

Figure 3-36: maximum Seebeck coefficient of theoretical value and measuring value

The data (Figure 3-81, 3-82, 3-83 and Table 3.13) showed that the more the n-type p-type pairs were, the power output and conversion were higher. The figure 3-35 showed the line of BTEM (D) and the line of BTEM (F) at (T_c=22℃, T_h=45℃) both had the same trend. The conversion efficiency was as high as belong the time. Oppositely, the conversion efficiency at (T_c=22℃, T_h=37℃) was getting lower belong the time. So, that showed the trends of conversion efficiency were the same of BTEM (F) (n-type and p-type pairs more) and BTEM (D). The figure 3-36 showed the trends of Seebeck coefficient were also the same of BTEM (F) (n-type and p-type pairs more) and BTEM (D).

3.1.2.6 Maximum Power Output per 1 cm^2 and Conversion Efficiency:

Table 3.27: load resistance in room temperature

BTEM	(A)	(B)	(C)	(D)	(E)	(F)
R_{RT}(Ω)	0.0691	0.0645	0.1021	0.9644	0.082	0.328

Table 3.28: maximum value of all BTEMs

	T_c=22℃, T_h=37℃					T_c=22℃, T_h=45℃				
BTEM	V(mV)	I(mA)	R(Ω)	P(μW)	η(x 10^{-6})	V(mV)	I(mA)	R(Ω)	P(μW)	η(x 10^{-6})
(A)	41.3	6.77	131.3	279.6	1.091	64	10.88	157.3	696.3	1.667
(B)	45.2	11.72	101.4	529.7	2.556	113.6	17.9	237	2033	6.997
(C)	37.8	5.38	101.6	203.3	0.505	54	8.28	120.3	447.1	2.807
(D)	46.4	8.35	100.5	387.4	11.91	65.3	13.63	140.7	890	9.136
(E)	58.5	8.13	126.8	475.6	29.36	87.8	12.23	190.8	1073	12.07
(F)	138.4	21.67	286.4	2999	10.73	208.9	34.19	1216	7142	16.53

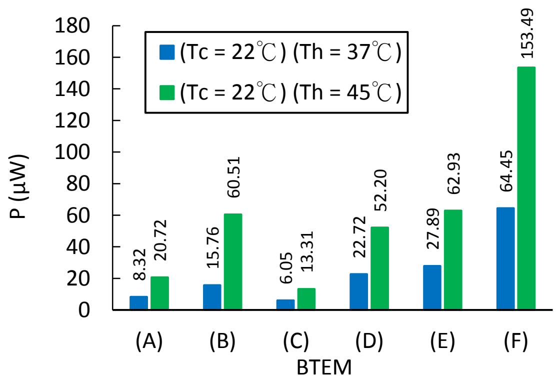

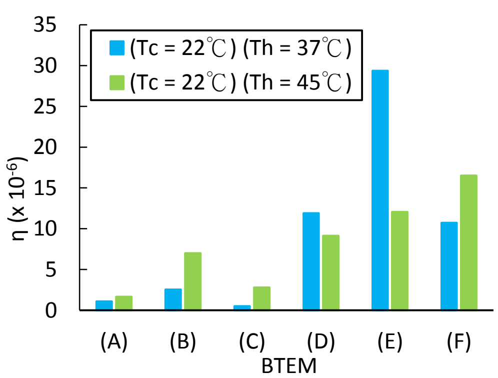

Figure 3-37: maximum power output of BTEMs per 1cm^2 Figure 3-38: maximum conversion efficiency

The figure 3-37 showed the power output was higher belong the temperature was higher. In this study, the data (BTEM (A) and (BTEM (C)), (BTEM (D) and BTEM (E) showed an important point that it was the relation of soldering and power output. And soldering well or worse was related to the variable pressure. Besides, making high power output and high efficiency module wasn't only having a way, the other way was raised the n-type and p-type pairs. The data (BTEM (D) and BTEM (F)) showed the power output and conversion efficiency were higher the n-type and p-type pairs more. Therefore, the study of BTEM could be got the conclusion which making high power output and high conversion efficiency modules must have 3 points. First, took the area of substrate smaller. Second, take the n-type and p-type pairs more. Third, modules made with improved fixator.

3.1.3 Theoretical Value Comparison of TTEM and FTEM:

The data (table 3.29 to 3.34 and figure 3-39, 3-40) of TTEM and FTEMs showed the theoretical of temperature difference, Seebeck coefficient and voltage every BTEM at (T_c=22℃, T_h=37℃) and (T_c=22℃, T_h=45℃).

Table 3.29: data of TTEM

Material	n-type	p-type	Copper	Ceramic	Bi/Sn Solder	Thermal grease
Touch Area(m^2)	9×10^{-6}	9×10^{-6}	9×10^{-6}	9×10^{-6}	9×10^{-6}	9×10^{-6}
Length (m)	2.4×10^{-3}	2.4×10^{-3}	3×10^{-4}	6.5×10^{-4}	5×10^{-5}	2×10^{-5}
Seebeck coefficient (VK^{-1})	-1.50×10^{-4}	1.96×10^{-4}	N/A	N/A	N/A	N/A
Resistivity (Ωm)	1.89×10^{-5}	1.53×10^{-5}	1.7×10^{-1}	1×10^{12}	3×10^{-8}	N/A
Thermal conductivity ($Wm^{-1}K^{-1}$)	1.75	1.57	401	22	2×10^{-1}	1
Thermal resistivity (KW^{-1})	1.524×10^{2}	1.698×10^{2}	1.1×10^{-1}	3.28283	3×10^{-1}	2.22222
Z (K^{-1})	2.45×10^{-3}	3.77×10^{-3}	N/A	N/A	N/A	N/A

Table 3.30: data of 1st FTEM

Material	n-type	p-type	Copper	Polyimide	Bi/Sn Solder	Thermal grease
Touch Area(m^2)	9×10^{-6}	9×10^{-6}	9×10^{-6}	9×10^{-6}	9×10^{-6}	9×10^{-6}
Length (m)	2.4×10^{-3}	2.4×10^{-3}	1.2×10^{-4}	2.5×10^{-4}	5×10^{-5}	2×10^{-5}
Seebeck coefficient (VK^{-1})	-1.50×10^{-4}	1.96×10^{-4}	N/A	N/A	N/A	N/A
Resistivity (Ωm)	1.89×10^{-5}	1.53×10^{-5}	1.7×10^{-1}	N/A	3×10^{-8}	N/A
Thermal conductivity ($Wm^{-1}K^{-1}$)	1.75	1.57	401	1.65×10^{-1}	2×10^{-1}	1
Thermal resistivity (KW^{-1})	1.524×10^{3}	1.698×10^{2}	3.3×10^{-2}	1.68×10^{2}	3×10^{-1}	2.22222
Z (K^{-1})	2.45×10^{-3}	3.77×10^{-3}	N/A	N/A	N/A	N/A

Table 3.31: data of 2nd FTEM

Material	n-type	p-type	Copper	Polyimide	Bi/Sn Solder	Thermal grease
Touch Area(m^2)	9×10^{-6}	9×10^{-6}	9×10^{-6}	9×10^{-6}	9×10^{-6}	9×10^{-6}
Length (m)	2.4×10^{-3}	2.4×10^{-3}	3.6×10^{-4}	2.5×10^{-4}	5×10^{-5}	2×10^{-5}
Seebeck coefficient (VK^{-1})	-1.50×10^{-4}	1.96×10^{-4}	N/A	N/A	N/A	N/A
Resistivity (Ωm)	1.89×10^{-5}	1.53×10^{-5}	1.7×10^{-1}	N/A	3×10^{-8}	N/A
Thermal conductivity ($Wm^{-1}K^{-1}$)	1.75	1.57	401	1.65×10^{-1}	2×10^{-1}	1
Thermal resistivity (KW^{-1})	1.524×10^{3}	1.698×10^{2}	1×10^{-1}	1.68×10^{2}	3×10^{-1}	2.22222
Z (K^{-1})	2.45×10^{-3}	3.77×10^{-3}	N/A	N/A	N/A	N/A

Table 3.32: equations of TTEM and FTEM practical temperature difference (ΔT_{TEM})

Module	ΔT_{TEM} equation
TTEM	$\Delta T_{TTEM} = 0.95766097 \times (T_h - T_c)$
1st FTEM	$\Delta T_{1^{st}\ FTEM} = 0.99910811 \times (T_h - T_c)$
2nd FTEM	$\Delta T_{2^{nd}\ FTEM} = 0.99910847 \times (T_h - T_c)$

Table 3.33: TTEM, 1st FTEM and 2nd FTEM theoretical value at T_c=22℃, T_h=37℃

Module	TTEM	1st FTEM	2nd FTEM
ΔT_{TEM} (℃)	14.36491449	14.98662172	14.98662704
Seebeck coefficient (mV/ΔT)	5.6329618	5.87675393	10.71643744
Voltage (mV)	84.49442703	88.15130893	160.74656166

Table 3.34: TTEM, 1st FTEM and 2nd FTEM theoretical value at T_c=22℃, T_h=45℃

Module	TTEM	1st FTEM	2nd FTEM
ΔT_{TEM} (℃)	22.02620222	22.97948663	22.9794948
Seebeck coefficient (mV/ΔT)	5.6329618	5.87675393	10.71643744
Voltage (mV)	129.55812144	135.16534036	246.47806122

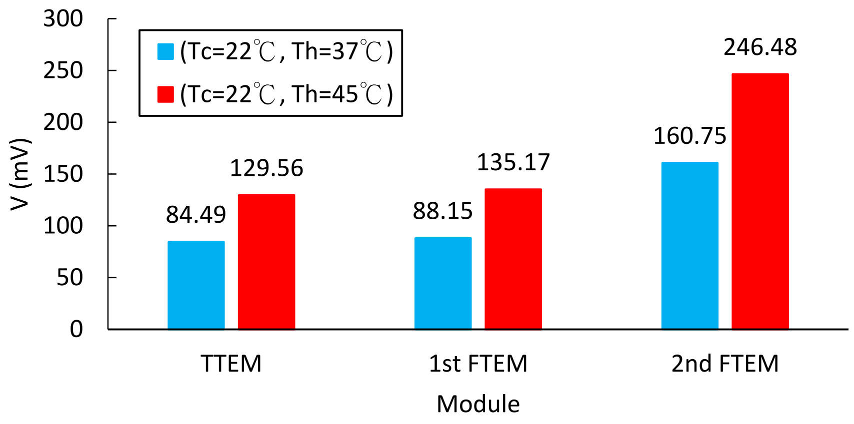

Figure 3-39: voltage of TTEM, FTEMs at (T_c=22℃, T_h=37℃) and (T_c=22℃, T_h=45℃)

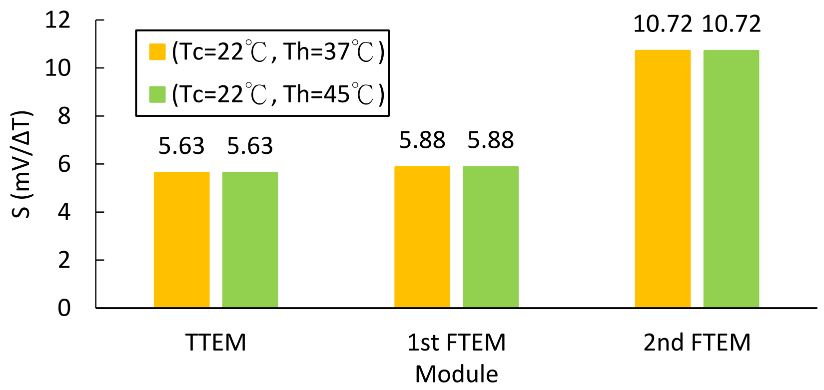

Figure 3-40: Seebeck coefficient of TTEM, FTEMs at (T_c=22℃, T_h=37℃) and (T_c=22℃, T_h=45℃)

The data (table 3.33, 3.34 and figure 3-39, 3-40) showed that the TTEM, FTEMs had the same Seebeck coefficient at (T_c=22℃, T_h=37℃) and (T_c=22℃, T_h=45℃) itself, and the FTEMs had the best voltage and Seebeck coefficient. It proved the assumption that the Eq. (1.15) $Z=S^2\sigma/\kappa$ for the different substrate of module, power factor ($S^2\sigma$) was supposed constant. Then the Z value was proportional to κ (thermal conductivity). The ceramic had higher thermal conductivity, and the Polyimide (PI) had less thermal conductivity, so the voltage of FTEMs were higher than TTEM.

3.1.4 Measuring Value of TTEM and FTEM (Flat Surface Measurement):

TTEM:

Table 3.35: Seebeck coefficient and current of TTEM at (T_c=22℃, T_h=37℃) and (T_c=22℃, T_h=45℃)

Seebeck coefficient and Current (I) / Time (Min)	Tc=22℃, Th=37℃, ΔT=15℃		Tc=22℃, Th=45℃, ΔT=23℃	
	S (mV/ΔT)	I (mA)	S (mV/ΔT)	I (mA)
0.5	3.887417219	13.18	6.064655172	20.57
1	3.887417219	13.16	6.008547009	20.5
1.5	3.894039735	13.18	6.056034483	20.42
2	3.906666667	13.19	6.021459227	20.39
2.5	4.006849315	13.2	6.025751073	20.31
3	3.886666667	13.21	6.104347826	20.23
3.5	3.906040268	13.25	6.095652174	20.21
4	3.952380952	13.28	6.004273504	20.2
4.5	3.945578231	13.28	6.113043478	20.2
5	3.97260274	13.24	6.108695652	20.15
5.5	3.918918919	13.21	6.082251082	20.11
6	3.873333333	13.21	6.135371179	20.07
6.5	3.925675676	13.21	6.056034483	20.03
7	3.88590604	13.23	6.030042918	20.01
7.5	3.925170068	13.24	6.193832599	20
8	3.905405405	13.24	6.042918455	20
8.5	3.88590604	13.21	6.095238095	20.03
9	3.95890411	13.2	6.117391304	20.02
9.5	3.993103448	13.19	6.090909091	20
10	3.925675676	13.17	6.012820513	20.02

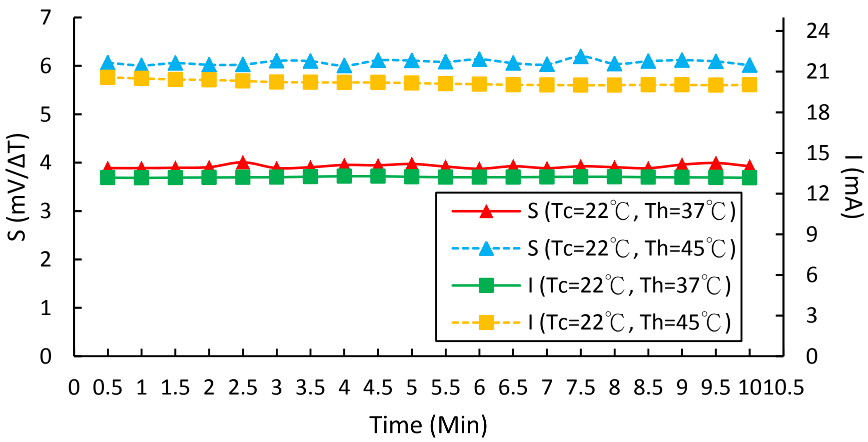

Figure 3-41: S-I-T of TTEM at (T_c=22℃, T_h=37℃) and (T_c=22℃, T_h=45℃)

Table 3.35 and figure 3-41 showed that the Seebeck coefficient at (T_c=22℃, T_h=45℃) was higher than Seebeck coefficient at (T_c=22℃, T_h=37℃), and the current also.

Table 3.36: power and conversion efficiency of TTEM at (T_c=22℃, T_h=37℃) and (T_c=22℃, T_h=45℃)

Time (Min) \ Power and conversion efficiency (η)	Tc=22℃, Th=37℃, ΔT=15℃		Tc=22℃, Th=45℃, ΔT=23℃	
	Power (μW)	η (x 10^{-6})	Power (μW)	η (x 10^{-6})
0.5	773.666	51.00646097	2894.199	19.08095332
1	772.492	25.46453059	2882.300	19.00250527
1.5	774.984	17.03111814	2869.010	18.9148866
2	772.934	25.47910074	2860.717	18.86021229
2.5	772.2	20.36392405	2851.524	18.79960443
3	770.143	25.38709784	2840.292	6.687697785
3.5	771.15	20.33623418	2833.442	6.124718994
4	771.568	20.34725738	2838.100	6.342746549
4.5	770.24	50.78059072	2840.120	6.040135429
5	767.92	25.31381857	2831.075	6.436133693
5.5	766.18	50.51292194	2825.455	6.423357249
6	767.501	20.24000527	2819.835	6.196894778
6.5	767.501	50.60001319	2814.215	6.397804361
7	766.017	25.25108782	2811.405	6.994379926
7.5	763.948	50.36577004	2812.000	6.995860202
8	765.272	50.45305907	2816.000	6.751054852
8.5	764.859	50.4258307	2820.224	6.523946998
9	762.96	25.15031646	2816.814	5.895481716
9.5	763.701	50.34948576	2814.000	5.984585545
10	765.177	50.44679589	2816.814	6.088776198

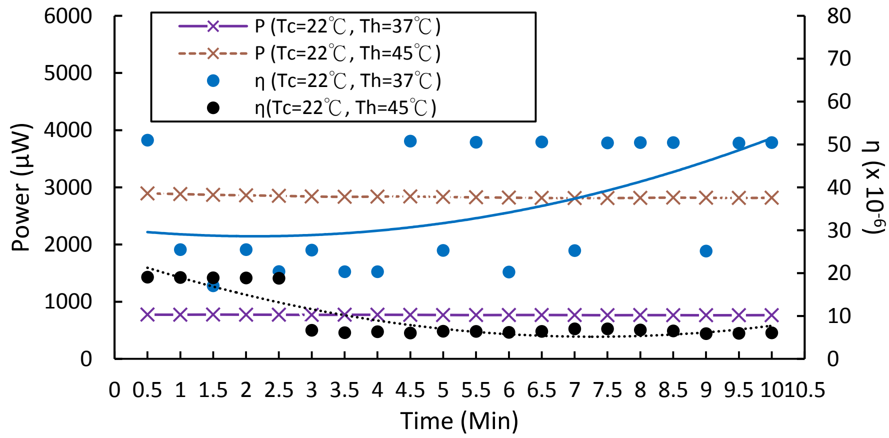

Figure 3-42: P-η-T of TTEM at (T_c=22℃, T_h=37℃) and (T_c=22℃, T_h=45℃)

Figure 3-42 and table 3.36 showed the conversion efficiency of TTEM at (T_c=22℃, T_h=37℃) was getting high belong the time, but the conversion efficiency at (T_c=22℃, T_h=45℃) was getting low belong the time. And the power output was as high as belong the temperature as high as.

1^{st} FTEM:

Table 3.37: Seebeck coefficient and current of 1^{st} FTEM at (T_c=22℃, T_h=37℃) and (T_c=22℃, T_h=45℃)

Seebeck coefficient and Current (I) / Time (Min)	Tc=22℃, Th=37℃, ΔT=15℃		Tc=22℃, Th=45℃, ΔT=23℃	
	S (mV/ΔT)	I (mA)	S (mV/ΔT)	I (mA)
0.5	6.647058824	16.03	7.01754386	24.38
1	6.597402597	15.98	7.035087719	24.39
1.5	6.697368421	15.94	7.039473684	24.4
2	6.690789474	15.88	6.952380952	24.4
2.5	6.715231788	15.82	6.991304348	24.39
3	6.726666667	15.77	7.057017544	24.37
3.5	6.72	15.73	7.021834061	24.38
4	6.77852349	15.69	6.995652174	24.4
4.5	6.785234899	15.66	7.052631579	24.39
5	6.785234899	15.63	7.017467249	24.38
5.5	6.798657718	15.61	7.052631579	24.39
6	6.721854305	15.6	7.061403509	24.39
6.5	6.715231788	15.59	7.026200873	24.34
7	6.708609272	15.59	7.083700441	24.32
7.5	6.671052632	15.59	6.991304348	24.37
8	6.708609272	15.57	6.892703863	24.41
8.5	6.701986755	15.57	6.991304348	24.43
9	6.664473684	15.55	7.083700441	24.41
9.5	6.721854305	15.54	7.017467249	24.39
10	6.786666667	15.56	6.97826087	24.37

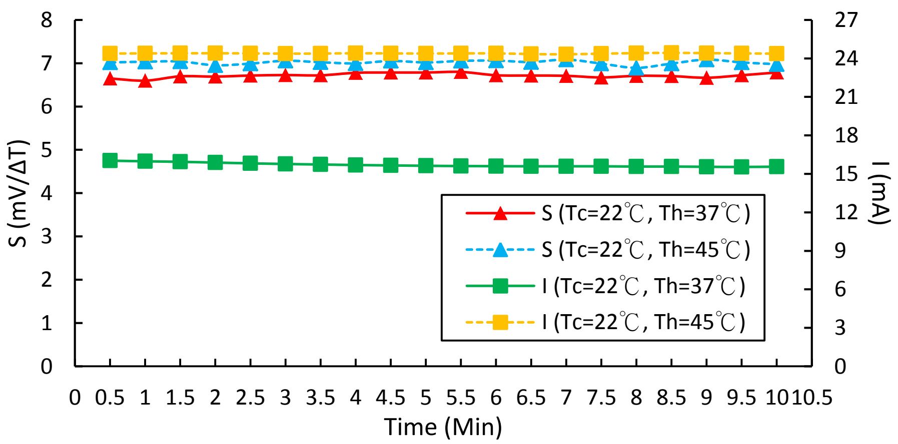

Figure 3-43: S-I-T of 1^{st} FTEM at (T_c=22℃, T_h=37℃) and (T_c=22℃, T_h=45℃)

Table 3.37 and figure 3-43 showed that the Seebeck coefficient at (T_c=22℃, T_h=45℃) was higher than Seebeck coefficient at (T_c=22℃, T_h=37℃), and the current also.

Table 3.38: power and conversion efficiency of 1st FTEM at (T_c=22℃, T_h=37℃) and (T_c=22℃, T_h=45℃)

Time (Min) \ Power and conversion efficiency (η)	Tc=22℃, Th=37℃, ΔT=15℃		Tc=22℃, Th=45℃, ΔT=23℃	
	Power (μW)	η (x 10^{-6})	Power (μW)	η (x 10^{-6})
0.5	1630.251	107.4796282	3900.800	9.351745301
1	1623.568	53.51951477	3912.156	9.73289348
1.5	1622.692	35.66042546	3916.200	9.93031889
2	1614.996	53.2369462	3918.640	9.394514768
2.5	1604.148	42.30348101	3921.912	9.576476793
3	1591.193	52.4523009	3921.133	9.232625546
3.5	1585.584	41.81392405	3920.304	8.474061009
4	1584.69	41.7903481	3925.960	8.773957663
4.5	1583.226	104.3793513	3921.912	8.340802368
5	1580.193	52.08969541	3917.866	8.906831987
5.5	1581.293	208.5038238	3921.912	8.916030118
6	1583.4	41.75632911	3926.790	8.629549051
6.5	1580.826	208.4422468	3916.306	8.903285501
7	1579.267	52.05917062	3910.656	9.729161691
7.5	1580.826	104.2211234	3918.696	9.749164079
8	1577.241	103.9847706	3920.246	9.398364979
8.5	1575.684	103.8821203	3928.344	9.087330668
9	1575.215	51.92559995	3925.128	8.215139642
9.5	1577.31	103.9893196	3919.473	8.335615302
10	1584.008	208.8618143	3911.385	8.454781853

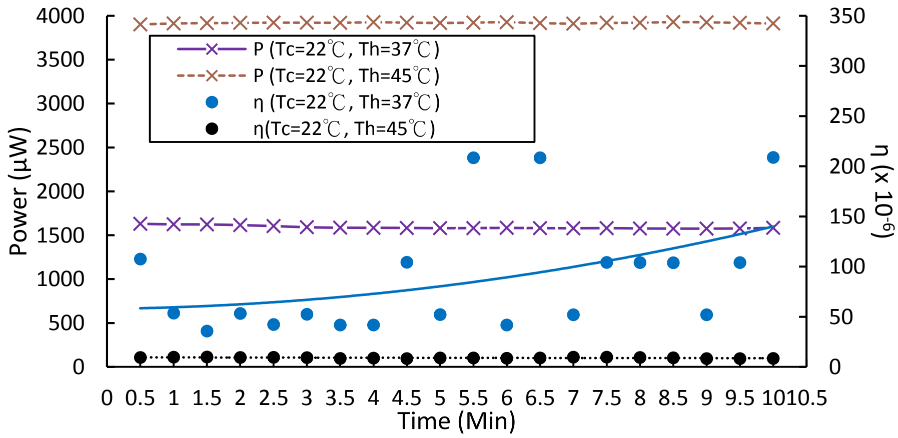

Figure 3-44: P-η-T of 1st FTEM at (T_c=22℃, T_h=37℃) and (T_c=22℃, T_h=45℃)

Figure 3-44 and table 3.38 showed the conversion efficiency of TTEM at (T_c=22℃, T_h=37℃) was getting high belong the time, but the conversion efficiency at (T_c=22℃, T_h=45℃) was getting low belong the time, the power output at (T_c=22℃, T_h=45℃) was also.

2nd FTEM:

Table 3.39: Seebeck coefficient and current of TTEM at (T_c=22℃, T_h=37℃) and (T_c=22℃, T_h=45℃)

Seebeck coefficient and Current (I) / Time (Min)	Tc=22℃, Th=37℃, ΔT=15℃		Tc=22℃, Th=45℃, ΔT=23℃	
	S (mV/ΔT)	I (mA)	S (mV/ΔT)	I (mA)
0.5	7.948051948	18.91	9.602678571	34
1	7.484662577	18.91	8.884297521	33.99
1.5	7.635220126	18.91	9.388646288	34.01
2	8.033112583	18.91	9.11440678	33.97
2.5	8.06	18.9	9.7239819	33.99
3	8.100671141	18.9	9.205128205	33.91
3.5	7.934210526	18.89	9.65470852	33.96
4	7.572327044	18.88	10.15566038	33.94
4.5	7.836601307	18.87	9.397379913	33.95
5	7.729032258	18.88	9.751131222	33.97
5.5	7.830065359	18.87	9.707207207	33.96
6	7.830065359	18.85	9.66367713	33.95
6.5	8.081081081	18.87	9.940092166	33.99
7	8.298611111	18.88	9.539823009	34.04
7.5	7.666666667	18.88	10.12206573	34.01
8	8.040268456	18.88	9.629464286	33.98
8.5	7.636942675	18.87	9.8	33.98
9	7.540880503	18.86	9.222222222	34.01
9.5	7.933774834	18.85	9.69058296	34.03
10	8.142857143	18.86	9.738738739	34.03

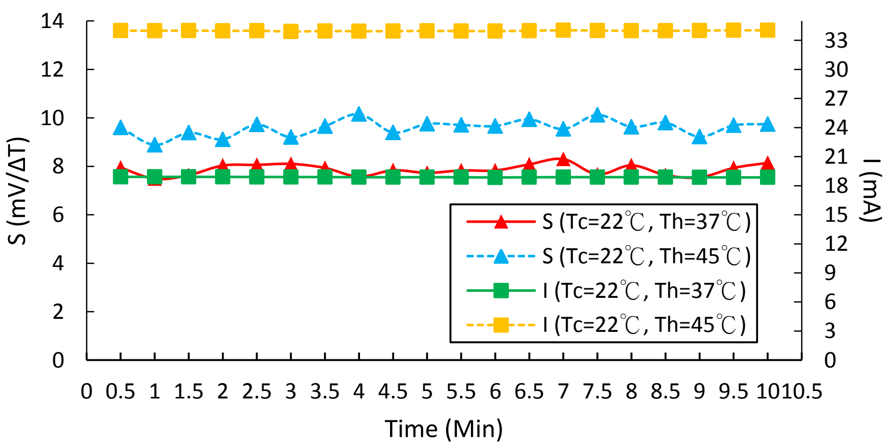

Figure 3-45: S-I-T of 2nd FTEM at (T_c=22℃, T_h=37℃) and (T_c=22℃, T_h=45℃)

Table 3.39 and figure 3-45 showed that the Seebeck coefficient at (T_c=22℃, T_h=45℃) was higher than Seebeck coefficient at (T_c=22℃, T_h=37℃).

Table 3.40: power and conversion efficiency of 2nd FTEM at (T_c=22℃, T_h=37℃) and (T_c=22℃, T_h=45℃)

Power and conversion efficiency (η) / Time (Min)	Tc=22℃, Th=37℃, ΔT=15℃		Tc=22℃, Th=45℃, ΔT=23℃	
	Power (μW)	η (x 10^{-6})	Power (μW)	η (x 10^{-6})
0.5	2314.584	21.79950271	7313.400	24.10799051
1	2307.02	50.69927918	7307.850	29.1996308
1.5	2295.674	37.83745385	7312.150	25.37249473
2	2293.783	20.16335267	7306.947	28.33731618
2.5	2285.01	21.52096519	7304.451	24.0784909
3	2281.23	18.79969343	7304.214	27.51738246
3.5	2278.134	25.03223892	7311.588	24.10201741
4	2273.152	29.97299578	7307.282	22.94078386
4.5	2262.513	24.86059467	7306.040	28.33379871
5	2261.824	21.30259192	7320.535	24.75026709
5.5	2260.626	21.29130877	7318.380	26.08043962
6	2258.23	18.61014966	7316.225	26.07275986
6.5	2256.852	21.25576401	7331.643	24.16812698
7	2256.16	15.65733955	7339.024	27.64852321
7.5	2258.048	21.26702833	7332.556	22.48477824
8	2261.824	19.88241913	7329.486	25.43264907
8.5	2262.513	29.83271361	7326.088	24.76904144
9	2261.314	33.12989334	7339.358	26.15519871
9.5	2258.23	22.90479958	7353.883	24.24143921
10	2257.542	21.26226266	7357.286	23.66112869

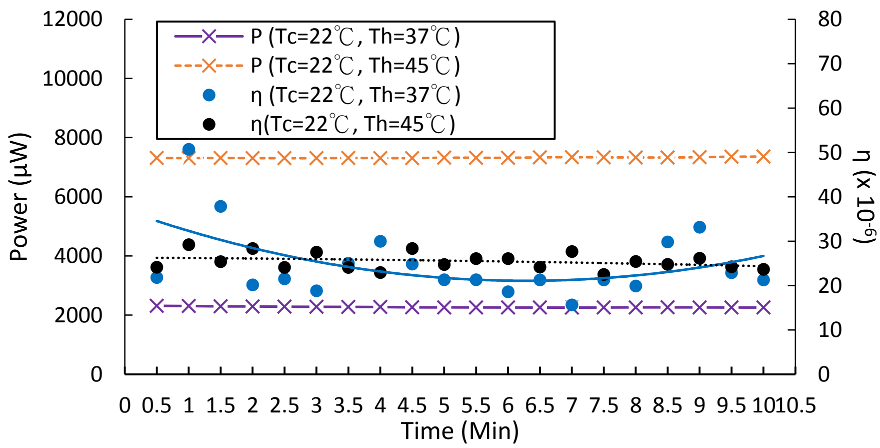

Figure 3-46: P-η-T of 2nd FTEM at (T_c=22℃, T_h=37℃) and (T_c=22℃, T_h=45℃)

Figure 3-46 and table 3.40 showed the conversion efficiency of TTEM at (T_c=22℃, T_h=37℃) had the minimum in 7 second, and the conversion efficiency of TTEM at (T_c=22℃, T_h=45℃) had the maximum in 1 second. And the power output was as high as belong the temperature as high as.

3.1.4.1 The Efficiency and Power of TTEM and 1st FTEM Comparison:

Table 3.41: TTEM and 1st FTEM menu

Module	TTEM	1st FTEM
Finished product		
Size	40mm x 40mm x 2.6mm	40mm x 40mm x 2.6mm
Further Explanation	1. Ceramic Substrate 2. 17 Pairs N-type P-type 3. Copper Foil Area (3mm x 9mm)	1. 2L FFCCL Substrate 2. 17 Pairs N-type P-type 3. Copper Foil Area: (3mm x 9mm)

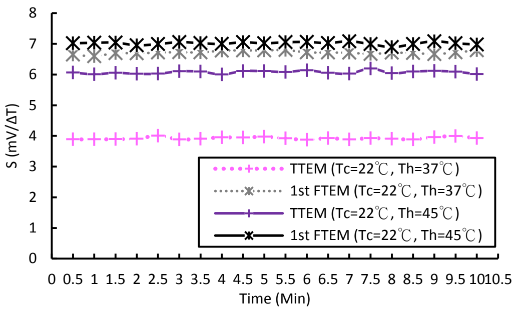

Figure 3-47: S-t in T_c=22℃, T_h=37℃ and 45℃

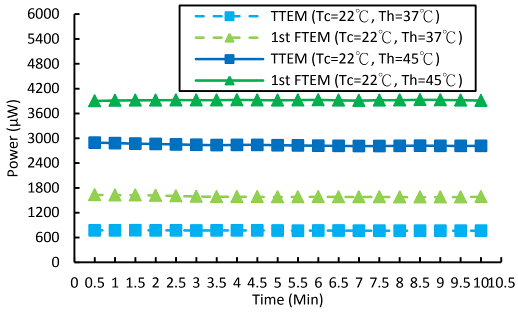

Figure 3-48: P-t in T_c=22℃, T_h=37℃ and 45℃

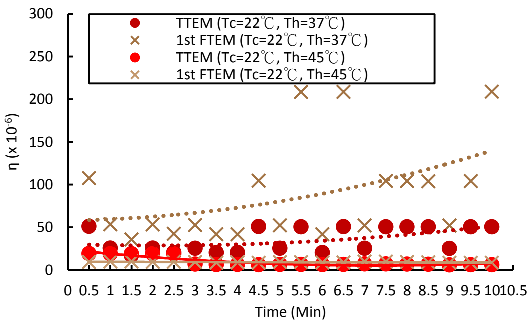

Figure 3-49: η-t in T_c=22℃, T_h=37℃ and 45℃

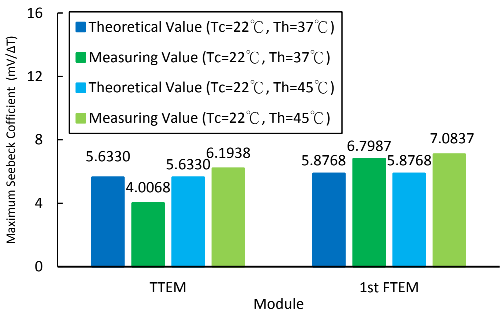

Figure 3-50: maximum Seebeck coefficient of theoretical value and measuring value

The data (Figure 3-47, 3-48, 3-49 and 3-50) showed that the Seebeck coefficient, power output and conversion efficiency of 1st FTEM are higher than TTEM. It proved the assumption that the Eq. (1.15) $Z=S^2\sigma/\kappa$ for the different surface materials of module, power factor ($S^2\sigma$) was supposed constant. Then the Z value was proportional to κ (thermal conductivity). The ceramic had higher thermal conductivity, and the Polyimide (PI) had less thermal conductivity, so the power output and conversion efficiency of 1st FTEM were higher than TTEM. The figure 3-50 showed the measuring value of TTEM at T_c=22℃, T_h=45℃ and the measuring value of 1st FTEM T_c=22℃, T_h=37℃ and 45℃ were higher the theoretical value.

3.1.4.2 The Efficiency and Power of 1st FTEM and 2nd FTEM Comparison:

Table 3.42: 1st FTEM and 2nd FTEM menu

Module	1st FTEM	2nd FTEM
Finished product		
Size	40mm x 40mm x 2.6mm	40mm x 40mm x 2.6mm
Further Explanation	1. 2L FCCL Substrate 2. 17 Pairs N-type P-type 3. Copper Foil Area: (3mm x 9mm)	1. 3L FCCL Substrate 2. 31 Pairs N-type P-type 3. Copper Foil Area: ($2 \times 9mm^2 + 2mm^2$)

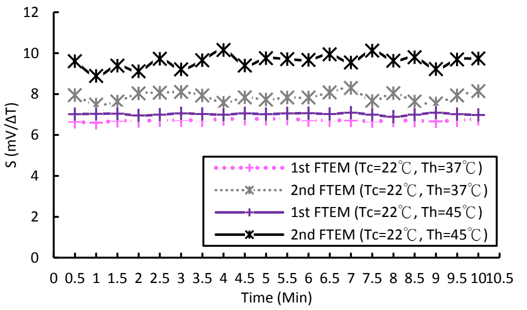

Figure 3-51: S-t in Tc=22℃, Th=37℃ and 45℃

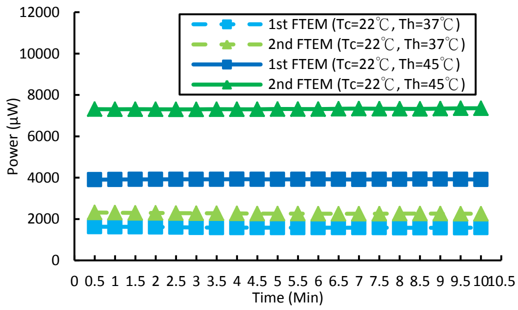

Figure 3-52: P-t in Tc=22℃, Th=37℃ and 45℃

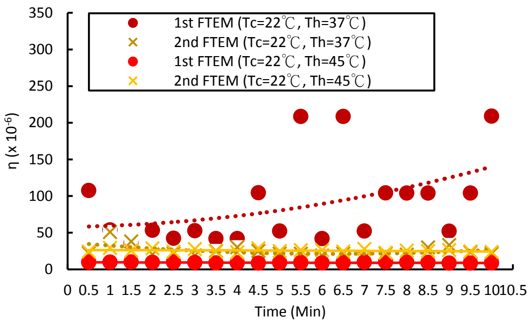

Figure 3-53: η-t in Tc=22℃, Th=37℃ and 45℃

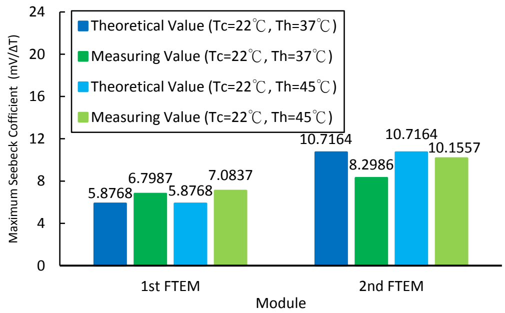

Figure 3-54: maximum Seebeck coefficient of theoretical value and measuring value

The data (figure 3-51, 3-52, 3-53 and 3-54) showed the Seebeck coefficient and power output of 2nd FTEM was higher than the Seebeck coefficient and power output of 1st FTEM, but the conversion efficiency of 2nd FTEM at T_c=22℃, T_h=37℃ was lower than the conversion efficiency of 1st FTEM at T_c=22℃, T_h=37℃. Due to the n-type and p-type pairs of 2nd FTEM was more than the n-type and p-type of 1st FTEM, the bulk material total area and the thermal energy flux into bulk material of 2nd FTEM were more than the bulk material total area and the thermal energy flux into bulk material of 1st FTEM. The equation $\mathrm{P} = Q_{flux} \times \eta$ could be explained that Q_{flux} of 2nd FTEM was higher than Q_{flux} of 1st FTEM, but η had no big difference. So, the power of 2nd FTEM was higher than the power of 1st FTEM.

3.1.4.3 Maximum Power Output per 1 cm^2 and Conversion Efficiency:

Table 3.43: load resistance in room temperature

Module	TTEM	1st FTEM	2nd FTEM
$R_{RT}(\Omega)$	0.0964	0.194	0.325

Table 3.44: maximum value of TTEM and FTEMs

	T_c=22℃, T_h=37℃					T_c=22℃, T_h=45℃				
Module	V(mV)	I(mA)	R(Ω)	P(μW)	η(10^{-6})	V(mV)	I(mA)	R(Ω)	P(μW)	η(10^{-6})
TTEM	58.8	13.18	130.4	774.9	51.01	140.7	20.57	294.3	2894	19.08
1st FTEM	101.7	16.03	219.0	1630	208.9	160.8	24.43	332.4	3928	9.930
2nd FTEM	122.4	18.91	244	2315	50.70	216.2	34.03	372	7357	29.20

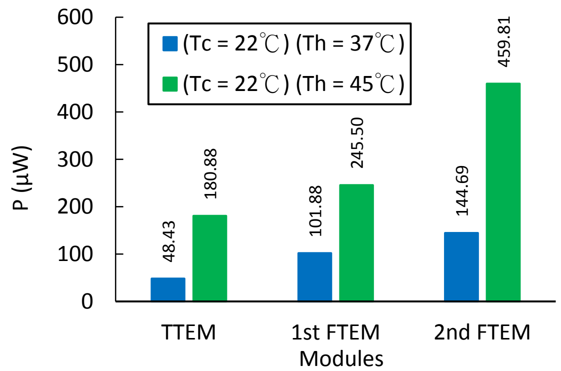

Figure 3-55: maximum power output per 1cm^2

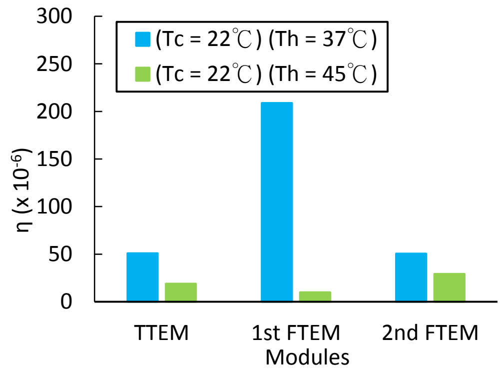

Figure 3-56: maximum conversion efficiency

The data (table 3.44 and figure 3-55) showed the 2nd FTEM had the best power output in the three modules at (T_c=22℃, T_h=37℃) and (T_c=22℃, T_h=45℃) because 2nd FTEM had the most pairs of n-type and p-type and the low thermal conductivity. Although the 2nd FTEM had the best, it had low conversion efficiency.

3.1.5 Measuring Value of TTEM and FTEM(Curved Surface Measurement):

TTEM:

Table 3.45: Seebeck coefficient and current of TTEM at (T_c=22℃, T_h=37℃) and (T_c=22℃, T_h=45℃)

Seebeck coefficient and Current (I) / Time (Min)	Tc=22℃, Th=37℃, ΔT=15℃		Tc=22℃, Th=45℃, ΔT=23℃	
	S (mV/ΔT)	I (mA)	S (mV/ΔT)	I (mA)
0.5	1.900662252	4.59	1.073913043	7.65
1	1.9	4.59	1.074235808	7.64
1.5	1.886666667	4.56	1.083700441	7.64
2	1.831168831	4.55	1.074889868	7.65
2.5	1.866666667	4.55	1.084444444	7.66
3	1.828947368	4.54	1.084821429	7.66
3.5	1.82781457	4.56	1.08	7.67
4	1.802631579	4.56	1.075555556	7.73
4.5	1.814569536	4.56	1.08	7.73
5	1.802631579	4.57	1.071111111	7.71
5.5	1.802631579	4.57	1.061946903	7.7
6	1.777777778	4.55	1.061946903	7.68
6.5	1.789473684	4.58	1.066666667	7.66
7	1.764705882	4.57	1.061674009	7.66
7.5	1.75974026	4.56	1.066371681	7.67
8	1.777777778	4.56	1.061674009	7.66
8.5	1.80794702	4.55	1.066371681	7.65
9	1.784313725	4.54	1.061674009	7.65
9.5	1.766233766	4.55	1.061674009	7.67
10	1.761290323	4.55	1.057017544	7.68

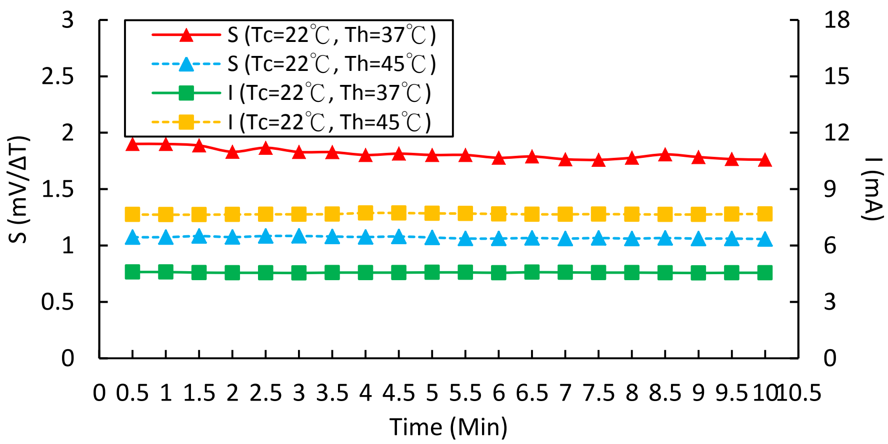

Figure 3-57: S-I-T of TTEM at (T_c=22℃, T_h=37℃) and (T_c=22℃, T_h=45℃)

The data (table 3.45 and figure 3-57) showed the Seebeck coefficient at (T_c=22℃, T_h=37℃) was higher than the Seebeck coefficient at (T_c=22℃, T_h=45℃).

Table 3.46: power and conversion efficiency of TTEM at (T_c=22℃, T_h=37℃) and (T_c=22℃, T_h=45℃)

Time (Min) \ Power and conversion efficiency (η)	Tc=22℃, Th=37℃, ΔT=15℃		Tc=22℃, Th=45℃, ΔT=23℃	
	Power (μW)	η (10^{-6})	Power (μW)	η (10^{-6})
0.5	131.733	5.789952532	188.955	1.311313291
1	130.815	3.449762658	187.944	1.304297135
1.5	129.048	2.835970464	187.944	1.548852848
2	128.31	3.383702532	186.660	1.640822785
2.5	127.4	4.199630802	186.904	1.449677339
3	126.212	3.328375527	186.138	1.887962512
3.5	125.856	2.370705244	186.381	1.890427215
4	124.944	5.491561181	187.066	1.761848252
4.5	124.944	4.118670886	187.839	1.54798754
5	125.218	3.302162447	185.811	1.884645813
5.5	125.218	4.127703059	184.800	2.030590717
6	123.76	4.07964135	184.320	1.869522882
6.5	124.576	4.106540084	183.840	1.731464738
7	123.39	4.06744462	184.606	1.622767229
7.5	123.576	5.431434599	184.847	1.354071437
8	124.032	4.088607595	184.606	1.431853438
8.5	124.215	2.339794304	184.365	1.519358188
9	123.942	3.268512658	184.365	1.736409358
9.5	123.76	3.26371308	184.847	1.523330367
10	124.215	2.729760021	185.088	1.435591958

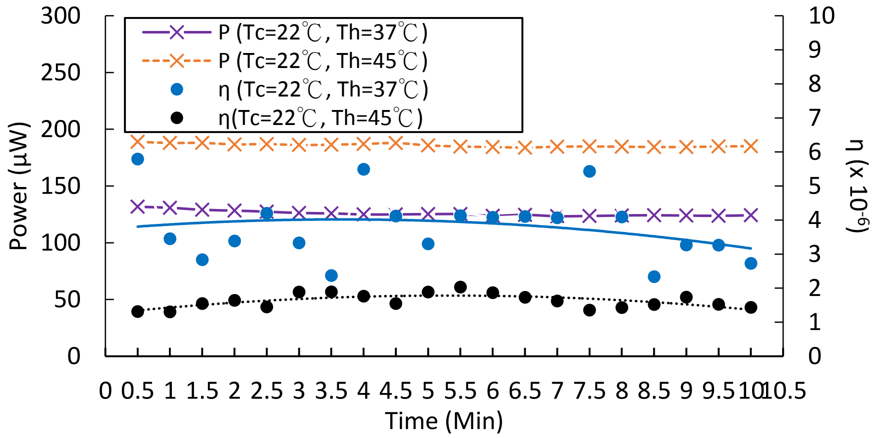

Figure 3-58: P-η-T of TTEM at (T_c=22℃, T_h=37℃) and (T_c=22℃, T_h=45℃)

The data (table 3.46 and figure 3-58) showed the conversion efficiency was getting lower because the substrate of TTEM was ceramic which it was inflexible. So, it couldn't catch the thermal energy completely on curved surface.

1st FTEM:

Table 3.47: Seebeck coefficient and current of TTEM at (T_c=22℃, T_h=37℃) and (T_c=22℃, T_h=45℃)

Seebeck coefficient and Current (I) / Time (Min)	Tc=22℃, Th=37℃, ΔT=15℃		Tc=22℃, Th=45℃, ΔT=23℃	
	S (mV/ΔT)	I (mA)	S (mV/ΔT)	I (mA)
0.5	3.863013699	8.24	4.128888889	15.1
1	3.567567568	8.27	4.115044248	15.1
1.5	3.560810811	8.26	3.982905983	15.07
2	3.703448276	8.25	3.965957447	15.08
2.5	3.513888889	8.23	4.069868996	15.06
3	3.573426573	8.22	3.982905983	15.03
3.5	3.482758621	8.25	4.0969163	15.04
4	3.425675676	8.23	4.056521739	15.07
4.5	3.38	8.23	4.038961039	15.11
5	3.402684564	8.22	4.091703057	15.11
5.5	3.364238411	8.24	4	15.09
6	3.361842105	8.24	4.03030303	15.08
6.5	3.452702703	8.27	4.017316017	15.06
7	3.4	8.27	4.101321586	15.05
7.5	3.370860927	8.24	4.105726872	15.06
8	3.38	8.24	4.043290043	15.05
8.5	3.350993377	8.24	4.118942731	15.06
9	3.370860927	8.24	4.211711712	15.05
9.5	3.342105263	8.28	4.201793722	15.07
10	3.863013699	8.27	4.230769231	15.1

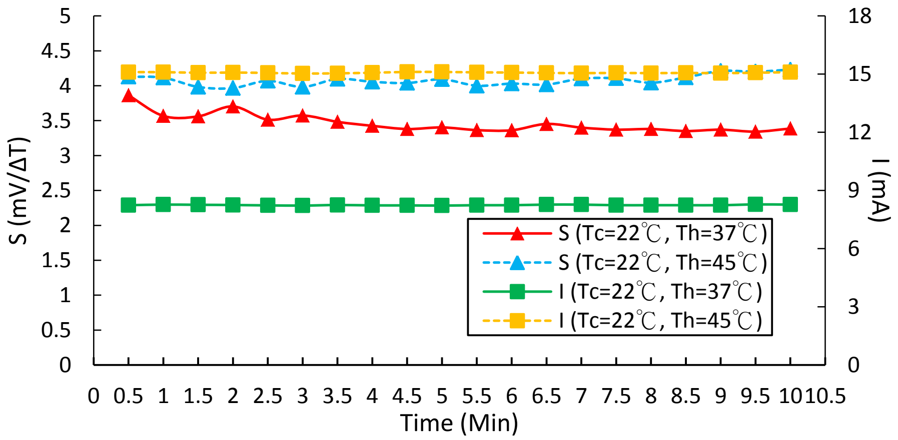

Figure 3-59: S-I-T of 1st FTEM at (T_c=22℃, T_h=37℃) and (T_c=22℃, T_h=45℃)

The data (table 3.47 and figure 3-59) showed the Seebeck coefficient at (T_c=22℃, T_h=45℃) was higher than the Seebeck coefficient at (T_c=22℃, T_h=37℃). And, the Seebeck coefficient at (T_c=22℃, T_h=37℃) was steadily in the 10 minutes.

Table 3.48: power and conversion efficiency of 1st FTEM at (T_c=22℃, T_h=37℃) and (T_c=22℃, T_h=45℃)

Time (Min) \ Power and conversion efficiency (η)	Tc=22℃, Th=37℃, ΔT=15℃		Tc=22℃, Th=45℃, ΔT=23℃	
	Power (μW)	η (10^{-6})	Power (μW)	η (10^{-6})
0.5	464.736	20.42616034	1402.790	36.99340717
1	436.656	14.39398734	1404.300	185.1661392
1.5	435.302	28.69870781	1404.524	185.1956751
2	443.025	19.47191456	1405.456	185.3185654
2.5	416.438	13.72751846	1403.592	61.69092827
3	420.042	55.38528481	1400.796	46.17602848
3.5	416.625	27.46736551	1398.720	184.4303797
4	417.261	13.75464794	1406.031	185.3943829
4.5	417.261	27.50929589	1409.763	92.94323576
5	416.754	18.31724684	1415.807	186.6834124
5.5	418.592	18.39803094	1412.424	186.2373418
6	421.064	27.7600211	1403.948	92.55986287
6.5	422.597	18.57405942	1397.568	92.13924051
7	421.77	9.268855485	1401.155	61.58381681
7.5	419.416	13.82568565	1403.592	46.2681962
8	417.768	18.36181435	1405.670	92.67339135
8.5	416.944	18.32559775	1408.110	92.83425633
9	419.416	27.65137131	1407.175	61.84840893
9.5	420.624	27.73101266	1412.059	93.09460707
10	420.116	27.6975211	1411.850	62.05388537

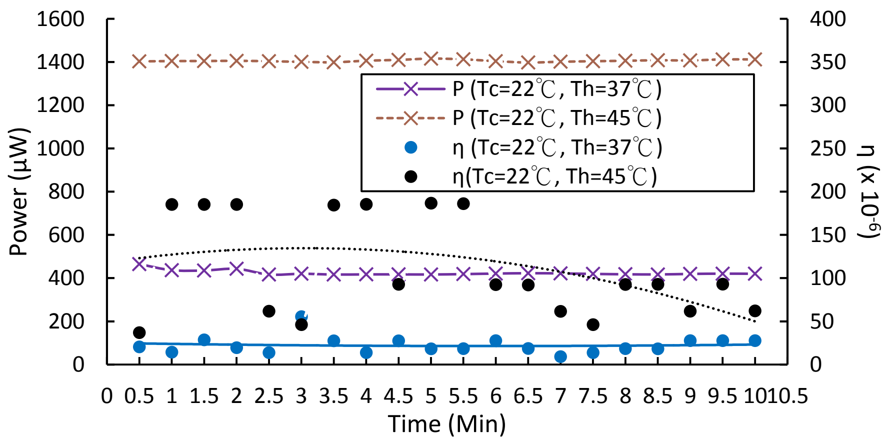

Figure 3-60: P-η-T of 1st FTEM at (T_c=22℃, T_h=37℃) and (T_c=22℃, T_h=45℃)

The data (table 3.48 and figure 3-60) showed the conversion efficiency at (T_c=22℃, T_h=45℃) was getting lower, and the conversion efficiency at (T_c=22℃, T_h=37℃) was more steadily than conversion efficiency at (T_c=22℃, T_h=45℃).

2^{nd} FTEM:

Table 3.49: Seebeck coefficient and current of 2^{nd} FTEM at (T_c=22℃, T_h=37℃) and (T_c=22℃, T_h=45℃)

Seebeck coefficient and Current (I) / Time (Min)	Tc=22℃, Th=37℃, ΔT=15℃		Tc=22℃, Th=45℃, ΔT=23℃	
	S (mV/ΔT)	I (mA)	S (mV/ΔT)	I (mA)
0.5	7.790540541	18.1	8.135135135	28.45
1	7.68	18.12	7.916666667	28.41
1.5	7.419354839	18.14	7.843478261	28.41
2	7.461038961	18.12	7.916666667	28.41
2.5	7.609271523	18.12	7.722222222	28.41
3	7.697986577	18.14	7.797413793	28.43
3.5	7.849315068	18.18	7.709401709	28.44
4	7.477124183	18.2	7.938325991	28.45
4.5	7.849315068	18.19	7.947136564	28.46
5	7.795918367	18.17	7.886462882	28.44
5.5	7.59602649	18.18	7.982300885	28.43
6	7.448051948	18.19	7.886462882	28.42
6.5	7.503267974	18.18	7.865217391	28.43
7	7.467532468	18.19	8.044444444	28.44
7.5	7.535947712	18.2	8.017699115	28.42
8	7.629139073	18.22	7.938596491	28.44
8.5	7.331210191	18.22	7.929824561	28.44
9	7.585526316	18.21	7.995575221	28.46
9.5	7.572368421	18.19	8.071428571	28.45
10	7.77027027	18.17	8.066964286	28.44

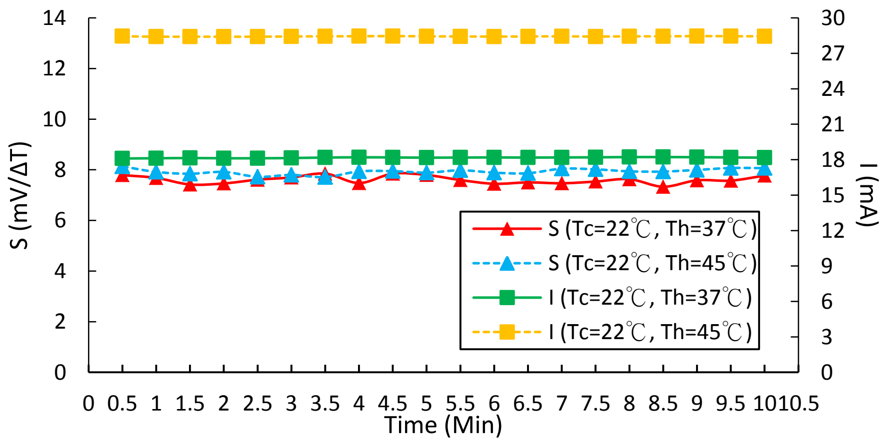

Figure 3-61: S-I-T of 2^{nd} FTEM at (T_c=22℃, T_h=37℃) and (T_c=22℃, T_h=45℃)

The data (table 3.49 and figure3-61) showed the Seebeck coefficient at (T_c=22℃, T_h=37℃) and (T_c=22℃, T_h=45℃) were similarly.

Table 3.50: power and conversion efficiency of 2nd FTEM at (T_c=22℃, T_h=37℃) and (T_c=22℃, T_h=45℃)

Time (Min) \ Power and conversion efficiency (η)	Tc=22℃, Th=37℃, ΔT=15℃		Tc=22℃, Th=45℃, ΔT=23℃	
	Power (μW)	η (x 10^{-6})	Power (μW)	η (x 10^{-6})
0.5	2086.93	68.7938423	5138.070	169.3720332
1	2087.424	137.6202532	5128.005	676.1609968
1.5	2086.1	91.68864276	5125.164	675.7863924
2	2081.988	91.50791139	5128.005	338.0804984
2.5	2081.988	274.5237342	5133.687	338.4551028
3	2080.658	274.348365	5142.987	678.1364715
3.5	2083.428	137.3568038	5130.576	169.125
4	2082.08	274.535865	5126.690	225.3292018
4.5	2084.574	91.62157173	5134.184	75.21952649
5	2082.282	137.28125	5136.264	677.25
5.5	2085.246	274.9533228	5128.772	112.7103551
6	2086.393	68.77614056	5132.652	676.7737342
6.5	2087.064	275.193038	5142.987	169.5341179
7	2091.85	275.8241034	5147.640	135.75
7.5	2098.46	276.6956751	5149.704	75.44690577
8	2098.944	276.7594937	5147.640	169.6875
8.5	2097.122	138.2596255	5141.952	113
9	2099.613	276.8477057	5142.722	226.0338432
9.5	2093.669	276.0639504	5143.760	61.65803606
10	2089.55	275.5208333	5139.108	67.7625

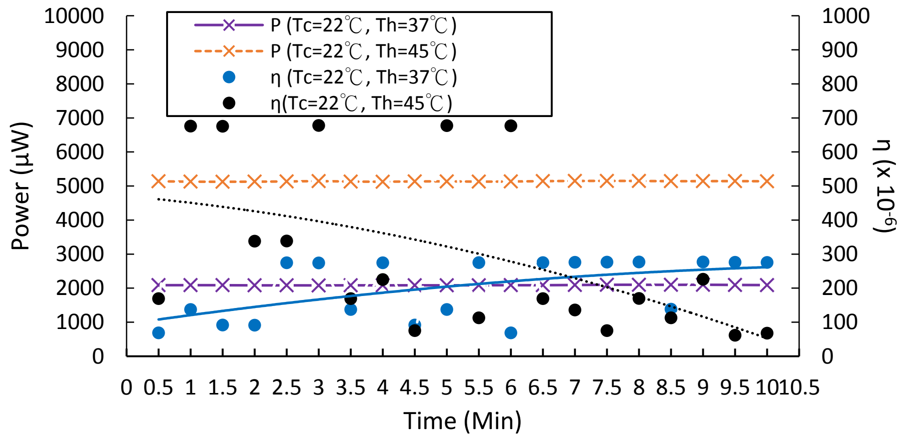

Figure 3-62: P-η-T of 2nd FTEM at (T_c=22℃, T_h=37℃) and (T_c=22℃, T_h=45℃)

The data (table 3.50 and figure3-62) showed the conversion efficiency at (T_c=22℃, T_h=37℃) became as high as, but the conversion efficiency at (T_c=22℃, T_h=45℃) became as low as.

3.1.5.1 The Efficiency and Power of TTEM and 1st FTEM Comparison:

Table 3.51: TTEM and 1st FTEM menu

Module	TTEM	1st FTEM
Finished product		
Size	40mm x 40mm x 2.6mm	40mm x 40mm x 2.6mm
Further Explanation	1. Ceramic Substrate 2. 17 Pairs N-type P-type 3. Copper Foil Area (3mm x 9mm)	1. 2L FFCCL Substrate 2. 17 Pairs N-type P-type 3. Copper Foil Area: (3mm x 9mm)

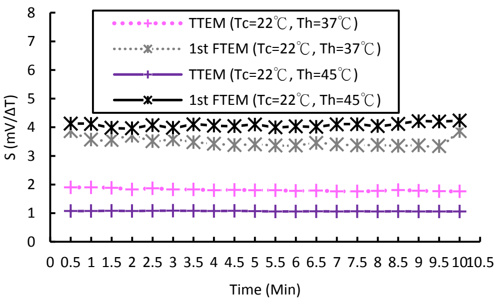

Figure 3-63: S-t in Tc=22℃, Th=37℃ and 45℃

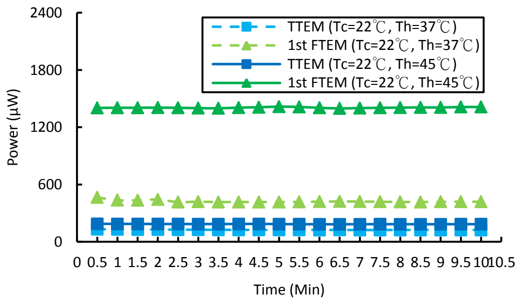

Figure 3-64: P-t in Tc=22℃, Th=37℃ and 45℃

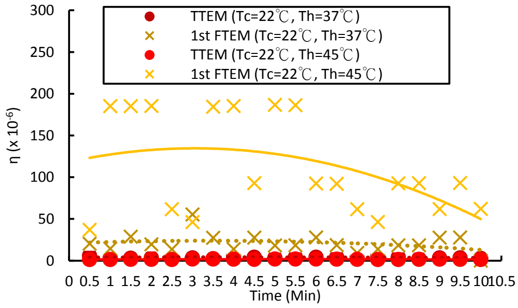

Figure 3-65: η-t in Tc=22℃, Th=37℃ and 45℃

The data (figure 3-63, 3-64 and 3-65) showed the Seebeck coefficient, power output and conversion efficiency of 1st FTEM were higher than TTEM due to the 2L FCCL substrate of 1st FTEM could be caught the more thermal energy than ceramic substrate of TTEM. The ceramic was inflexible, but the 2L FCCL was flexible. The figure 3-65 showed conversion efficiency of 1st FTEM was getting lower belong the time. The conversion efficiency of TTEM was more stable than the conversion of 1st FTEM.

3.1.5.2 The Efficiency and Power of 1st FTEM and 2nd FTEM Comparison:

Table 3.52: 1st FTEM and 2nd FTEM menu

Module	1st FTEM	2nd FTEM
Finished product		
Size	40mm x 40mm x 2.6mm	40mm x 40mm x 2.6mm
Further Explanation	1. 2L FCCL Substrate 2. 17 Pairs N-type P-type 3. Copper Foil Area: (3mm x 9mm)	1. 3L FCCL Substrate 2. 31 Pairs N-type P-type 3. Copper Foil Area: ($2 \times 9mm^2 + 2mm^2$)

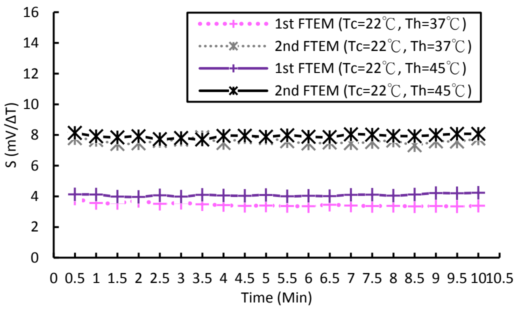

Figure 3-66: S-t in Tc=22℃, Th=37℃ and 45℃

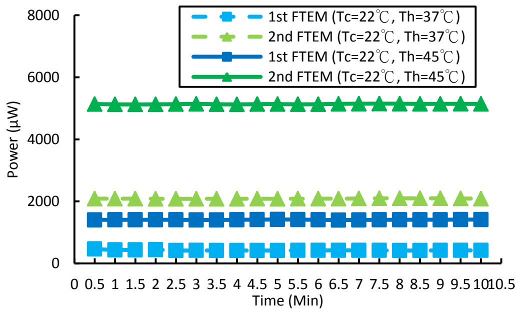

Figure 3-67: P-t in Tc=22℃, Th=37℃ and 45℃

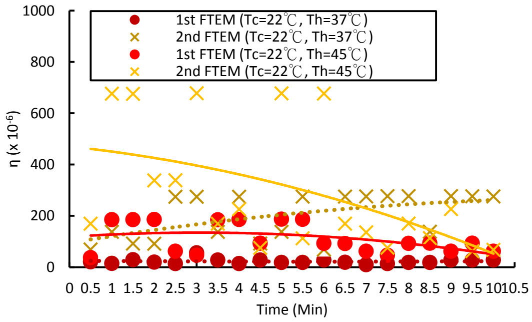

Figure 3-68: η-t in Tc=22℃, Th=37℃ and 45℃

The data (figure 3-66, 3-67 and 3-68) showed the Seebeck coefficient, power output and conversion efficiency of 2nd FTEM were higher than 1st FTEM because the 3L FCCL substrate of 2nd FTEM had higher flexible ability than 2L FCCL substrate of 1st FTEM. The material 3L FCCL had one more layer of copper foil than 2L FCCL, so the outside copper foil of 2nd FTEM could be offset the gap when the 2nd FTEM was used on curved surface material. Therefore, the 2nd FTEM could get more thermal power than 1st FTEM.

3.1.5.3 Maximum Power Output per 1 cm^2 and Conversion Efficiency:

Table 3.53: load resistance in room temperature

Module	TTEM	1st FTEM	2nd FTEM
$R_{RT}(\Omega)$	0.0964	0.194	0.325

Table 3.54: maximum value of TTEM and FTEMs

	T_c=22℃, T_h=37℃				T_c=22℃, T_h=45℃			
Module	V_{oc}(mV)	I(mA)	P(μW)	η(10^{-6})	V_{oc}(mV)	I(mA)	P(μW)	η(10^{-6})
TTEM	28.7	4.59	131.7	5.79	24.7	7.65	189	2.03
1st FTEM	56.4	8.24	464.7	55.39	93.7	15.11	1416	186.7
2nd FTEM	115.2	18.22	2099	276.8	181.2	28.42	5150	678.1

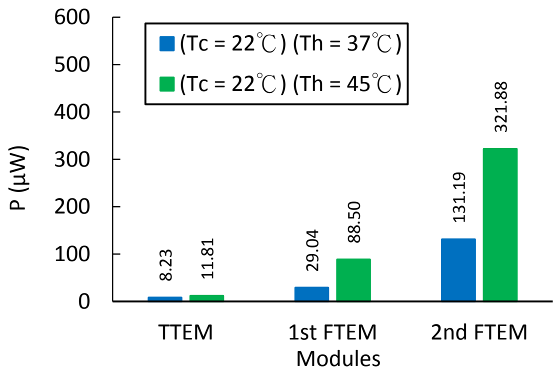

Figure 3-69: maximum power output per 1cm^2

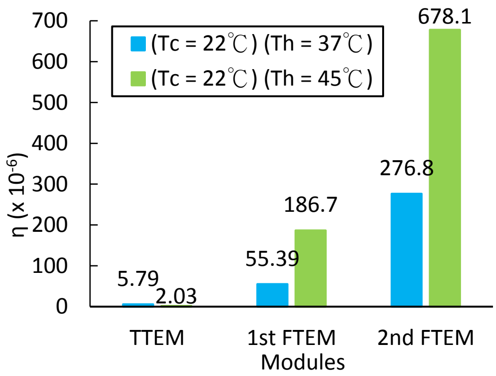

Figure 3-70: maximum conversion efficiency

The data (figure 3-69 and 3-70) showed the 2nd FTEM had the best power output and conversion efficiency in the three modules. So, it also showed the 2nd FTEM had the best flexible ability. The 2L FCCL substrate of 1st FTEM could be caught the more thermal energy than ceramic substrate of TTEM. But the 2L FCCL substrate still was not caught the thermal energy completely when it was flexible. The gap between the n-type and p-type had nothing to stuff so it still lost much thermal energy. Therefore, the 2nd FTEM was used 3L FCCL substrate to improve the defects and to increase the power output of the n-type and p-type.

3.2 Cooling Performance:

3.2.1 Measuring Value of TTEM and FTEM:

TTEM:

Table 3.55: the temperature of TTEM at current = 1A

Temperature (℃) / Time (min)	T_{c1}	T_{c2}	T_{c3}	T_{c4}	T_{c5}	T_{h1}	T_{h2}	T_{h3}	T_{h4}	T_{h5}	T_{ca}	T_{ha}
0.5	21.3	21.2	21.3	21.3	21.3	25.9	25.6	25.6	25.6	25.3	21.28	25.6
1	21.5	21.4	21.4	21.5	21.4	26.1	25.7	25.6	25.7	25.4	21.44	25.7
1.5	21.4	21.4	21.4	21.5	21.5	26.3	25.9	25.5	25.7	25.6	21.44	25.8
2	21.4	21.3	21.4	21.4	21.3	26.6	26	25.8	26	25.8	21.36	26.04
2.5	21.4	21.3	21.4	21.4	21.3	26.6	26.1	26.3	26.2	25.7	21.36	26.18
3	21.3	21.3	21.4	21.4	21.3	26.8	26.3	26.4	26.4	25.9	21.34	26.36
3.5	21.5	21.5	21.5	21.5	21.5	26.8	26.5	26.7	26.4	26	21.5	26.48
4	21.6	21.6	21.6	21.6	21.6	27.1	26.5	26.5	26.4	26.1	21.6	26.52
4.5	21.6	21.6	21.6	21.6	21.5	27.1	26.5	26.6	26.6	26.2	21.58	26.6
5	21.5	21.5	21.6	21.6	21.5	27.6	26.8	26.7	26.8	26.5	21.54	26.88
5.5	21.6	21.6	21.6	21.6	21.5	27.6	26.9	26.8	26.9	26.6	21.58	26.96
6	21.6	21.6	21.6	21.6	21.5	27.6	26.9	27.2	27	26.6	21.58	27.06
6.5	21.7	21.7	21.7	21.7	21.6	27.8	27.2	27.3	27.2	26.7	21.68	27.24
7	21.7	21.7	21.7	21.7	21.6	27.8	27.2	27.5	27.3	26.8	21.68	27.32
7.5	21.7	21.7	21.7	21.7	21.6	28.2	27.3	27.3	27.4	27	21.68	27.44
8	21.8	21.8	21.8	21.7	21.7	28.3	27.4	27.6	27.6	27	21.76	27.58
8.5	21.9	21.9	21.9	21.8	21.8	28.4	27.7	27.7	27.7	27.2	21.86	27.74
9	21.9	21.9	21.9	21.8	21.8	28.4	27.6	27.8	27.7	27.1	21.86	27.72
9.5	22	22	22	21.9	21.9	28.3	27.8	28.1	27.8	27.3	21.96	27.86
10	22	22	22	21.9	21.9	28.4	27.8	28.1	27.9	27.3	21.96	27.9

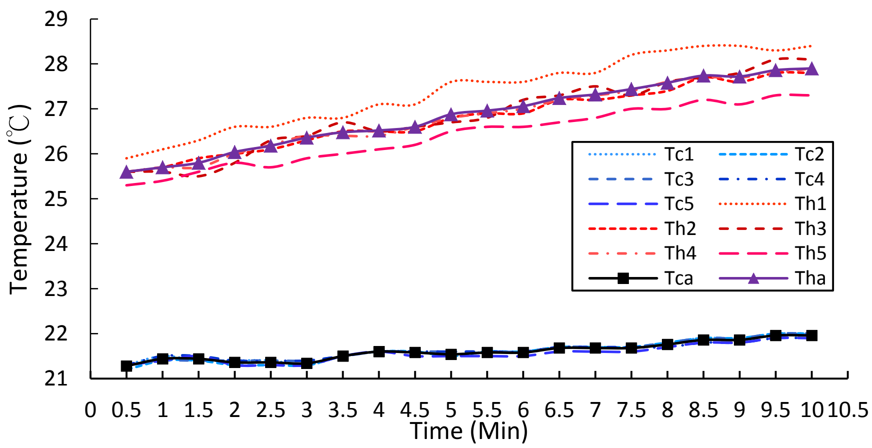

Figure 3-71: the temperature of TTEM at current = 1A

The figure 3-71 and table 3.55 showed the T_h, T_C and ΔT were higher belong the time. The 5 points of T_c were more stable than the 5 points of T_c.

Table 3.56: the temperature of TTEM at current = 2A

Temperature (℃) / Time (min)	T_{c1}	T_{c2}	T_{c3}	T_{c4}	T_{c5}	T_{h1}	T_{h2}	T_{h3}	T_{h4}	T_{h5}	T_{ca}	T_{ha}
0.5	24.5	24.6	24.7	23.9	24.2	38.7	36.5	36.7	36.9	35.4	24.38	36.84
1	25.2	25.3	25.4	24.4	24.8	38.1	37.1	37.7	37.1	35.4	25.02	37.08
1.5	25.4	25.8	25.6	24.6	25.1	38.5	37.1	38.4	37.5	35.7	25.3	37.44
2	25.6	26	25.8	24.8	25.3	38.8	36.9	38.6	38	35.9	25.5	37.64
2.5	25.9	26.2	26.1	25	25.6	39.7	37.8	38.9	38.4	36.6	25.76	38.28
3	26	26.4	26.3	25.1	25.7	40.1	38.2	39.1	38.6	36.9	25.9	38.58
3.5	26.2	26.4	26.6	25.3	25.9	40.1	39	39	38.7	36.9	26.08	38.74
4	26.4	26.7	26.7	25.3	26	40.1	38.6	39.8	39	36.9	26.22	38.88
4.5	26.4	26.8	26.9	25.5	26.1	41.4	39.1	38.9	39.2	37.5	26.34	39.22
5	26.6	27	26.9	25.6	26.3	40.5	39.1	40.2	39.5	37.4	26.48	39.34
5.5	26.8	27.2	27.2	25.7	26.4	40.7	39.4	40	39.5	37.5	26.66	39.42
6	27	27.3	27.3	25.8	26.6	40.8	39.5	40.4	39.8	37.5	26.8	39.6
6.5	27	27.4	27.3	25.9	26.7	41.5	39.5	40.5	39.9	38	26.86	39.88
7	26.9	27.2	27.3	25.8	26.7	40.9	39.8	40.4	40	37.9	26.78	39.8
7.5	27	27.3	27.5	26.2	26.7	41.6	40.2	39.6	40.3	38.1	26.94	39.96
8	27	27.4	27.5	26	26.8	42.2	40.3	39.5	40.3	38.2	26.94	40.1
8.5	27.2	27.5	27.6	26.2	26.9	42.4	40	40.2	40.4	38.6	27.08	40.32
9	27.3	27.6	27.6	26.2	26.9	42	39.9	40.4	40.5	38.5	27.12	40.26
9.5	27.3	27.7	27.7	26.2	27	41.9	40	40.8	40.7	38.3	27.18	40.34
10	27.3	27.7	27.7	26.2	27.1	42.2	40	40.9	40.7	38.7	27.2	40.5

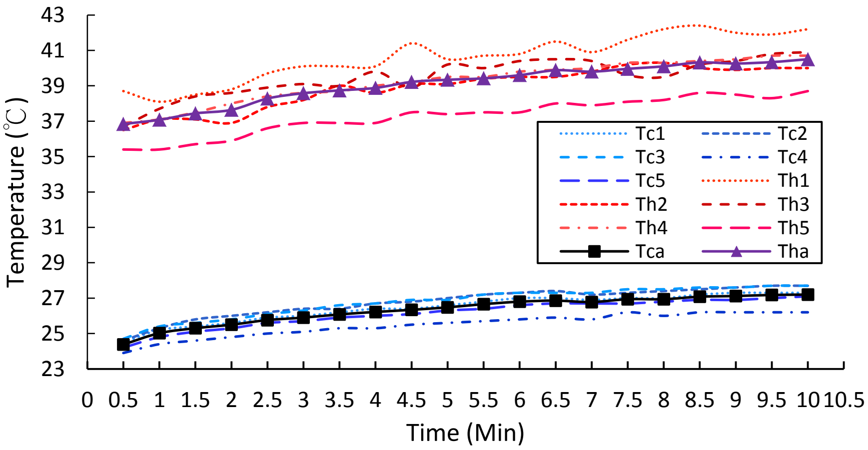

Figure 3-72: the temperature of TTEM at current = 2A

The figure 3-72 and table 3.56 showed the T_h, T_C and ΔT were higher belong the time. The 5 points of T_c were more stable than the 5 points of T_h. The T_{h1} and T_{h5} were a wide range of the T_{ha} in hot side.

Table 3.57: the temperature of TTEM at current = 3A

Temperature (℃) / Time (min)	T_{c1}	T_{c2}	T_{c3}	T_{c4}	T_{c5}	T_{h1}	T_{h2}	T_{h3}	T_{h4}	T_{h5}	T_{ca}	T_{ha}
0.5	33.2	33.4	34.1	30.9	32.6	57.9	55.4	56.5	56.4	51.8	32.84	55.6
1	33.9	34.6	34.6	31.6	33.5	59.8	55.9	56.9	57.6	53.1	33.64	56.66
1.5	34.9	35.5	35.3	31.9	34.3	60.2	56.5	58.6	57.8	53.4	34.38	57.3
2	35.2	36	35.9	32.3	34.8	61.3	56.7	59.3	59.1	53.9	34.84	58.06
2.5	35.6	36.7	36.3	32.8	35.3	61.8	57.2	59.5	59.8	54.3	35.34	58.52
3	36.4	37.1	36.8	33.1	35.7	61.9	58.2	59.1	59.8	55	35.82	58.8
3.5	36.5	37.3	37.1	33.3	36	62.8	58.9	60.6	60.1	55.5	36.04	59.58
4	36.4	37.5	37.1	33.2	36.2	63.1	58.3	61.5	60.4	55.4	36.08	59.74
4.5	36.5	37.6	37.5	33.8	36.3	65.2	58.8	60.5	61.7	56.3	36.34	60.5
5	37	38.2	37.6	33.8	36.8	64.4	58.9	61.8	61.5	56	36.68	60.52
5.5	37	38.2	37.9	34.2	36.9	65.6	59.4	61.7	61.7	56.8	36.84	61.04
6	37.5	38.4	38.1	34.3	37	64.4	59.8	61.9	61.7	57	37.06	60.96
6.5	37.6	38.7	38.4	34.6	37.1	65.7	60	61.6	62.6	57.3	37.28	61.44
7	37.4	38.5	38.1	34.1	37.3	64.9	59.7	62.4	61.9	56.8	37.08	61.14
7.5	37.4	38.7	38.2	34.4	37.4	65.8	58.9	61.4	63.1	57	37.22	61.24
8	37.5	38.7	38.5	34.8	37.3	66.1	60.2	60.8	62.9	57.9	37.36	61.58
8.5	37.7	38.7	38.6	34.5	37.5	65.9	60.4	62	63	57.5	37.4	61.76
9	37.4	38.8	38.4	34.4	37.6	66.1	59.9	61.9	63.3	57.1	37.32	61.66
9.5	37.5	38.8	38.4	34.9	37.5	67	59.9	61.7	63.1	57.7	37.42	61.88
10	37.9	39.1	39	35.3	37.7	66.9	60.1	60.7	63.7	58.3	37.8	61.94

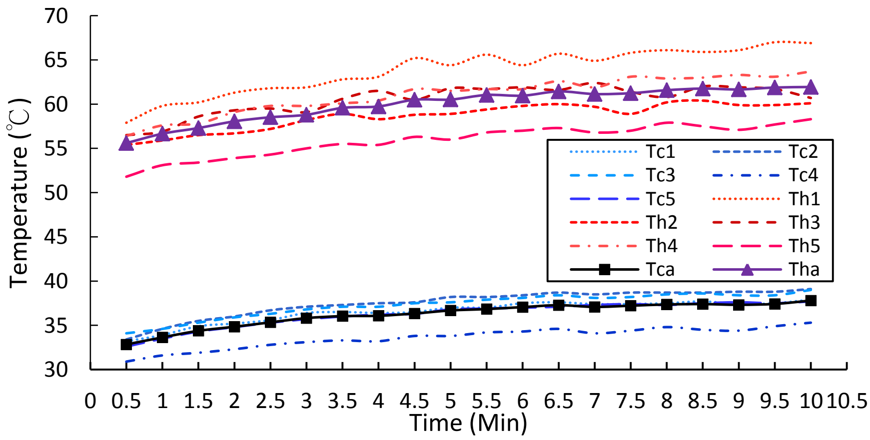

Figure 3-73: the temperature of TTEM at current = 3A

The figure 3-73 and table 3.57 showed the T_h, T_C and ΔT were higher belong the time. The 5 points of T_c were more stable than the 5 points of T_h. In cold side, the T_{c4} was a wide range of the T_{ca}. The T_{h1} and T_{h5} were a wide range of the T_{ha} in hot side.

1st FTEM:

Table 3.58: the temperature of 1st FTEM at current = 1A

Temperature (℃) / Time (min)	T_{c1}	T_{c2}	T_{c3}	T_{c4}	T_{c5}	T_{h1}	T_{h2}	T_{h3}	T_{h4}	T_{h5}	T_{ca}	T_{ha}
0.5	32.3	24.6	24	26.8	29.2	47.6	36.9	30.8	39.7	42.7	27.38	39.54
1	34	26.2	24.6	27.5	30.7	50.3	37.3	33.1	41.6	43.4	28.6	41.14
1.5	34.9	26.9	24.7	27.7	31.3	51.4	37.3	33.7	42.3	43.6	29.1	41.66
2	35.7	27.1	25.2	28.4	31.6	52.4	37.8	33.6	42.4	44.5	29.6	42.14
2.5	35.6	27.4	24.8	28.1	31.7	52.5	37.4	34.5	42.6	44.2	29.52	42.24
3	35.8	27.1	25.5	28.4	31.7	52.8	38.1	33.6	42.4	44.6	29.7	42.3
3.5	35.8	27.1	25.6	28.5	31.7	53.6	38.2	33.2	41.8	44.9	29.74	42.34
4	35.9	27.1	25.6	28.6	31.8	53.7	38.4	33.6	42.5	45.1	29.8	42.66
4.5	36	27	25.8	28.7	31.6	53.9	38.5	33.2	42.2	45.3	29.82	42.62
5	35.8	27.1	25.5	28.7	31.7	53.7	38.4	33.7	42.5	45.1	29.76	42.68
5.5	35.8	27.4	25.2	28.6	31.8	53.6	37.8	34.1	42.6	45.2	29.76	42.66
6	36.2	27.2	25.4	28.9	31.9	53.9	38	33.7	42.6	45.4	29.92	42.72
6.5	35.9	27.2	25.2	28.6	31.8	53.5	37.8	33.7	42.5	44.9	29.74	42.48
7	36.1	27.5	25.2	28.7	31.8	53.1	37.7	34.2	42.7	45.1	29.86	42.56
7.5	36.1	27.5	25.2	28.9	31.8	53.4	37.9	34.2	42.5	45.5	29.9	42.7
8	35.9	27.2	25.2	28.7	31.8	53.7	38.1	34.1	42.6	45.3	29.76	42.76
8.5	36.3	27.1	25.8	29	31.8	53.8	38.5	33.4	42.5	45.5	30	42.74
9	36.3	27	25.9	28.9	31.8	54.5	38.9	32.9	42.2	45.8	29.98	42.86
9.5	36.2	27.1	25.8	29.2	31.7	54.5	38.5	33.5	42.4	46	30	42.98
10	36.1	27.1	25.6	29	31.7	54.5	38.5	33.2	42.2	45.8	29.9	42.84

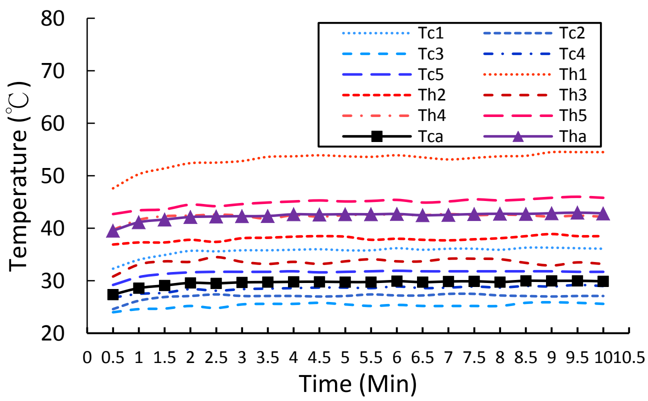

Figure 3-74: the temperature of 1st FTEM at current = 1A

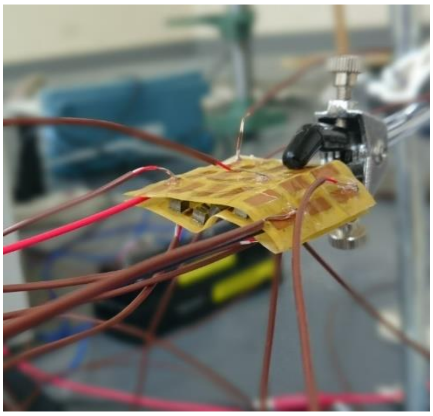

Figure 3-75: the measurement of 1st FTEM at current = 2A

In cold side, the T_{c3} was a wide range of the T_{ca}. The T_{h1} and T_{h3} were a wide range of the T_{ha} in hot side. The figure 3-75 showed the 1st FTEM was disordered because the 1st FTEM had more Joule than it could be lost. So, temperature was over than electric load could be received range when it was measured at current = 2A.

2^{nd} FTEM:

Table 3.59: the temperature of 2^{nd} FTEM at current = 1A

Temperature (℃) / Time (min)	T_{c1}	T_{c2}	T_{c3}	T_{c4}	T_{c5}	T_{h1}	T_{h2}	T_{h3}	T_{h4}	T_{h5}	T_{ca}	T_{ha}
0.5	33.2	29.3	30.1	28.4	31.5	45.6	41.6	43.2	39.1	42.4	30.5	42.38
1	36.3	31.8	32.4	30.4	33.9	49.5	44.4	44.9	40.5	45.2	32.96	44.9
1.5	37.9	32.8	33.7	31.8	35.1	51.4	45.5	47.3	42.9	46	34.26	46.62
2	38.7	33.4	34.2	31.7	35.7	52.6	46.6	49.7	43.5	46.5	34.74	47.78
2.5	39.3	34	34.9	32.1	36.4	52.8	46	51	44.6	46.4	35.34	48.16
3	39.4	34.5	34.3	32	36.7	52.2	45.6	52.7	44.9	46.7	35.38	48.42
3.5	39.7	34.6	34.9	32.6	37	51.8	45.6	53.1	45.8	46.9	35.76	48.64
4	39.9	34.6	35	32.7	37	52.6	46.2	52.3	44.6	47.4	35.84	48.62
4.5	39.9	34.4	35.2	31.9	37	53.6	46.7	52.3	44.7	46.2	35.68	48.7
5	40	34.7	34.6	32.1	37.1	53.6	46.4	53.3	45.1	46.7	35.7	49.02
5.5	39.7	35	34	31.9	37.3	52.2	45.9	54.6	45.4	46.9	35.58	49
6	39.6	34.7	33.8	31.7	37.2	52.9	46	54.1	45.9	47	35.4	49.18
6.5	39.6	34.7	33.8	31.7	37.3	52.2	45.6	53.9	46.5	46.6	35.42	48.96
7	39.4	34.8	33.5	31.5	37.4	52.2	45.3	53.5	45.7	46.1	35.32	48.56
7.5	39.5	34.5	33.9	31.9	37.3	52.2	45.1	53.9	46.2	46.9	35.42	48.86
8	39.6	34.6	34	31.7	37.4	53.1	45.9	53.9	46.6	46.2	35.46	49.14
8.5	39.7	34.8	34	31.7	37.3	52.5	45.7	54.5	45.8	46.8	35.5	49.06
9	39.8	34.9	34.1	31.9	37.6	52.8	45.8	53.5	46	46.5	35.66	48.92
9.5	39.5	35.1	33.7	31.7	37.6	51.8	44.5	54	46.6	46.2	35.52	48.62
10	39.1	35	33	31.2	37.8	51.6	44.2	53.8	46.7	45.9	35.22	48.44

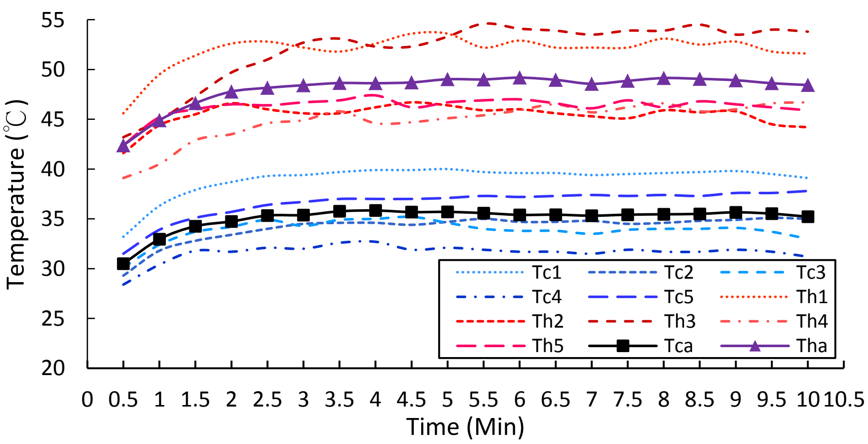

Figure 3-76: the temperature of 2^{nd} FTEM at current = 1A

The figure 3-76 and table 59 showed the T_c and T_h were raised in the 0.5 minutes to 2.5 minutes. In cold side, the T_{c4} and T_{c1} were a wide range of the T_{ca}. And, the T_{h1} and T_{h3} were a wide range of the T_{ha} in hot side.

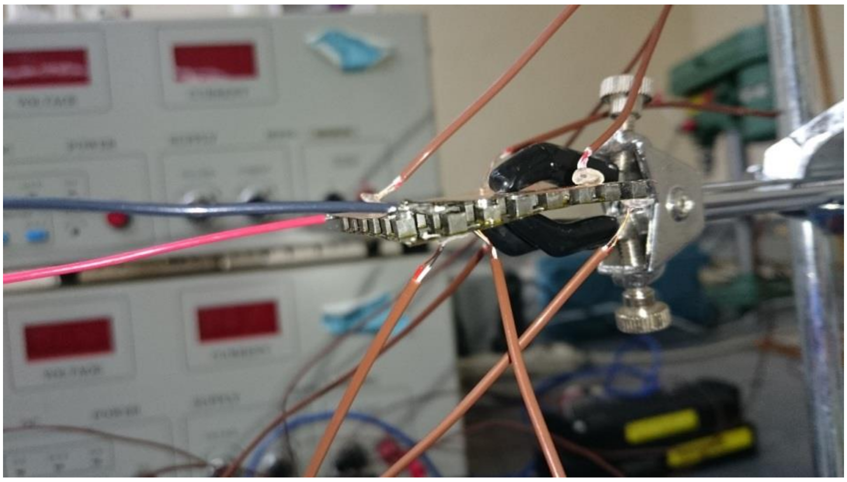

Figure 3-77: the measurement of 2nd FTEM at current = 2A

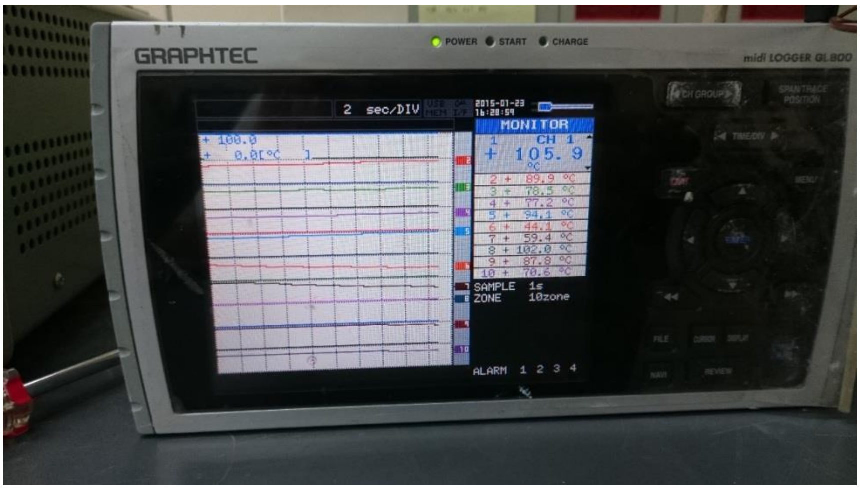

Figure 3-78: the 10 points of T_c and T_h in the measurement of 2nd FTEM at current = 2A

The figure 3-77 showed the 2nd FTEM was disordered because the 2nd FTEM had more Joule than it could be lost. So, the temperature was over than electric load could be received range when it was measured at current = 2A. The figure 3-78 (the figure was taken before the 2nd FTEM disordered completely) showed the 10 points temperature of 2nd FTEM, the 2nd FTEM could generated the 105.9℃. So, it meaned the 2nd FTEM cooling conversion efficiency was very well.

3.2.1.1 The Cooling Efficiency of TTEM and FTEMs Comparison:

Table 3.60: TTEM and FTEMs menu

Module	TTEM	1st FTEM	2nd FTEM
Finished product			
Size	40mm x 40mm x 2.6mm	40mm x 40mm x 2.6mm	40mm x 40mm x 2.6mm
Further Explanation	1. Ceramic Substrate 2. 17 Pairs N-type P-type 3. Copper Foil Area (3mm x 9mm)	1. 2L FFCCL Substrate 2. 17 Pairs N-type P-type 3. Copper Foil Area: (3mm x 9mm)	1. 3L FCCL Substrate 2. 31 Pairs N-type P-type 3. Copper Foil Area: ($2 \times 9mm^2 + 2mm^2$)

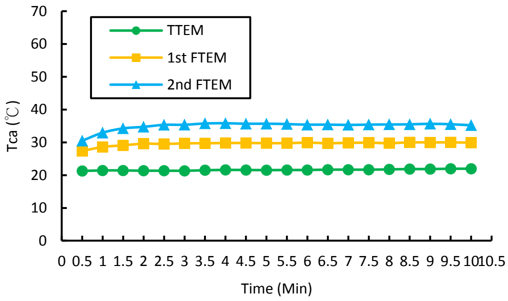

Figure 3-79: T_{ca}-t at current = 1A

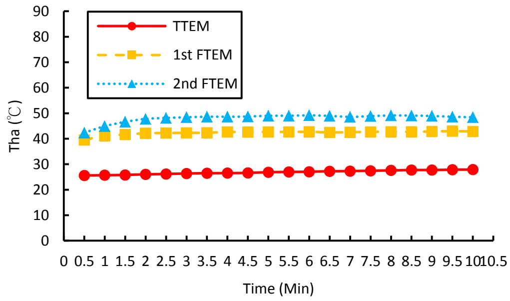

Figure 3-80: T_{ha}-t at current = 1A

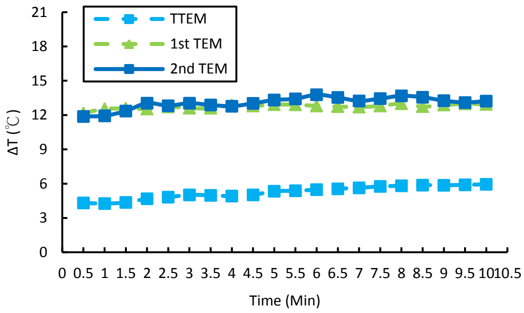

Figure 3-81: ΔT-t at current = 1A

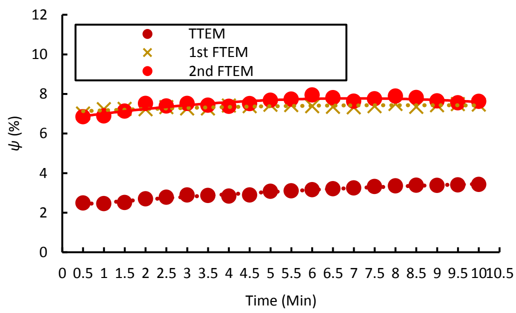

Figure 3-82: ψ-t at current = 1A

The data (figure 3-79, 3-80, 3-81 and 3-82) showed the 2nd FTEM was the best cooling performance. The figure 3-81 showed the temperature difference was getting higher, so the cooling performance was also getting higher. Therefore, it could be assumed it should be the great cooling performance when it was applied in 2nd FTEM wristlet.

3.3 1st Wristlet Performance:

Table 3.61: 1st wristlet generating at human body temperature

Time (min)	Voltage (mV)	I (mA)	Power (μW)
0.5	9.4	1.13	10.622
1	8.3	1.18	9.794
1.5	7.7	1.17	9.009
2	8.7	1.14	9.918
2.5	6.5	1.11	7.215
3	6.1	1.12	6.832
3.5	5.5	1.13	6.215
4	5.7	1.13	6.441
4.5	5.7	1.13	6.441
5	5.7	1.13	6.441
5.5	5.8	1.15	6.670
6	6.1	1.14	6.954
6.5	6.1	1.12	6.832
7	6	1.13	6.780
7.5	5.9	1.11	6.549
8	5.7	1.11	6.327
8.5	5.6	1.13	6.328
9	5.9	1.14	6.726
9.5	5.8	1.15	6.670
10	5.8	1.17	6.786

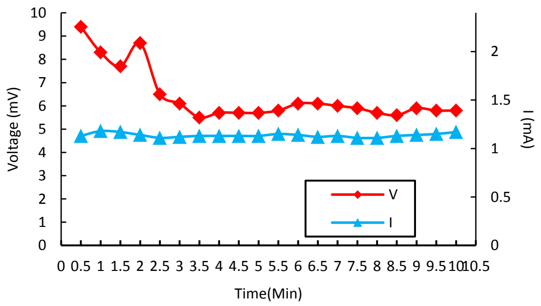

Figure 3-83: V-I-t at human body temperature

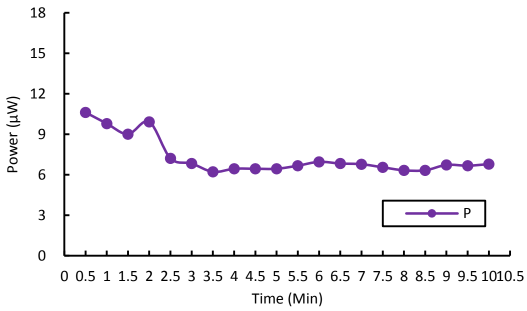

Figure 3-84: P-t at human body temperature

The data (table 3.61, figure 3-83 and 3-84) showed the voltage was getting lower from 0.5 minute and 3.5 minute. Meanwhile, the power output was also getting lower from 0.5 minute and 3.5 minute. Therefore, the 1st wristlet had stable power output and voltage after 3.5 minute.

3.4 2nd Wristlet Performance:

Table 3.62: 2nd wristlet performance at human body temperature

Time (min)	Generator			Cooler		Heater	
	Voltage (mV)	I (mA)	Power (μW)	T_c (℃)	T_h (℃)	T_c (℃)	T_h (℃)
0.5	18.7	2.08	38.896	32.1	40.3	30.4	40.2
1	17.5	2.07	36.225	32.4	40.5	30.4	40.2
1.5	16.4	2.07	33.948	32.5	40.8	30.4	40.5
2	16.3	2.04	33.252	32.8	40.9	30.5	40.8
2.5	15.7	2.03	31.871	32.9	41.1	30.4	41
3	13.5	2.02	27.27	33.4	41.1	30.7	41.2
3.5	12.3	2.03	24.969	33.6	41.5	30.6	41.3
4	10.2	2.03	20.706	33.7	41.5	30.8	41.5
4.5	9.7	2.02	19.594	33.7	41.8	30.9	41.7
5	9.7	2.02	19.594	33.7	41.8	31	41.7
5.5	9.6	2.04	19.584	33.9	42.3	31.2	41.7
6	9.6	2.04	19.584	34.2	42.7	31.2	41.9
6.5	9.3	2.01	18.693	34.2	42.7	31.1	42
7	9.3	2.03	18.879	34.6	42.9	31.4	42
7.5	9.3	2.02	18.786	34.7	43.3	31.5	41.8
8	9.1	2.02	18.382	34.8	43.8	31.3	41.9
8.5	9.1	2.03	18.473	35	44.2	31.5	42
9	9.1	2.04	18.564	35	44.6	31.3	42
9.5	8.9	2.04	18.156	35.3	44.6	31.2	42.1
10	8.8	2.02	17.776	35.5	44.6	31.1	42

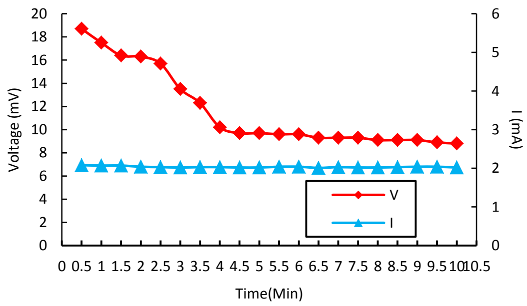

Figure 3-85: V-I-t at human body temperature

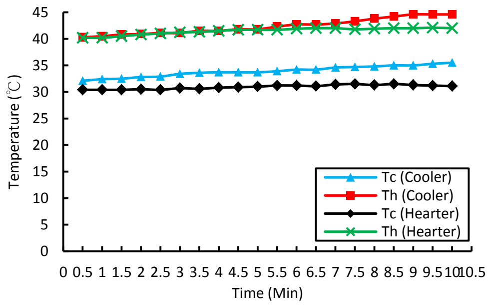

Figure 3-86: T-t at human body temperature

The data (table 3.62, figure 3-85 and 3-86) showed the power output and voltage of 2nd wristlet was getting lower. The cooler and heater performance were with respect to the time.

3.5 Application on Clothes for Body Warming up, Cooling down and for Battery Charging:

Table 3.63: generating, warming and cooling clothes performance

Time (min)	Generator			Cooler		Heater	
	Voltage (mV)	I (mA)	Power (μW)	T_c (℃)	T_h (℃)	T_c (℃)	T_h (℃)
0.5	37.2	2.82	104.904	32.2	40.2	30.2	40.2
1	34.8	2.805	97.614	32.5	40.1	30.5	40.2
1.5	32.7	2.805	91.7235	32.4	40.7	30.5	40.5
2	32.4	2.76	89.424	32.3	40.8	30.3	40.7
2.5	31.2	2.7	84.24	32.7	41.1	30.2	41
3	27.7	2.73	75.621	33.3	41.2	30.8	41.2
3.5	24.4	2.75	67.1	33.5	41.3	30.8	41.3
4	20.2	2.75	55.55	33.6	41.4	30.7	41.4
4.5	19.2	2.73	52.416	33.4	41.6	30.9	41.7
5	19.2	2.73	52.416	33.3	41.4	31	41.7
5.5	19	2.76	52.44	33.5	42.5	31.1	41.7
6	19	2.76	52.44	34.3	42.8	31.2	41.9
6.5	18.4	2.72	50.048	34.5	42.7	31	42
7	18.4	2.75	50.6	34.7	42.9	31.4	42
7.5	18.4	2.73	50.232	34.3	43.3	31.5	41.7
8	18	2.73	49.14	34.7	43.8	31.3	41.9
8.5	18	2.4	43.2	34.8	44.1	31.5	42
9	18	2.76	49.68	34.5	44.6	31.2	42
9.5	17.6	2.76	48.576	35.3	44.7	31.2	42.2
10	17.4	2.73	47.502	35.5	44.6	31.1	42

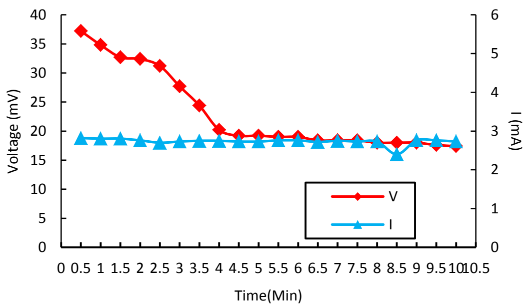

Figure 3-87: V-I-t at human body temperature

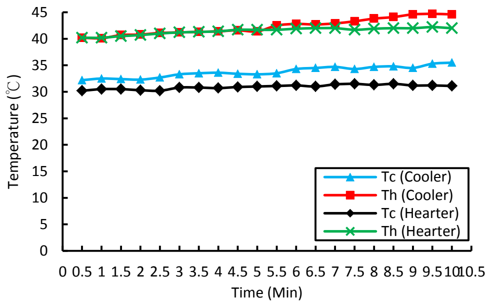

Figure 3-88: T-t at human body temperature

The data (table 3.63, figure 3-87 and 3-88) showed the power output and voltage of clothes was getting lower. The cooler and heater performance were as high as belong the time.

3.6 Cost Comparison:

Table 3.64: cost comparison

Module	TTEM	1st FTEM	2nd FTEM
Substrate	750	3	5
Bulk Material	600	600	1240
Total	1350	603	1245

The table 3.64 showed the TTEM was the most expensive among all modules. The reason was the cost of 2L FCCL substrate and 3L FCCL of FTEM were lower than the cost of ceramic substrate. Besides, the producing cost of ceramic was very expensive (ceramic substrate produced under high temperature) and it was also difficult to put into mass production. Oppositely, producing the material FCCL were not necessary to be under high temperature that it was cheap. And, FCCL was easy to put into mass production.

Chapter 4 Conclusion

In this study, the Basic Thermoelectric Module showed to be the high performance thermoelectric module. There were three conditions to make high performance thermoelectric modules. First, the copper foil should be shorter and thicker. Second, more pairs of the n-type and p-type could get higher power output. Third, fixators were indispensable to make modules.

The study of Traditional Thermoelectric Module Flexible and Thermoelectric Module showed that it was successful to make flexible thermoelectric module. The power output, generating conversion efficiency and cooling conversion efficiency of flexible thermoelectric modules were much higher than traditional thermoelectric modules. Besides, the flexible thermoelectric modules were much cheaper than traditional thermoelectric modules. This study also proved the assumption that the Eq. (1.15) $Z=S^2\sigma/\kappa$ for the different substrate materials of modules, power factor ($S^2\sigma$) supposed to be constant. The lower κ (thermal conductivity) is, the higher Z is. So, the conversion efficiency of flexible thermoelectric modules (FCCL substrate had low thermal conductivity) were higher than traditional thermoelectric modules (ceramic substrate had high thermal conductivity).

The flexible thermoelectric module was successfully for application in therapy usage (wristlet and clothes for examples). And it was also successful for application in circumstances of low-temperature.

Chapter 5 References

[1] Fu-Feng Tsai (2012), "Reflections and Reflections of 311 Nuclear Event Fukushima Japan", Taipower Nuclear, 351.

[2] Ying-Ru Chen (2012), "The risk perception of climate change and nuclear energy after Fukushima nuclear disaster", National Central University Graduate Institute of Industrial Economics M.S.

[3] British Petroleum (2013)," BP Statistical Review of World Energy 2013".

[4] IEA (2011), "world energy outlook 2011".

[5] Deutsche Shell, http://www.shell.de/ .

[6] R.O.C. Ministry of Economic Affairs Bureau of Energy (2014), "Total energy supply", Energy Statistics Monthly Report, August 14 update.

[7] Rowe DM (1999), "Thermoelectrics, an environmentally-friendly source of electrical power", Renewable Energy, 16, 1-4.

[8] T. J. Seebeck (1821), "Magnetische polarization der metalle und erzedurch temperature-differenze.Abhand deut," Akad. Wiss. , 265.

[9] Hsu-Shen Chu (2004), "theory and application of thermoelectric materials and device", electron and material magazine, 22, 78-89.

[10] W. Thomson (1851), "On the dynamical theory of heat; with numerical results deduced from Mr. Joule's equivalent of a thermal unit and M.Regnault's observations on steam", Math. and Phys. Papers 1, 175-183 ,1851.

[11] Y.M. Tan, W. Fan, K.M. Chua, Z. F. Shi and C. K. Wang (2005), "Fabriction of Thermoelectric Cooler for Device Integration", Proceedings of Electrics Packaging Technology Conference, pp.802-805.

[12] http://www.noahprecision.com/thermoelectric-overview.html

[13] D.J.Yao (2011)," In-plane MEMS thermoelectric microcooler", Ph. D, dissertation of UCLA.

[14] Lauryn L. Baranowski, G. Jeffrey Snyder and Eric S. Toberer (2012), " Concentrated solar thermoelectric generators", Energy Environ. Sci., 5.

[15] Terry M.Tritt and M.A. Subramanian (2006), " Thermoelectric Materials, Phenomena, and Applications: A Bird's Eye View", MRS BULLETIN VOLUME, pp.188~198.

[16] V.E. Altenkirch (1909), *Physikalische Zeitschrift*, 10, 560.

[17] A. F. Ioffe (1957), "Semiconductor Thermoelements and ThermoelectricCooling" , Infosearch.

[18] Jing-Hui Meng, Xin-Xin Zhang, Xiao-Dong Wang (2014), "Multi-objective and multi-parameter optimization of a thermoelectric generator module", Energy, 71, 367–376.

[19] F.J. Disalvo (1999), "Thermoelectric cooling and power generation", Science, 285, 703–706.

[20] W.H. Chen, C.C. Wang, C.I. Hung, C.C. Yang, R.C. Juang (2014), "Modeling and simulation for the design of thermal-concentrated solar thermoelectric generator", Energy, 64, 287–297.

[21] A.Z. Sahin, B.S. Yilbas (2014), "Thermodynamic irreversibility and performance characteristics of thermoelectric power generator", Energy, 55, 899–904.

[22] H.L. Lua, T. Wu, S.Q. Bai, K.C. Xu, Y.J. Huang, W.M. Gao, et al. (2013), "Experiment on thermal uniformity and pressure drop of exhaust heat exchanger for automotive thermoelectric generator", Energy, 54, 372–377.

[23] L.E. Bell (2008), "Cooling, heating, generating power, and recovering waste heat with thermoelectric systems", Science, 321, 1457–1461.

[24] D.M. Rowe (2006), "Thermoelectrics handbook: macro to nano", CRC Press.

[25] Heat2power, http://www.heat2power.net/en_benchmark.php

[26] China Steel Corporation, http://www.csc.com.tw/csc_e/hr/green4.htm

[27] Ming Ma, Jianlin Yu (2014), "An analysis on a two-stage cascade thermoelectric cooler for electronics cooling applications", International Journal of Refrigeration, 38, 352–357.

[28] http://web.mit.edu/imoyer/www/portfolio/absolutzero/index.html

[29] Industrial Technology Research Institute.

[30] Yury M. Belov, Sergei M. Maniakin, and Igor V. Morgunov (2006), "Review of Methods of Thermoelectric Materials Mass Production", Thermoelectrics Handbook Macro to Nano, 20-1~20-12.

【評語】120006

本作品利用熱電晶片冷端與熱端的溫度差產生電的特性，將環境廢熱回收成為可用的電能，此構想可應用於工業製程廢熱及家電廢熱。本作品以人體體溫為發電對象，利用 Peltier 效應，作為醫療用冷敷或熱敷之器材，應用價值仍待進一步評估。